



Attorney's Docket N°

IN THE UNITED STATES PATENT AND TRADEMARK OFFICE

IN RE APPLICATION OF:

Martial RUAT, et al.

SERIAL No.:10/543,004 :

FILED: JANUARY 22, 2004 :

FOR: NOVEL USE OF MIFEPRISTONE AND DERIVATIVES THEREFOR AS  
HEDGEHOG PROTEIN SIGNALLING PATHWAY MODULATORS AND  
APPLICATION OF SAME

DECLARATION UNDER 37 C.F.R. § 1.132

ASSISTANT COMMISSIONER FOR PATENT  
ALEXANDRIA, VIRGINIA 22313

SIR:

I, Martial RUAT, Research Director at the Institut National de la Santé Et de la Recherche Médicale (INSERM) and co-applicant of the Patent Application No.10/543,004 filed on January 22, 2004, hereby declare and state as follows:

1. I am a graduate of INSA of Lyon where I received my Engineer diploma in Biochemistry.
2. I am a graduate of University Lyon II, where I received my DEA diploma in Microbiology.
3. I am a graduate of the University Paris 6, where I received my PhD in Molecular and Integrative Neurobiology.
4. I am a graduate of the John Hopkins Hospital, Departement of Neuroscience, where I received my Post-doctoral fellowship in Neuroscience.

5. I am, since 1996, Head of ATIPE Team "Signal Transduction and Developmental Neuroparmacology" in Laboratoire de Neurobiologie Cellulaire et Moléculaire, UPR9040 CNRS Gif-sur-Yvette (Director: G. Baux).
6. The following experiments were performed by me or under my supervision.
7. The following experiment describes tests demonstrating the effect of mifepristone on the activity of the Hedgehog signaling pathway in neural progenitor cells, precursors of brain tumors.
8. The effect of mifepristone has been evaluated *in vivo* on the incorporation of the proliferation marker Bromodeoxyuridine (BrdU) by persistent neural progenitors in the adult brain in two neurogenic regions: the sub-ventricular zone (ZSV) of lateral ventricles and sub-granular zone (ZSG) in the hippocampus.
9. These cells are the precursors of brain tumors (Vescovi *et al.*, Nat Rev Neurosci, 2006, 6, 425-436).
10. In these two brain areas, by blocking the Smo receptor of the Sonic hedgehog pathway with cyclopamine, the first antagonist identified for this receptor, a decrease in the number of proliferating cells is induced (Palma *et al*, Development, 2005, Lai *et al*, Nat Neurosci, 2003).

#### 11. Experimental protocol

Mifepristone has been injected subcutaneously to adult mice and the effect of this administration on the number of proliferating cells in these two regions was analyzed.

**Injections:** Two injections of mifepristone (25 mg/kg) in a volume of 100 µl are administered by daily subcutaneous (sc) injection to 8 weeks old, adult OF1 male mice (30-32 g, Charles Rivers) for 4 or 10 days (n = 7-8 animals per group).

In parallel, two groups of animals (n = 7-8) received daily injections of vehicle (ethanol 10% in propane-diol) used for the dissolution of mifepristone.

The day after the last injection, the animals received 2 intraperitoneal injections of BrdU spaced 2 hours (as described in Loulia *et al.*, J. Neurochem, 2006).

**Anti-BrdU immunohistochemistry:** The protocol used is described in Loulia *et al*, J Neurochem, 2006. Briefly, after completion of serial sections of the brain of each animal (slides), DNA is denatured by immersion of the slides in a solution of 2N hydrochloric acid in phosphate buffer saline (PBS). After 3 washes in PBS, sections were covered with a blocking solution (Normal Goat Serum (NGS) 10% in PBS) and incubated over night at 4°C with primary antibody anti-BrdU (1/ 200). After 3 washes, the slides were incubated with appropriate biotinylated secondary antibody and the immunostaining was revealed using the avidin biotin complex and 3,3'-diaminobenzidine tétrahydrochloride (DAB) as substrate of the enzymatic reaction.

**Cell counts:** double-blind cell counts are performed under the 20X objective of a conventional microscope (DMRXA2, Leica Microsystems). The cells were counted in the ZSG and in the ZSV of the two cerebral hemispheres on 4 to 6 sections per animal located at comparable levels for each animal. The results reflect the average number of BrdU<sup>+</sup> cells per section of tissue ± SEM in all sections of the same group of animals. For statistical analysis, the Student test was applied (\* p <0.05).

12.        Results

The daily injection of mifepristone (25 mg/kg) for 4 or 10 days did not induce alteration of the apparent general condition of animals.

The immunohistochemical analysis of frontal sections of brains of mice treated with mifepristone or vehicle allowed counting the number of BrdU<sup>+</sup> cells / section in the ZSV and in the ZSG in 4 groups of animals described above.

After 4 days of treatment, a significant decrease in the density of BrdU<sup>+</sup> cells in the ZSV is observed in the animals treated with mifepristone compared to control animals, respectively  $84 \pm 3$  and  $113 \pm 3$  BrdU<sup>+</sup> cells / section (total number of cells counted, respectively  $n = 5239$  and  $n = 5448$ ,  $p < 0.001$ ).

After 10 days of treatment, a comparable decrease is observed. In this case, the number of cells evaluated in animals treated by mifepristone or vehicle is  $117 \pm 3$  and  $145 \pm 3$  BrdU<sup>+</sup> cells / section (total number of cells counted, respectively,  $n = 5156$  and  $5826$ ,  $p < 0.001$ ).

In ZSG, the number of proliferating cells also decreased, but to a lesser degree in the 2 analyzed conditions of time in the animals receiving mifepristone.

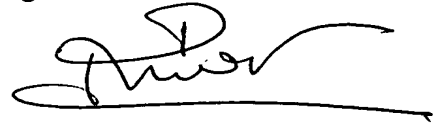
The number of BrdU<sup>+</sup> cells / section in mifepristone-treated animals compared to control animals is  $4.2 \pm 0.4$  and  $5.3 \pm 0.4$  (total number of counted cells  $n = 153$  and  $n = 201$ ,  $p < 0.05$ ) after 4 days of treatment, and  $6 \pm 0.3$  and  $7.0 \pm 0.4$  (total number of counted cells  $n = 418$  and  $n = 491$ ,  $p < 0.05$ ) after 10 days of treatment.

13. These results indicate that mifepristone induces a decrease in the number of proliferating cells in the two main areas of neurogenesis in the adult brain, the sub-ventricular zone (ZSV) of lateral ventricles and the sub-granular zone (ZSG) in the hippocampus.
14. A similar effect has been described after blocking Shh signaling by the molecule first described as a Smo receptor antagonist, the cyclopamine (Palma *et al.*, Development, 2005, Lai *et al.*, Nat Neurosci, 2003). We have also identified a decrease in the number of cells incorporating BrdU after administration of another Smo antagonist, the Cur61414.
15. Mifepristone shows the same behavior than the first molecule described as a Smo receptor antagonist of the Hedgehog protein signaling pathway, the cyclopamine.
16. Several studies have reported that increases in corticosterone inhibit neurogenesis in the *hippocampus* (Gould *et al.* J. Neurosci., 1992, 12 (9): 3642-3650; Stranahan *et al.* Nat. Neurosci., 2008, 11 (3): 309-317); more recently, Lau *et al.* have reported that corticosteroids also reduce cell proliferation in the ZSV (Lau *et al.* Restaur. Neurol. Neurosci., 2007, 25: 17-23).
17. The expected action of mifepristone, which is known as a glucocorticoid receptors antagonist, should lead to an increase in the number of proliferating cells in the ZSG and ZSV (*i.e.* the opposite effect of those observed with a corticosteroid).
18. The expected action of mifepristone should not lead to the decrease observed in the present results.

19. These results thus indicate that mifepristone shows an unexpected effect compared to knowledge of the state of the art: its effect on neural progenitor is similar to a corticosteroid hormone when it is an antagonist corticosteroids.
20. These results demonstrate that mifepristone does not act on neural progenitors via the glucocorticoid receptors.
21. These results indicate that mifepristone has the ability to inhibit the proliferation of neural progenitors via the Hedgehog protein signaling pathway.
22. The neural progenitors have a broad potential for differentiation. Clarke *et al.*'s review (Science, 2000, 288: 1666-1663) describes the ability of adult neural progenitor cells to differentiate into muscle cells (page 1661, left column, lines 23-25), in cells of mesonephric tubules (page 1661, middle column, line 10) and epidermal cells (page 1661, middle column, line 11) (see also Table 1, page 1663); all of these cells, therefore, share the common characteristic of having a proliferation regulated by the Hedgehog signaling pathway.
23. Thus, tumors associated with a hyperactivation of the Hedgehog proteins signaling pathway of brain cells (*medulloblastomas, glioblastomas, oligodendrogliomas*), muscle cells (*rhabdomyosarcoma*), skin cells (basal cell *carcinoma, trichoepithelioma*) and kidney cells (renal tumors) will have a behavior identical to that of neural progenitors in the presence of mifepristone: mifepristone will be able to inhibit their proliferation.
24. These data confirm the inhibitory effect of mifepristone on cell proliferation via the hyperactivation of the Hedgehog protein signaling pathway; which is consistent with the results obtained in the *in vitro* differentiation of the C3H10T1/2 cell line described in Example 1 of the present Patent Application.
25. In addition, the use of mifepristone for the treatment of tumors associated with a hyperactivation of the signaling pathway of the Hedgehog protein chosen among *medulloblastomas, glioblastomas, oligodendrogliomas*, the basal cell carcinoma, *trichoepithelioma, rhabdomyosarcoma* and tumors of the kidney, is not obvious from Haak *et al.*, Reiner *et al.* nor Gettys *et al.* which describe mifepristone as a progesterone antagonist, a ABC transporter blocker and a glucocorticoid antagonist, respectively.
26. In particular, these documents teach that mifepristone is effective **only** in the treatment of tumors whose growth is dependent on progesterone or glucocorticoids; the skilled person would have been deterred from using mifepristone to treat other tumors whose growth is linked to a hyperactivation of the Hedgehog protein signaling pathway that involves neither the progesterone receptor nor glucocorticoid.
27. In my opinion, one skilled in the art would not have expected mifepristone to inhibit the proliferation of neural progenitors via the glucocorticoid receptors. Further, I am of the opinion that this result is important and commercially significant.

28. The undersigned petitioner declares further that all statements made herein of his own knowledge are true and that all statements made on information and belief are believed to be true; and further that these statements were with the knowledge that wilful false statements and the like so made are punishable by fine or imprisonment, or both, under Section 1001 of Title 18 of the United States Code and that such wilful false statements may jeopardize the validity of this Application or any Patent Issuing thereon.

Signature: Martial RUAT

A handwritten signature in black ink, appearing to read 'Martial RUAT', with a long horizontal flourish extending to the right.

Date

28/09/2009

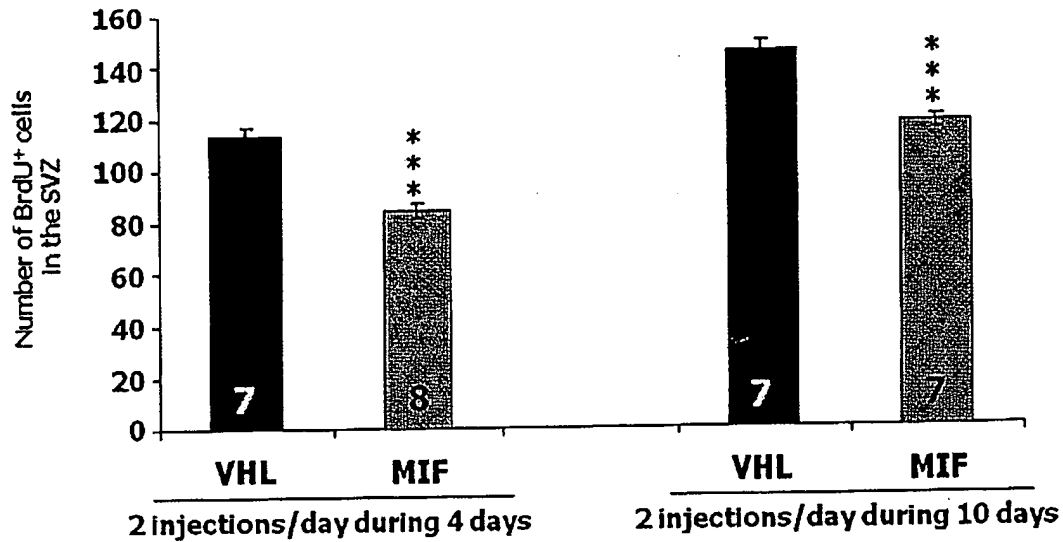


**Figure 1: Decrease of the number of BrdU<sup>+</sup> cells in the ventricular zone (ZSV) of animals treated with mifepristone.** Histograms displaying the number of BrdU<sup>+</sup> cells / section in the ZSV in animals that received 4 respectively (left panel) or 10 (right panel) days of treatment with mifepristone (MIF, gray bars) or vehicle (VHL, black bars). The figures at the base of bars indicate the number of animals analyzed. Values represent the mean  $\pm$  SEM of 4-6 sections for each animal analyzed. \*\*\*  $p < 0.001$ .

After 4 days of treatment, a significant decrease in the density of BrdU<sup>+</sup> cells in the ZSV is observed in the animals treated with mifepristone compared to control animals, respectively  $84 \pm 3$  and  $113 \pm 3$  BrdU<sup>+</sup> cells / section (total number of cells counted, respectively  $n = 5239$  and  $n = 5448$ ,  $p < 0.001$ , Figure 1).

After 10 days of treatment, a comparable decrease is observed. In this case, the number of cells evaluated in animals treated by mifepristone or vehicle is  $117 \pm 3$  and  $145 \pm 3$  BrdU<sup>+</sup> cells / section (total number of cells counted, respectively,  $n = 5156$  and  $5826$ ,  $p < 0.001$ , Figure 1).

In ZSG, the number of proliferating cells also decreased, but to a lesser degree in the 2 analyzed conditions of time in the animals receiving mifepristone.

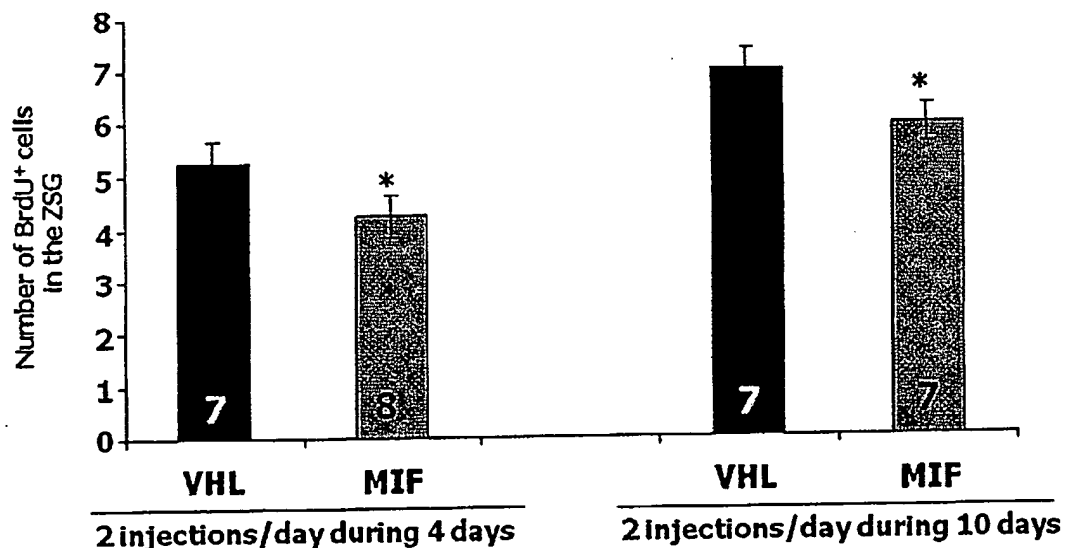


**Figure 2: Decrease of the number of BrdU<sup>+</sup> cells in the area of the hippocampus Granular (ZSG) of animals treated with mifepristone.** Histograms displaying the number of BrdU<sup>+</sup> cells / section in the ZSG in animals that received 4 (left panel) or 10 (right panel) days of treatment with mifepristone (MIF, gray bars) or vehicle (VHL, black bars). The figures at the base of bars indicate the number of animals analyzed. Values represent the mean  $\pm$  SEM of 4-6 sections for each animal analyzed. \*,  $p < 0.05$ .

The number of BrdU<sup>+</sup> cells / section in mifepristone-treated animals compared to control animals is  $4.2 \pm 0.4$  and  $5.3 \pm 0.4$  (total number of counted cells  $n = 153$  and  $n = 201$ ,  $p < 0.05$ , Figure 2) after 4 days of treatment, and  $6 \pm 0.3$  and  $7.0 \pm 0.4$  (total number of counted cells  $n = 418$  and  $n = 491$ ,  $p < 0.05$ , Figure 2) after 10 days of treatment.

### **Discussion**

These results indicate that mifepristone induces a decrease of the number of proliferating cells in the two main areas of adult brain neurogenesis. A similar effect has been described after blocking Shh signaling by the molecule first described as a Smo receptor antagonist, the cyclopamine (Palma *et al*, 2005). We have also identified a decrease in the number of cells incorporating BrdU after administration of another Smo antagonist, the Cur61414 (unpublished results).

## Brain tumour stem cells

Angelo L. Vescovi\*, Rossella Galli<sup>†</sup> and Brent A. Reynolds<sup>§</sup>

**Abstract** | The dogma that the genesis of new cells is a negligible event in the adult mammalian brain has long influenced our perception and understanding of the origin and development of CNS tumours. The discovery that new neurons and glia are produced throughout life from neural stem cells provides new possibilities for the candidate cells of origin of CNS neoplasias. The emerging hypothesis is that alterations in the cellular and genetic mechanisms that control adult neurogenesis might contribute to brain tumorigenesis, thereby allowing the identification of new therapeutic strategies.

**Abnormal ionic flux**  
Alterations in the transit of ions through specific channels (NMDA receptors) that is generated by the massive release of glutamate from damaged cells and which leads to excitotoxicity.

**Reperfusion**  
CNS injury that is produced by tumour-induced transient ischaemia followed by blood re-oxygenation, which induces neural damage through the generation of reactive oxygen species.

The central role of the brain in every aspect of bodily function, and the dramatic functional disturbances that arise with minimal disturbance to the neural cyto-architecture or circuitry, account for the severity of many brain tumours. These tumours are often lethal, as conventional anti-cancer treatments have limited or no efficacy.

There is now increasing awareness that a principal hurdle in understanding and successfully treating these cancers might be overcome by the identification of a defined cell that could function as a therapeutic target. Similar to haematopoietic and breast cancers, only a few atypical cells within the cancerous mass might be responsible for the growth and recurrence of some brain tumours. Evidence indicates that the real culprit is a peculiar, transformed CNS cell type that has the defining properties of somatic stem cells, as well as cancer-initiating ability — a brain tumour stem cell.

Here, we review the findings that demonstrate the presence and involvement of brain tumour stem cells in the initiation and propagation of brain tumours, particularly glioblastomas, medulloblastomas and ependymomas, for which the identification of specific tumour stem cells has recently been described. We provide a comparative analysis of the functional properties of brain tumour stem cells relative to normal neural stem cells and in the context of adult cell genesis. We also discuss the origin of brain tumour stem cells from normal adult neural stem cells or progenitor cells, and cover the possible involvement of normal neurogenetic regulatory mechanisms in the physiology of brain tumours and brain tumour stem cells. The theoretical and practical consequences of the idea that brain tumour stem cells are 'diseased' cells with deregulated self-renewal will be analysed, together with the conceptual and clinical implications.

### Characteristics of malignant brain tumours

Different types of tumour of neuroepithelial origin have been identified and classified according to the cell types that predominate within the tumour mass (BOX 1). Whereas grade IV gliomas are the most frequent primary intraparenchymal neoplasm in the elderly, medulloblastomas have the highest incidence in children.

The therapy of intracranial tumours presents many problems that result from the inherent vulnerability of the brain parenchyma. Abnormal ionic flux, excitotoxicity that is related to glutamate release from dead cells, reperfusion and compressive forces often cause irreversible damage to CNS tissues. In addition, the tendency of specific brain tumours, such as the astrocytic and embryonal subtypes, to extensively infiltrate the neighbouring brain structures and to relapse, often progressing toward malignancy, makes the prognosis of these cancers poor.

On the basis of World Health Organization classification, the most malignant form of glioma is grade IV, which is commonly known as glioblastoma multiforme. This highly aggressive tumour develops either *de novo* (primary glioblastoma multiforme) or as the result of the malignant progression from a low-grade glioma (secondary glioblastoma multiforme)<sup>1</sup>. In both cases, prognosis is poor and the median survival when radiotherapy and chemotherapy are combined is 14.6 months<sup>2</sup>. Most importantly, glioblastoma multiforme is characterized by a diffuse tissue-distribution pattern, with extensive dissemination of the tumour cells within the brain that hinders complete surgical resection<sup>3</sup>. Similarly, medulloblastoma, which is thought to arise from the malignant transformation of progenitors of the external granular layer of the cerebellum, is a highly malignant paediatric cancer with a poor prognosis, although there has been some progress recently. As opposed to glial tumours, medulloblastoma is primarily characterized by neuronal differentiation and is considered an embryonal tumour<sup>4</sup>.

\*Department of Biotechnology and Biosciences, University of Milan Bicocca, Milan 20126, Italy.

<sup>†</sup>Stem Cell Research Institute, DIBIT, San Raffaele Scientific Institute, Via Olgettina 58, Milan 20132, Italy.

<sup>§</sup>University of Queensland, Brisbane 4072, Australia. Correspondence to A.L.V. e-mail: vescovi@tin.it doi:10.1038/nrc1889



## At a glance

- Adult somatic stem cells are a rare population of long-lived cells that have significant proliferative capacity, show extensive self-renewal and have a wide differentiation potential.
- Cells that have the cardinal properties of stem cells have been identified in restricted regions of the CNS, where they are arranged in specific lineage hierarchies.
- Similar to other adult stem cells, neural stem cells or their immediate progeny, which are called transiently dividing progenitors, can be considered a credible target for malignant transformation. This concept is supported by the finding that many of the molecular determinants that regulate normal neurogenesis seem also to be involved in tumorigenesis.
- Brain tumour stem cells have been identified and isolated from different types of brain tumour: in particular, glioblastoma multiforme and medulloblastoma.
- Brain tumour stem cells show all the features of stem cells, including the ability to generate new tumours that faithfully reproduce the phenotype of the human disease.
- The availability of brain tumour stem-cell lines provides a model system for the identification of specific antigenic and molecular markers that might target the tumour-initiating cell.
- The development of agents that selectively target and inhibit the tumour-initiating and propagation potential of brain tumour stem cells might reduce or eliminate primary tumour establishment, growth and recurrence.

## Stem cells in the adult CNS

Cancer arises from a series of mutations that occurs in few or even single founder cells. These cells eventually acquire unlimited and uncontrolled proliferation potential<sup>5</sup>. Two hypothetical models can explain this phenomenon (BOX 2). The stochastic model predicts that all the cells in a tumour have a similar tumorigenic potential, which is activated asynchronously and at a low frequency in certain cells<sup>6</sup>. Conversely, the hierarchical

model holds that only a rare subset of cells within the tumour have significant proliferation capacity and, particularly, the ability to generate new tumours, with the remainder of the tumour cells representing differentiating or terminally differentiated cells<sup>6</sup>. The latter hypothesis fits with the cancer-stem-cell theory and is now supported by a plethora of recent observations<sup>7-9</sup>.

Recently, the concept of cancer stem cells has been extended to tumours of the brain, whose archetypically quiescent tissue has long been thought not to undergo significant cell turnover. This concept, known as the 'no new neuron' dogma, and the implied absence of brain stem cells in adulthood, was challenged in the early 1960s when the genesis of new, functional brain cells (neurogenesis) was described in the adult mammalian CNS<sup>10-12</sup>. However, the 'no new neuron' dogma withstood the challenge: although resting embryonic-like tissue remnants, which can persist within the CNS parenchyma, were also envisioned as the possible cellular source of brain tumours<sup>13</sup>, tumour cells in the brain were hypothesized to derive mostly from the transformation of maturer neural cells such as astrocytes, oligodendrocytes or neuronal precursors.

However, in the early 1990s, following on from the pioneering work of Fernando Nottebohm's laboratory that showed the functional relevance of adult neurogenesis in songbirds<sup>14</sup>, Reynolds and Weiss reported the isolation of a neural stem cell from the adult mouse brain<sup>15</sup>. A flurry of studies followed, which described persistent neurogenesis in the adult brains of rodents, tree shrews<sup>16</sup>, monkeys<sup>17</sup> and humans<sup>18</sup> (reviewed in REF. 19). Therefore, neurogenesis of mature cells persists throughout adult life within discrete brain regions, primarily in the dentate gyrus of the hippocampus and in the subventricular zone of the forebrain lateral ventricles (FIG. 1). This process is central to the generation and integration of new neurons into pre-existing neural circuitry, and is probably crucial for the maintenance of brain integrity, plasticity and optimal function<sup>20</sup>.

The main implication of continued adult neurogenesis is the presence of undifferentiated, mitotically active stem and progenitor cells within discrete regions of the mature brain. Like those that are found in other renewing tissues, these populations might function as a source of cells for transformation, giving rise to tumour stem cells.

The overall structure of the cell neogenetic process in the adult brain, its basic cellular compartments and the fundamental organization of the lineage hierarchy within neurogenetic areas are comparable to those of other renewing tissues (FIG. 2). The stem-cell compartment contains highly undifferentiated cells that are endowed with an extensive proliferative potential, and is responsible for the whole process of tissue cell homeostasis throughout the life of the organism. Stem cells often produce the entire range of mature cell types that are found in the tissue of origin (multipotency). Most importantly, they have extensive self-renewal capacity — that is, the ability to maintain their number in adult tissues at a steady level throughout life. Stem cells can accomplish self-renewal by undergoing asymmetric divisions, by which a faithful

## Box 1 | WHO classification of brain tumours

### Astrocytic tumours

- Diffuse astrocytoma (grade II)
- Anaplastic astrocytoma (grade III)
- Glioblastoma (grade IV)

### Oligodendroglial tumours

- Oligodendroglioma

### Mixed gliomas

- Oligoastrocytoma

### Ependymal tumours

- Ependymoma

### Neuronal and mixed tumours

- Gangliocytoma

### Neuronal/glia tumours

- Dysembryoplastic neuroepithelial tumour
- Ganglioglioma

### Embryonal tumours

- Medulloblastoma
- Ependymoblastoma
- Neuroblastoma

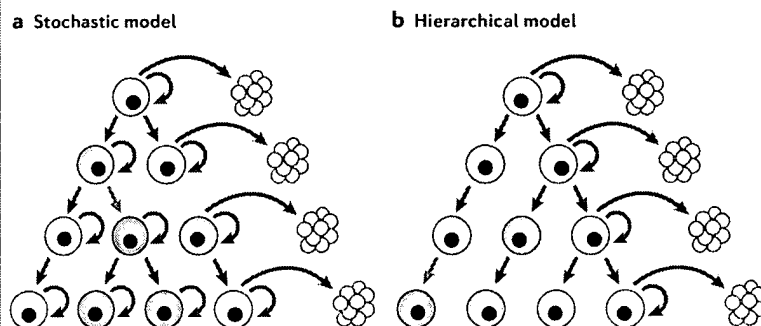
### Primitive neuroectodermal tumours

- Medulloblastoma

Resting embryonic-like tissue  
Remnants of cells that maintain the features of embryonic cells but are located in a semi-quiescent mature tissue.

## Box 2 | Tumour initiation and development

Two alternative models have been put forward to explain how tumours initiate and develop. The stochastic model (a) proposes that tumour cells are heterogeneous, but that virtually all of them can function as a tumour-founding cell, although this might happen only rarely. Conversely, the hierarchical model (b) implies that only a small subpopulation of tumour stem cells can proliferate extensively and sustain the growth and progression of a neoplastic clone. Figure reproduced with permission from REF. 6 © (2001) Macmillan Publishers Ltd.



copy of the mother cell, together with a maturer progenitor, is generated. The same result is achieved when, within a given stem-cell pool, equivalent numbers of symmetrical cell cycles take place, yielding either two stem cells or two maturer progenitors<sup>21</sup>. Extensive self-renewal is often used to distinguish somatic stem cells from their immediate descendants, which constitute the transiently dividing progenitor compartment and can only reproduce themselves in a limited fashion. These descendants eventually give rise to the terminally differentiated elements of the mature cell compartment. Disruption of the regulatory mechanisms that control self-renewal are probably involved in the genesis of cancer-initiating stem-like cells<sup>6,22</sup>.

### Neurogenesis in the mature CNS

The largest neurogenetic region in the adult mammalian brain is the subventricular zone, which is located between the lateral ventricle and the parenchyma of the striatum (FIG. 1a). Despite previous controversies about their actual identity and nature, a subset of the subventricular zone cells that express the astroglial marker glial fibrillary acidic protein (GFAP) have been identified as the putative adult neural stem cells in this region<sup>23</sup>. These cells can reconstruct the entire neurogenetic structure when all of the other mitotically active cells have been ablated. Relatively quiescent, with a proposed cell-cycle time of 28 days, these astrocyte-like adult neural stem cells are called type B cells and represent a small subset of the total astrocyte population in the subventricular zone<sup>23</sup>. Notably, they can be distinguished from mature astrocytes, particularly those of the mature brain parenchyma, as these do not seem to possess stem-cell properties. *In vivo*, adult neural stem cells generate transiently dividing progenitor cells that are characterized by a cell-cycle time of about 12 hours<sup>24</sup>. These progenitors, which are called type C cells, retain multipotency and give rise to maturer transiently dividing progenitors that are restricted to neurons and are called type A cells.

These type A cells migrate in bundles through the rostral extension of the subventricular zone into the olfactory bulb, where they integrate as new interneurons in the cortical layers (FIG. 1a).

Interestingly, the subventricular zone seems to be present in the human adult brain<sup>25–27</sup>. However, in humans, newly generated cells do not migrate in bundles towards the olfactory bulb, but instead leave the periventricular region as single cells, the destination of which remains to be identified<sup>25,27</sup> (FIG. 1c).

There is a similar hierarchical neurogenetic system in the subgranular zone of rodents<sup>28,29</sup> (FIG. 1b) and humans<sup>18,30</sup> (FIG. 1d). The subgranular zone is located between the hippocampal granular layer and the hilus, and contains astrocytes that are tightly associated with blood vessels to form foci of proliferating cells. Similar to their subventricular-zone equivalents, subgranular-zone astrocytes operate as neural stem cells and give rise to transiently amplifying precursors, which are called type D cells, from which new neuronal precursors are generated that migrate a short distance to functionally integrate into the granule-cell layer (reviewed in REF. 20).

The persistence of germinal regions and the presence of stem cells and transiently dividing progenitor compartments in the adult CNS has important conceptual and practical implications, and reinforces the idea that mature neural cells are not the only possible source of tumour cells in the adult mammalian brain.

### Identifying neural stem cells and tumour stem cells

A valuable feature of adult neural stem cells is that they are readily and extensively expandable when placed in culture and stimulated with the appropriate growth factors, such as epidermal growth factor (EGF)<sup>15,23,31</sup> and fibroblast growth factor 2 (FGF2)<sup>32,33</sup>. This culture condition allows adult neural stem cells to be isolated, and their functional characteristics and developmental potential to be investigated. This was demonstrated by Reynolds and Weiss in 1992 who isolated a small population of cells (<0.1% of total cells) from the adult striatum that could proliferate and generate multipotent clones of cells — neurospheres — *in vitro*<sup>15</sup>.

This neurosphere approach represents a serum-free, selective culture system in which most differentiating or differentiated cells rapidly die, whereas neural stem cells respond to mitogens, divide and form neurospheres that can be dissociated and re-plated to generate secondary spheres. This process can be repeated by serial subculturing, which results in an exponential increase in the total number of cells and neurospheres that are generated<sup>34</sup> (FIG. 3). It is worth emphasizing that the neural stem-cell content in this system is variable and depends on the stage of the culture. The neural stem-cell titre is actually extremely high (although it never reaches absolute purity) soon after the dissociation and re-plating (which selects against cells other than neural stem cells), but tends to decline progressively until the next subculturing step is carried out. This is due to the production of maturer precursors that occurs spontaneously during cell proliferation and neurosphere formation. Notably, on mitogen removal, the progeny of the growth-factor-responsive

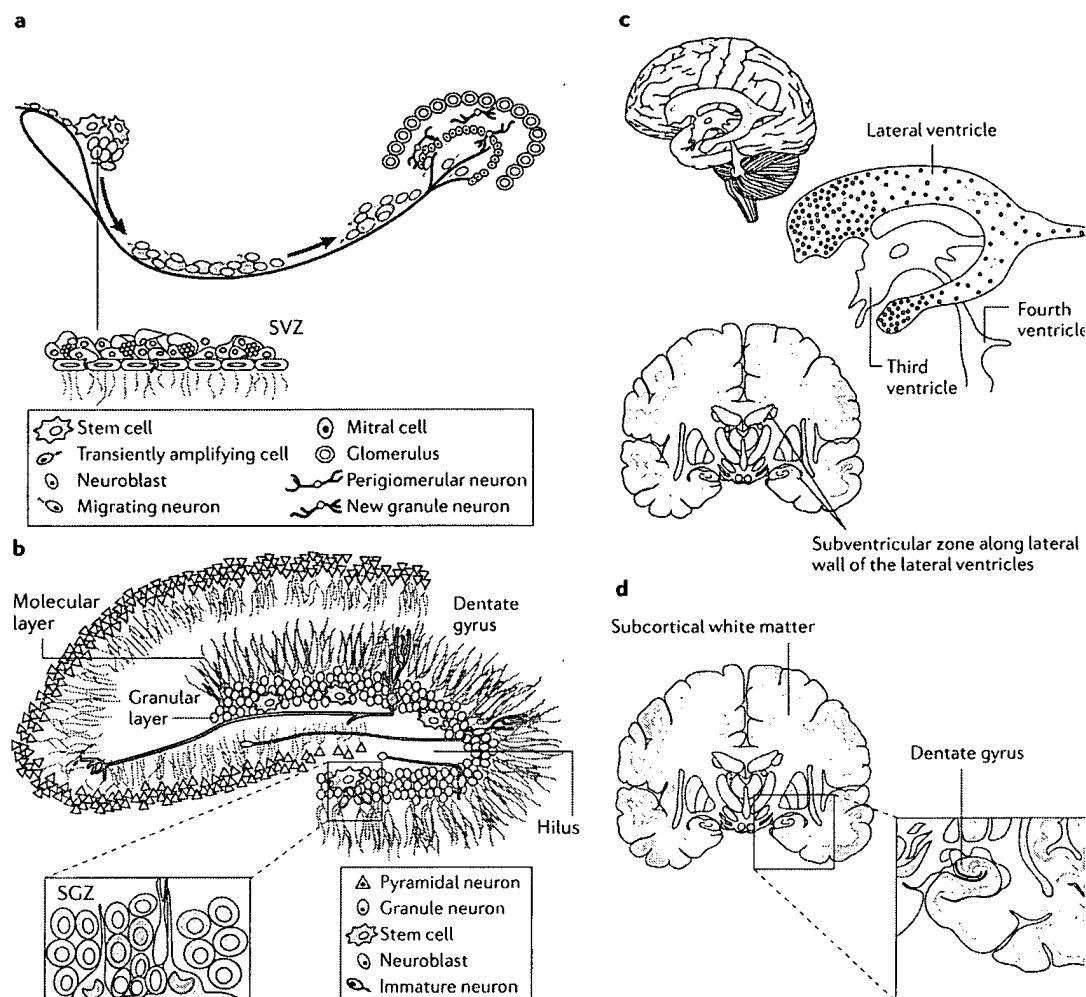


**Figure 1 | The anatomy and functioning of the subventricular zone and subgranular zone in rodents and humans.** **a** | A sagittal section through the lateral ventricle that shows the larger area of adult neurogenesis; that is, the subventricular zone (SVZ). This region lines the lateral ventricles of the forebrain and is comprised of three main cell types. The multipotent, type B astrocytes, that have been identified as the *bona fide* SVZ stem cells, give rise to fast-cycling transiently proliferating precursor cells that are called type C precursors and that, in turn, generate mitotically active type A neuroblasts. The type A cells, while dividing, migrate tangentially towards the olfactory bulbs where they integrate as new interneurons. **b** | An additional adult neurogenetic region is found in the subgranular zone (SGZ), which is located within the dentate gyrus of the hippocampus. A cellular hierarchy, somewhat similar to that of the SVZ, is seen in the SGZ in which the true stem cell is probably the type B astrocyte, which produces the intermediate type D precursor that eventually gives rise to the type G granule neurons. These neurons integrate functionally into the granule cell layer. **c** | In the adult human brain, a population of SVZ astrocytes that is organized as a periventricular ribbon has been identified as comprising neural stem cells. In contrast to the rodent SVZ, no signs of tangential neuronal chain migration were detected from the corresponding human area. **d** | The germinal zone of the adult human hippocampus is located within the dentate gyrus. Neurogenesis in this region has been demonstrated to take place in adult humans. Parts **a** and **b** are reproduced with permission from REF. 20 © (2005) Annual Reviews. Parts **c** and **d** are reproduced with permission from REF. 26 © (2005) Massachusetts Medical Society.

cells can be differentiated into neurons, astrocytes and oligodendrocytes. Under these conditions, growth-factor-responsive neural stem cells that are derived from the embryonic and adult CNS can be passaged and expanded indefinitely with little change in their growth or differentiation characteristics<sup>32,33,35,36</sup>. These results indicate that adult neural stem cells possess the fundamental stem-cell criteria of self-renewal, multipotency and the generation of many progeny<sup>15,33,37–39</sup>.

The neurosphere assay<sup>15</sup> is a simple and robust assay for the isolation, expansion and identification of neural stem cells (FIG. 3), and has become the method of choice to study potential expanded neural stem-cell populations *in vitro*. Cells with stem-cell characteristics in culture have subsequently been found to line the entire mouse ventricular neuroaxis<sup>40,41</sup>, to be present in the human fetal and adult CNS<sup>25,36,42,43</sup>, and to participate in adult rodent neurogenesis<sup>44–48</sup>. Recently, the conditions of the

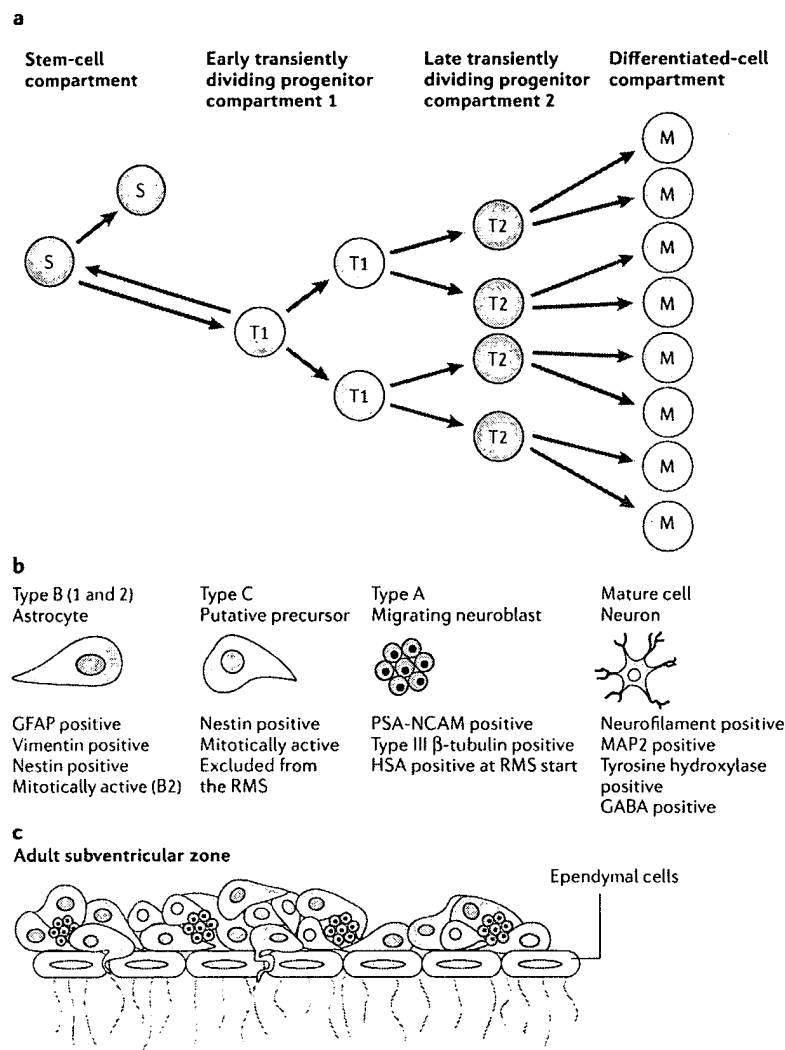


**Figure 2 | Hierarchical organization of the functional compartments in renewing tissues.** **a** | The stem-cell compartment (purple), early transiently dividing progenitor compartment (orange), late transiently dividing progenitor compartment (red) and differentiated-cell compartment (green) are schematically described. Cells in the stem-cell and transiently dividing progenitor compartments could be the target of the onco-transformation that leads to the formation of tumour stem cells. **b** | The neural precursors that make up similar functional compartments in the neurogenetic regions of the adult brain and that might be the source of brain tumour stem cells. **c** | The structure of the subventricular zone, showing how these precursors fit and are organized in the germinal neuroepithelium of the largest neurogenetic region of the adult brain. GABA,  $\gamma$ -aminobutyric acid; GFAP, glial fibrillary acid protein; HSA, heat-stable antigen; MAP2, microtubule-associated protein 2; NCAM1, neural cell adhesion molecule 1; PSA, polysialic acid; RMS, rostral migratory stream.

neurosphere assay have been used to isolate other types of candidate stem cell from various tissues, including skin<sup>49</sup>, heart<sup>50</sup> and breast<sup>51</sup>, and, significantly, to identify brain tumour stem cells.

**Brain tumour stem cells.** The identification and isolation of brain tumour stem cells remains a difficult and confusing issue, as the term 'brain tumour stem cell' is often applied to cells that have been identified by different methods and criteria, and that have varying

characteristics. Although this is probably a consequence of the relatively recent identification of these cells, it also reflects the current state of flux in neurobiology in attempting to provide a general definition of neural stem cells and to identify neural stem-cell-specific markers. The most widely used neural lineage markers often label intracellular antigens<sup>20</sup>, and adult neural stem-cell-specific antigens are still being identified. This shortcoming hinders the enrichment and purification of adult neural stem cells by flow cytometry. The situation is now improving with the identification of cell-surface antigens and methods that are used to identify putative neural stem cells in rodents<sup>52–54</sup> and humans<sup>43</sup> and that might eventually be used to purify brain tumour stem cells<sup>55</sup>. However, despite the modifications that cell culturing might bring about in tumour stem cells, to date all of the reports that describe the isolation and characterization of putative brain tumour stem cells have used the neurosphere assay (in some form) to help confirm the existence of a stem-cell population.

The first evidence of the existence of cells with stem-like characteristics in human brain tumours was reported by Steindler and colleagues<sup>56</sup>, who isolated clonogenic, neurosphere-forming precursors from post-surgery specimens of human glioblastoma multiforme. These stem-like cells expressed both neuronal and astroglial markers on differentiation, together with several key determinants of neural stem-cell fate. Later, two independent groups extended these findings, showing that both glioblastoma multiforme and medulloblastoma contain neurosphere-forming cells that can give rise to neuronal and astroglial-like cells<sup>57,58</sup>. Medulloblastoma cells were also shown to express many genes that are characteristic of neural stem cells, including proteins such as SOX2, BMI1 and Musashi 1, and to give rise to dysplastic tissue following intracerebral transplantation<sup>58</sup>.

The relevance of these findings is manifold. First, they confirm that different brain tumours contain transformed, undifferentiated neural precursors that respond to the same mitogens that activate adult neural stem cells. Second, they indicate that tumour stem-like cells possess some of the molecular features of neural stem cells. Third, they show that CD133, a 120 kDa cell-surface protein that is a marker of normal human neural precursors<sup>43,59,60</sup>, can be used for the enrichment of tumour stem-like cells from brain tumours<sup>55,57</sup>.

However, these observations do not show whether the stem-like cells that are derived from these tumours have the identifying characteristics of true stem cells (that is, long-term self-renewal, multipotency and generation of many progeny), and, most importantly, whether they have cancer-initiating capacity as would be expected of brain tumour stem cells.

By applying the same conditions that are used for the isolation of human neural stem cells, we were able to isolate clonogenic, neurosphere-forming progenitors from adult human glioblastoma multiforme<sup>61</sup>. These cells were isolated at a frequency comparable to that of the CD133<sup>+</sup> cells that were previously isolated from brain tumours<sup>55,57</sup>, and they had the key *in vitro* stem-cell characteristics of extensive self-renewal, multipotency and generation

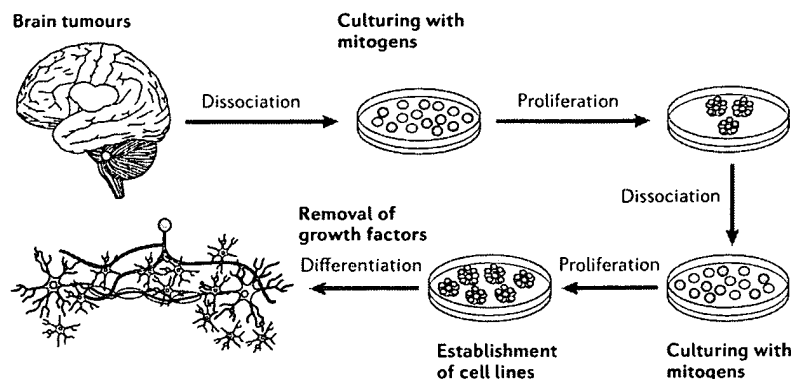


**Figure 3 | Isolation and perpetuation of brain tumour stem cells in culture.** The neurosphere assay is a defined serum-free culture system that allows the isolation and propagation of CNS-derived stem cells. Adult precursors are dissociated and plated in a liquid growth medium that contains the stem-cell mitogens epidermal growth factor and/or fibroblast growth factor 2. Because of the lack of serum and the low plating density, most cells die, except those that divide in response to the stem-cell mitogens. The growth-factor-responsive cells proliferate to form floating clusters of cells that are referred to as neurospheres. These can be further dissociated into a single-cell suspension and then re-plated in fresh medium to produce secondary neurospheres. The process can be repeated, resulting in a geometric expansion in the number of cells that are generated at each passage. Upon mitogen removal, the progeny of the proliferating precursors can be differentiated into neurons, astrocytes and oligodendrocytes, which are the three primary cell types that are found in the adult mammalian CNS. Under these conditions, the growth-factor-responsive precursors can be expanded indefinitely with little change in their growth or differentiation characteristics. These results indicate the existence of an adult neural stem cell as these cells possess the fundamental stem-cell features of extensive self-renewal, generation of many progeny and the ability to give rise to the primary cell types of the tissue from which they were obtained.

of many progeny. Most importantly, when clonally derived, they could initiate new tumours when transplanted into the striatum of adult immunodeficient mice<sup>61</sup>. These tumours showed the classic *in vivo* features of human glioblastoma multiforme, having extensive migratory and infiltrative capacity, which indicated that the *in vitro* defined brain tumour stem cells could recapitulate the *in vivo* histological features of glioblastoma multiforme. In addition, stem-like cells could be re-isolated from these tumours and could re-establish secondary stem-cell lines with the same functional characteristics as the parental cell lines. Furthermore, following intracranial transplantation, these secondary brain tumour cells gave rise to new tumours, which demonstrated their self-renewal *in vivo*.

As this population of cells has the cardinal properties of stem cells, it seems likely that they are brain tumour stem cells<sup>61</sup>. Recently, a report from the Dirks group has described the presence of similar, *in vivo* self-renewing, CD133<sup>+</sup> cancer-initiating precursors in short-term neurosphere cultures that had been established from human glioblastoma multiforme and medulloblastoma<sup>55</sup>. Although it remains unclear which subset of the CD133<sup>+</sup> precursor pool can initiate tumour formation *in vivo*, the CD133<sup>+</sup> fraction was shown to lack any tumorigenic capacity. Despite the fact that the actual identity of the true tumour-initiating stem cells in both neurosphere cultures and AC133<sup>+</sup> populations

remains to be established conclusively, these findings clearly support the existence of brain tumour stem cells in human glioblastoma multiforme.

This field is expanding rapidly and new studies<sup>62,63</sup> are corroborating the view that the cancer-initiating cells in glioblastoma multiforme and medulloblastoma are brain tumour stem cells. Interestingly, this concept has now been extended to include other brain tumours, such as ependymomas<sup>64</sup>. It has been reported that multipotent CD133<sup>+</sup> cells, which show features of radial glia — the progenitors that are known to give rise to both ependymal cells and adult neural stem cells in the postnatal subventricular zone<sup>65</sup> — can be cultured from human ependymomas using the neurosphere assay<sup>64</sup>.

Several crucial considerations arise from these studies. The definition of brain tumour stem cells is often loosely applied, such that it includes cells of unknown or limited self-renewal and differentiation potential. Worryingly, the term might be applied to candidate cells in the absence of any reported cancer-initiating capability. This lack of rigour in the characterization of a putative brain tumour stem cell confuses the field as it groups cells with *bona fide* tumour stem-cell features together with those that do not satisfy these criteria. The undesired consequence of this situation is the allocation of divergent and contradictory properties to cells with different natures and identities that are then all called brain tumour stem cells.

We propose that the term brain tumour stem cell be applied only to cells with the cardinal features that are listed in BOX 3. The development of a rigorous definition and its application across the field would standardize and guide future work, allowing groups to compare and contrast their findings on the basis of reasonable and generally accepted criteria.

**The origin of brain tumour stem cells.** Different interpretations have been proposed about the nature of the neural cell type that is targeted by transformation and results in subsequent tumorigenesis. To date, evidence indicates that brain tumours might derive from the transformation of undifferentiated precursor cells, which are found not only in germinal regions of the developing and early-postnatal CNS — such as those that are involved in the genesis of the cerebellar external granular layer from which medulloblastoma develops<sup>66</sup> — but also in areas of the mature brain, in which neurogenesis persists throughout adulthood. Amongst these, the subventricular zone emerges as the most likely source of gliomas<sup>26</sup>. Many tumours develop near this region and exposure to oncogenic viruses or administration of carcinogens results in the preferential formation of tumours in germinal regions as opposed to the non-proliferative brain parenchyma<sup>26</sup>. Tumours arise with much greater frequency when carcinogens are administered in the subventricular zone rather than in the peripheral cortex<sup>67</sup>. This is further supported by the finding that tumours that are found in the white matter of dogs that have been exposed to avian sarcoma virus early in postnatal life originate in the subventricular zone and subsequently migrate to their final location<sup>68</sup>.

## Box 3 | Definition of brain tumour stem cells

Brain tumour cells should qualify as brain tumour stem cells if they are characterized by:

- Cancer-initiating ability upon orthotopic implantation (tumours should be a phenocopy of the tumour of origin)
- Extensive self-renewal ability, demonstrated either *ex vivo* (by showing both sequential-clonogenic and population-kinetic analyses<sup>37,61</sup>) or *in vivo* (by serial, orthotopic transplantation<sup>55,61</sup>)
- Karyotypic or genetic alterations
- Aberrant differentiation properties
- Capacity to generate non-tumorigenic end cells
- Multilineage differentiation capacity\*

\* Not a defining characteristic in all circumstances.

Recently, Parada and colleagues established a double-mutant mouse in which they combined mutations in tumour suppressor p53 (*Trp53*) and the neural-specific neurofibromatosis type 1 gene (*Nf1*), which activates Ras and therefore increases the formation of astrocytomas in humans. They suggested that some of the astrocytoma-like lesions that they observed developed within the subventricular zone<sup>69</sup>. Similarly, a series of classic studies proposed that deletion of tumour suppressors and/or activation of oncogenes, such as Ras and Akt, in undifferentiated nestin-expressing cells results in a higher frequency of tumour formation than such alterations in GFAP-expressing astrocytes<sup>70,71</sup>. Likewise, overexpression of platelet-derived growth factor- $\beta$  (PDGFR $\beta$ ) in either nestin-expressing progenitors or GFAP-expressing astrocytes caused a significant increase in the rate of glioma formation, with the highest frequency observed following nestin-directed targeting<sup>72</sup>. However, mature astroglia have also been shown to be more susceptible to oncogenic transformation when a more immature phenotype is targeted. The combined loss of the *CDKN2A* locus (which encodes the INK4a and ARF tumour suppressors) and the expression of constitutively active EGF receptor (EGFR) in mature astrocytes led to the formation of glioma-like lesions following intracranial transplantation<sup>73</sup>.

However, the observation that, in patients, the site of glioma origin is often distinct from the site where the tumour eventually develops might be explained by the hypothesis that a brain tumour stem cell, through asymmetric divisions, generates another brain tumour stem cell that remains within the subventricular zone, and a progenitor cell that migrates away to give rise to the tumour mass<sup>74</sup>.

In the same way, persistence of neurogenesis in the hippocampus throughout life entails the persistence of undifferentiated, mitotic neural precursors within this area. As these precursors are a probable target of tumorigenic transformation<sup>20</sup>, it remains unclear why there is currently no clear evidence of increased tumour frequency in the regions that are adjacent to the hippocampus. A possible explanation can be found in the recent observation that the actual neural stem cells that give rise to subgranular-zone neurons might reside outside the subgranular zone itself<sup>75,76</sup>.

These studies provide compelling evidence that mitotically active precursors are the most likely source of many brain tumours; however, the specific identity of these cells within the neurogenetic regions of the brain remains unresolved. It has been suggested that between four and seven independent mutations must occur within a normal somatic cell before a cancerous phenotype results<sup>5</sup>. Some of these alterations might be acquired early in development, predisposing certain adult cells to cancer<sup>77</sup>. Nonetheless, oncogenic mutations are rare, stochastic events, that are thought to accumulate over a considerable period of time. Transiently dividing progenitors exist only briefly before differentiating into cells that are often quiescent or die because of normal turnover or damage. Therefore, mutagenic events might not have the opportunity to accumulate in transiently dividing progenitors and their terminally differentiated progeny, as time spent in the transformation-prone phase is short and mutated cells might be discarded through differentiation and normal cell loss. Conversely, somatic stem cells are perennial cells with a significant proliferation and self-renewal potential that lasts the lifetime of the animal, making them a preferential target for tumorigenesis. It is thought that this might be the case in acute myeloid leukaemia and several solid-tissue malignancies<sup>78</sup>. However, as the transiently dividing progenitors are the immediate descendants of somatic stem cells, which will pass down their mutations, it is arguable that the rapidly and transiently dividing cells could accumulate additional tumour-promoting events, eventually leading to the transformation of these cells into cells with the properties of tumour stem cells (FIG. 2).

The role of transiently dividing progenitors (type C cells) as the possible source of brain tumour stem cells is supported by the finding that in the adult subventricular zone these progenitors express EGFR<sup>31</sup>. The activity of this receptor is altered in more than 50% of human gliomas<sup>79</sup> and its constitutive activation can cause glioma formation in the CNS<sup>73</sup>. Strikingly, *in vivo* exposure to EGFR ligands, such as transforming growth factor- $\alpha$  (TGF $\alpha$ ) or EGF<sup>31,80</sup>, produces the formation of tumour-like structures that protrude into the ventricle, and an aberrant and invasive pattern of neural cell proliferation. This leads to many progeny being displaced, throughout the CNS parenchyma, at significant distances away from the periventricular region<sup>80,81</sup>. *In vitro*, transiently dividing progenitors that are derived from the subventricular-zone population can revert to a stem-cell-like phenotype as they form neurospheres and show some proliferative ability. This supports the potential of this population to be a target for further oncogenic transformation<sup>31</sup>.

Intuitively, given the lack of an intrinsic self-renewal capacity and the ephemeral nature of transiently dividing progenitors, this indicates that the frequency with which they give rise to tumour stem cells is much lower than that of somatic stem cells, which retain a proliferative capacity throughout the lifetime of an animal. But this might not be the case — the size of the transiently dividing progenitor compartment is at least one order of magnitude larger than that of the somatic stem-cell compartment (FIG. 2), which

Nestin-expressing cells  
Undifferentiated neural  
precursors that express the  
neuroepithelial intermediate  
filament nestin.

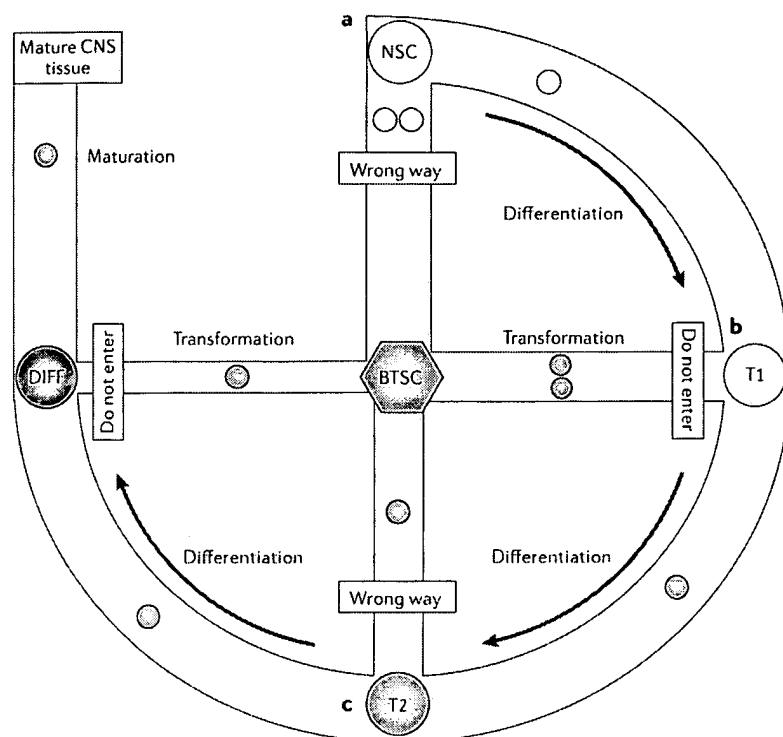


**Figure 4 | Neurogenetic compartments as developmental 'beltways'.** Brain tumour stem cells (BTSCs), despite the fact that they have stem-cell properties, might be derived from many of the mostly undifferentiated cells that are found in the neurogenetic areas of the adult brain. During this process, sequential cell lineages are generated that progressively acquire properties of greater differentiation. Therefore, cells in the neurogenetic process can be envisioned as rolling along a developmental 'beltway'. They start as neural stem cells (NSCs), which give rise to progressively maturer, transiently dividing progenitors (T1 and T2) until they leave the beltway (terminally differentiate: DIFF) to become either functional mature neurons or other cells. Throughout this process and at different stages of differentiation mistakes can occur, and cells on the beltway can enter some of the 'forbidden' beltway exits that, regardless of where they start, all lead to the same result: the formation of BTSCs. The widths of the horizontal and vertical arms that take cells from the beltway to their final BTSC fate become progressively narrower closer to the exit to the compartment of differentiated cells. This represents the fact that the more mature a cell is, the less likely it will turn into a BTSC.

increases the overall probability of cell transformation within the former population. This is particularly true in complex tissues that contain many mature cell types, as the dimensions of the transiently dividing progenitor compartment — and therefore the size of the pool of mitotically active cells — increase with the number of terminally differentiated cell lineages that are generated in a given tissue<sup>82</sup>. Most importantly, the de-differentiation of transiently dividing progenitors into somatic stem cells has been shown to occur under physiological conditions, both *in vivo* and *in vitro*, without the need for transformation<sup>31,83</sup>. Furthermore, although somatic stem cells have a lifelong proliferation potential, the global number of divisions that they undergo might not be any greater than that of the transiently dividing progenitor population, which expresses its full proliferative potential over a relatively short time. This concept is strengthened by the observation that forced cycling of haematopoietic

stem cells, either through serial transplantation or genetic disruption of key negative cell-cycle regulators, affects the functional integrity of stem cells over time. This indicates that, similar to transiently dividing progenitors, the total number of divisions that is allowed for somatic stem cells might be limited<sup>84,85</sup>.

Additional factors decrease the actual frequency at which somatic stem cells undergo transformation. For instance, Cairns proposed that somatic stem cells retain their original, or template, DNA strands at each cycle, thereby protecting themselves effectively against DNA-replication errors<sup>86</sup>. This immortal-strand hypothesis, as it has become known, has now found experimental support in studies of small-intestinal and neural stem cells<sup>87,88</sup>.

Therefore, it seems plausible that the anatomical origin of brain tumour stem cells might be in regions of the CNS that have the greatest degree of cell proliferation, such as the subventricular zone. The transformation of normal somatic stem cells or of their progeny, the transiently dividing cells, are equally conceivable hypotheses for the cellular origin of brain tumour stem cells within these proliferative zones (FIG. 4).

Although we think that brain tumour stem cells are best defined on the basis of functional competence rather than on the identity of the cell that underwent the original oncogenic transformation, the need to identify accurately the cellular origin of such stem cells is not superfluous. In fact, brain tumour stem cells are likely to retain many of their parental characteristics<sup>55,57,58,61,63</sup>. As adult neural stem cells and neural transiently dividing progenitors have specific functional, molecular and antigenic attributes (FIG. 2), these might be used to develop better classification and diagnostic assays, as heterogeneity exceeds the sensitivity of the current classification system<sup>89</sup>. These differential antigenic and molecular attributes might also be exploited to devise cell-enrichment procedures to establish nearly pure preparations of tumour-initiating cells, which might enable the identification of a more specific pathway to target for brain tumour therapy and the devising of exclusive immunotherapy approaches. Furthermore, they might lead to a more reliable identification of tumour-initiating stem cells and the development of novel and accurate assays that enable the number of true tumour stem cells in different brain tumours, or in the same brain tumour type from different patients, to be identified. The experimental and clinical benefits of these findings could be considerable. It is also imperative to define the functional, regulatory, molecular and antigenic features that distinguish normal from tumour stem cells. This will allow us to devise therapeutic strategies that specifically target the tumour population, but leave normal stem and precursor cells unharmed.

**Regulation of neural stem-cell division: insights into tumour stem-cell biology.** The finding that adult germinal, neural precursors might provide the origin of brain tumour stem cells indicates the presence of common regulatory pathways. There is evidence that the same key mechanisms that control the activity of

normal neurogenetic progenitors are altered in brain tumours. As this topic has recently been covered in a series of excellent articles<sup>26</sup>, here we provide only a brief overview of the most relevant pathways.

EGFR expression is upregulated during tumour formation, is correlated with malignancy and response to treatment<sup>79</sup>, and is considered a reliable marker for primary glioblastoma multiforme<sup>1</sup>. Similarly, FGFs, which have been shown to regulate neural stem-cell proliferation<sup>44,32</sup> and cell-fate commitment<sup>80</sup>, have been proposed as glioma-promoting autocrine factors that are involved in the proliferation of tumour cells<sup>91</sup> and the induction of angiogenesis<sup>92</sup>.

Likewise, overexpression of Notch receptors and their ligands Delta-like 1 (DLK1) and Jagged 1 (JAG1) correlates with the proliferative capacity of human glioma cells<sup>93</sup>. Therefore, Notch has been suggested to function as a positive effector of self-renewal in adult neural stem cells<sup>94,95</sup>.

Another gene that has recently been implicated in the regulation of self-renewal of normal neural stem cells<sup>96,97</sup> and in CNS tumorigenesis<sup>98</sup> is BMI1. This belongs to the Polycomb group of genes and has been shown to positively regulate cell proliferation and self-renewal through repression of the tumour suppressors INK4a and ARF<sup>96</sup>. Intriguingly, BMI1 expression is significantly increased in human medulloblastomas, directly linking the deregulation of BMI1-dependent self-renewal to tumour development<sup>98</sup>.

Similarly, Sonic Hedgehog (SHH) and its downstream effectors glioma-associated oncogene homologue 1 (GLI1), GLI2 and GLI3 have been shown to specifically regulate neurogenesis and self-renewal within the external granular layer of the early postnatal cerebellum and to control precursor proliferation in the adult subventricular zone<sup>99</sup>. Therefore, mutations in this pathway are directly implicated in the genesis of medulloblastoma<sup>100,101</sup>.

Other genes, the expression of which links normal regulation of neural stem cells to aberrant function in brain tumours, include PTEN and elements of the canonical Wnt- $\beta$ -catenin signalling pathway<sup>102,103</sup>. PTEN is a tumour suppressor with an important function in the control of proliferation of neural stem cells and progenitor cells *in vivo* and *in vitro*<sup>104</sup>. It has also been shown to control migration in the adult subventricular zone<sup>105</sup>. Importantly, PTEN is often inactivated in glioblastomas<sup>66,106</sup> and, as a result, maintenance of its expression has been closely associated with a favourable prognosis in patients with glioblastoma multiforme<sup>79</sup>.

Finally, the Wnt- $\beta$ -catenin pathway has recently been implicated in the regulation of adult neurogenesis<sup>107,108</sup>. Although a direct correlation between the deregulation of the Wnt regulatory system has been documented in the pathogenesis of medulloblastomas<sup>109</sup>, evidence for its involvement in gliomagenesis is less obvious. However, interfering with Wnt signalling through the ectopic expression of soluble Wnt modulators such as the secreted Frizzled-related proteins (sFRPs) has been shown to promote the growth of malignant glioma cells while inhibiting their invasive ability<sup>110</sup>.

## Perspectives

### *A new system for drug/target discovery and validation.*

The hallmarks of tumour cells are exacerbated proliferation and aberrant self-renewal, which indicates that cells from CNS cancers could be used to establish brain tumour stem-cell lines from adult human specimens. This possibility is true for brain tumour stem cells from glioblastoma multiforme and, to a much lesser extent, from medulloblastoma<sup>61</sup>, and it has considerable practical implications. Brain tumour stem cells, even at the single-cell level, have the genetic information that is required to generate a faithful phenocopy of the original tumour from which they are derived<sup>55,61</sup>. The increasing number of copies of the original brain tumour stem cells that are produced during serial subculturing generates a renewable and stable source of cancer-initiating cells that retain patient-specific features, such as growth characteristics, an aberrant differentiation phenotype and a specific molecular fingerprint<sup>61</sup>. These personalized brain tumour stem-cell lines can be used both as a means to identify novel molecular markers and as a source of material for patient-specific drug-screening protocols. We predict that these brain tumour stem-cell-based assays will result in a more meaningful and predictive model of the actual therapy responsiveness of brain tumours than the standard glioma cell lines that are currently available.

**A new target.** The discovery of putative brain tumour stem cells identifies a new cellular target that might be amenable to novel or traditional treatments.

One feature that contributes to the ability of a stem cell to survive throughout the lifespan of an animal is its inherent resistance to drugs and toxins. A peculiarity of many stem-cell populations is their relatively high expression of ATP-binding cassette (ABC) drug transporters, which can protect cells from cytotoxic agents<sup>111</sup>. Haematopoietic stem cells have been isolated on the basis of their expression of these transporters and their ability to efflux the fluorescent dye Hoechst 33342, which give them a unique profile, referred to as the side population, when analysed by flow cytometry. Side-population cells have also been isolated from the CNS<sup>54</sup>. Although somatic and tumour stem cells can be identified within the side population, not all of the stem-cell population is contained within this group, nor does the side population contain a pure stem-cell population, therefore negating the use of this technique as a method to purify tumour stem cells. However, the presence of drug-resistance genes in the tumour population and their non-selective expression in a putative tumour stem-cell population indicates the hypothetical possibility that drug resistance and, in particular, tumour recurrence might be related to the inability of cytotoxic compounds to eliminate the tumour-initiating cells. The next generation of chemotherapy agents might be a combination of chemosensitizers and cytotoxic agents that alters ABC-transporter activity, leading to better clinical outcomes<sup>111</sup>.



**Normal stem cells to target tumour stem cells?** A particularly innovative approach indicates that normal neural stem cells can be used to target and deliver molecules to CNS tumours<sup>112</sup>. Endogenous neural stem cells<sup>113</sup>, as well as neural stem cells that have been engineered to secrete interleukin 4 (IL-4)<sup>114</sup>, IL-12 (REF. 115) or a fragment of metalloproteinase-2 called PEX<sup>116</sup>, can produce tumour regression and increase survival in experimental intracranial gliomas. Similarly, immortalized neural stem cells that were placed near the tumour or at a distant site through intravascular delivery could migrate towards and integrate with the previously implanted tumour cells<sup>117</sup>. The transplanted neural stem cells surrounded the expanding tumour mass, even seeking out and attaching to the infiltrating tumour cells. Furthermore, migratory, tumour-seeking neural stem cells could be genetically engineered to deliver a therapeutically relevant molecule. This intriguing approach has been confirmed with other neural precursors<sup>118,119</sup> and the tropism of these cells for glioblastoma multiforme cells has been shown to be dependent on the vascular endothelial growth factor (VEGF) that is secreted by these cells<sup>120</sup> and on their expression of the chemokine receptor CXCR4 (REF. 121). It should be noted that the strategy of using neural stem cells and progenitor cells as 'Trojan horses' with anti-glioma homing capacity has, to date, only been shown using experimentally implanted cell lines and that the same phenomenon ought also to be demonstrated with tumours that arise spontaneously in the brain. This notwithstanding, this innovative approach might prove useful not only for

the site-specific delivery of cytotoxic agents or virally mediated genetic elements, but also for the widespread release of molecules that regulate the proliferation, differentiation and migration of the tumour stem cells.

## Conclusions

The discovery that brain tumours, particularly glioblastoma multiforme, contain tumour-founding cells with the defining features of neural stem cells strongly indicates that immature precursors within neurogenic areas represent the cellular origin of brain tumour stem cells. The latter ought not to be exclusively viewed as the result of transformation of normal neural stem cells, as our knowledge of the mechanisms that regulate adult neurogenesis indicates that it is equally likely that brain tumour stem cells might derive from transiently dividing progenitors. According to this view, and while we await the identification of specific brain tumour stem-cell-lineage antigens, it seems reasonable to define brain tumour stem cells as cancer-initiating precursors that show defining stem-cell properties and, principally, a long-term capacity for self-renewal *in vitro* or *in vivo*. The tumours that are generated from these cells must be a faithful, possibly patient-specific, phenocopy of the original neoplasia (BOX 3). The capacity to culture brain tumour stem cells *in vitro* might give us an opportunity to devise new and more-specific therapeutic approaches to target incurable brain tumours.

There is hope that the identification of brain tumour stem cells as possibly the long-sought culprit in brain cancers might revolutionize the way that we approach brain tumour physiology, diagnosis and therapy.

- Behin, A., Hoang-Xuan, K., Carpentier, A. F. & Delattre, J. Y. Primary brain tumours in adults. *Lancet* **361**, 323–331 (2003).
- Stupp, R. *et al.* Radiotherapy plus concomitant and adjuvant temozolomide for glioblastoma. *N. Engl. J. Med.* **352**, 987–996 (2005).
- Holland, E. C. Glioblastoma multiforme: the terminator. *Proc. Natl Acad. Sci. USA* **97**, 6242–6244 (2000).
- Ellison, D. Classifying the medulloblastoma: insights from morphology and molecular genetics. *Neuropathol. Appl. Neurobiol.* **28**, 257–282 (2002).
- Hanahan, D. & Weinberg, R. A. The hallmarks of cancer. *Cell* **100**, 57–70 (2000).
- Reya, T., Morrison, S. J., Clarke, M. F. & Weissman, I. L. Stem cells, cancer, and cancer stem cells. *Nature* **414**, 105–111 (2001).
- Bonnet, D. & Dick, J. E. Human acute myeloid leukemia is organized as a hierarchy that originates from a primitive hematopoietic cell. *Nature Med.* **3**, 730–737 (1997).  
**Describes for the first time the identification of stem-like cells in haematopoietic malignancies.**
- Hope, K. J., Jin, L. & Dick, J. E. Acute myeloid leukemia originates from a hierarchy of leukemic stem cell classes that differ in self-renewal capacity. *Nature Immunol.* **5**, 738–743 (2004).
- Al-Hajj, M., Wicha, M. S., Benito-Hernandez, A., Morrison, S. J. & Clarke, M. F. Prospective identification of tumorigenic breast cancer cells. *Proc. Natl Acad. Sci. USA* **100**, 3983–3988 (2003).
- Altman, J. & Das, G. D. Autoradiographic and histological evidence of postnatal hippocampal neurogenesis in rats. *J. Comp. Neurol.* **124**, 319–335 (1965).
- Altman, J. Proliferation and migration of undifferentiated precursor cells in the rat during postnatal gliogenesis. *Exp. Neurol.* **16**, 263–278 (1966).
- Dacey, M. L. & Wallace, R. B. Postnatal neurogenesis in the feline cerebellum: a structural-functional investigation. *Acta Neurobiol. Exp. (Wars.)* **34**, 253–263 (1974).
- Sell, S. Stem cell origin of cancer and differentiation therapy. *Crit. Rev. Oncol. Hematol.* **51**, 1–28 (2004).
- Nottebohm, F. The road we travelled: discovery, choreography, and significance of brain replaceable neurons. *Ann. N. Y. Acad. Sci.* **1016**, 628–658 (2004).
- Reynolds, B. A. & Weiss, S. Generation of neurons and astrocytes from isolated cells of the adult mammalian central nervous system. *Science* **255**, 1707–1710 (1992).  
**Reports the initial evidence that multipotent neural stem cells that reside in the adult rodent brain can be identified and isolated *in vitro* following mitogen stimulation.**
- Gould, E., McEwen, B. S., Tanapat, P., Galea, L. A. & Fuchs, E. Neurogenesis in the dentate gyrus of the adult tree shrew is regulated by psychosocial stress and NMDA receptor activation. *J. Neurosci.* **17**, 2492–2498 (1997).
- Gould, E., Tanapat, P., McEwen, B. S., Flugge, G. & Fuchs, E. Proliferation of granule cell precursors in the dentate gyrus of adult monkeys is diminished by stress. *Proc. Natl Acad. Sci. USA* **95**, 3168–3171 (1998).
- Eriksson, P. S. *et al.* Neurogenesis in the adult human hippocampus. *Nature Med.* **4**, 1313–1317 (1998).
- Lie, D. C., Song, H., Colaninno, S. A., Ming, G. L. & Gage, F. H. Neurogenesis in the adult brain: new strategies for central nervous system diseases. *Annu. Rev. Pharmacol. Toxicol.* **44**, 399–421 (2004).
- Ming, G. L. & Song, H. Adult neurogenesis in the mammalian central nervous system. *Annu. Rev. Neurosci.* **28**, 223–250 (2005).
- Loeffler, M. and Potten, C. in *Stem Cells and Cellular Pedigrees — A Conceptual Introduction*. (ed. Potten, C.) Ch. 1 (Academic Press, London, 1997).
- Passegue, E. J. C., Ailles, L. E. & Weissman, I. L. Normal and leukemic hematopoiesis: are leukemias a stem cell disorder or a reacquisition of stem cell characteristics? *Proc. Natl Acad. Sci. USA* **100**, 11842–11849 (2003).
- Doetsch, F., Caille, L., Lim, D. A., Garcia-Verdugo, J. M. & Alvarez-Buylla, A. Subventricular zone astrocytes are neural stem cells in the adult mammalian brain. *Cell* **97**, 703–716 (1999).  
**Results in this paper show that the bona fide subventricular-zone stem cell is the type B cell, which shows features of a differentiated astrocyte.**
- Morshead, C. M. *et al.* Neural stem cells in the adult mammalian forebrain: a relatively quiescent subpopulation of subependymal cells. *Neuron* **13**, 1071–1082 (1994).
- Sanai, N. *et al.* Unique astrocyte ribbon in adult human brain contains neural stem cells but lacks chain migration. *Nature* **427**, 740–744 (2004).  
**Provides the first evidence of the existence of neural stem cells in the subventricular zone of the adult human brain, and highlights the differences from the same compartment in rodents and the implications for the origin of brain tumours.**
- Sanai, N., Alvarez-Buylla, A. & Berger, M. S. Neural stem cells and the origin of gliomas. *N. Engl. J. Med.* **353**, 811–822 (2005).
- Quinones-Hinojosa, A. *et al.* Cellular composition and cytoarchitecture of the adult human subventricular zone: A niche of neural stem cells. *J. Comp. Neurol.* **494**, 415–434 (2006).
- Seri, B., Garcia-Verdugo, J. M., McEwen, B. S. & Alvarez-Buylla, A. Astrocytes give rise to new neurons in the adult mammalian hippocampus. *J. Neurosci.* **21**, 7153–7160 (2001).

29. Seri, B., Garcia-Verdugo, J. M., Collado-Morente, L., McEwen, B. S. & Alvarez-Buylla, A. Cell types, lineage, and architecture of the germinal zone in the adult dentate gyrus. *J. Comp. Neurol.* **478**, 359–378 (2004).
30. Roy, N. S. *et al.* *In vitro* neurogenesis by progenitor cells isolated from the adult human hippocampus. *Nature Med.* **6**, 271–277 (2000).
31. Doetsch, F., Petreanu, L., Caille, I., Garcia-Verdugo, J. M. & Alvarez-Buylla, A. EGF converts transit-amplifying neurogenic precursors in the adult brain into multipotent stem cells. *Neuron* **36**, 1021–1034 (2002).
32. Gritti, A. *et al.* Multipotential stem cells from the adult mouse brain proliferate and self-renew in response to basic fibroblast growth factor. *J. Neurosci.* **16**, 1091–1100 (1996).
33. Gritti, A. *et al.* Epidermal and fibroblast growth factors behave as mitogenic regulators for a single multipotent stem cell-like population from the subventricular region of the adult mouse forebrain. *J. Neurosci.* **19**, 3287–3297 (1999).
34. Reynolds, B. A. & Rietze, R. L. Neural stem cells and neurospheres — re-evaluating the relationship. *Nature Methods* **2**, 333–336 (2005).
35. Reynolds, B. A. & Weiss, S. Clonal and population analyses demonstrate that an EGF-responsive mammalian embryonic CNS precursor is a stem cell. *Dev. Biol.* **175**, 1–13 (1996).
36. Vescovi, A. L. *et al.* Isolation and cloning of multipotential stem cells from the embryonic human CNS and establishment of transplantable human neural stem cell lines by epigenetic stimulation. *Exp. Neurol.* **156**, 71–83 (1999).
37. Galli, R. *et al.* Emx2 regulates the proliferation of stem cells of the adult mammalian central nervous system. *Development* **129**, 1633–1644 (2002).
38. Parras, C. M. *et al.* Mash1 specifies neurons and oligodendrocytes in the postnatal brain. *EMBO J.* **23**, 4495–4505 (2004).
39. Soria, J. M. *et al.* Defective postnatal neurogenesis and disorganization of the rostral migratory stream in absence of the *Vox1* homeobox gene. *J. Neurosci.* **24**, 11171–11181 (2004).
40. Weiss, S. *et al.* Multipotent CNS stem cells are present in the adult mammalian spinal cord and ventricular neuroaxis. *J. Neurosci.* **16**, 7599–7609 (1996).
41. Gritti, A. *et al.* Multipotent neural stem cells reside into the rostral extension and olfactory bulb of adult rodents. *J. Neurosci.* **22**, 437–445 (2002).
42. Svendsen, C. N., Caldwell, M. A. & Ostenfeld, T. Human neural stem cells: isolation, expansion and transplantation. *Brain Pathol.* **9**, 499–513 (1999).
43. Uchida, N. *et al.* Direct isolation of human central nervous system stem cells. *Proc. Natl Acad. Sci. USA* **97**, 14720–14725 (2000).
44. Palmer, T. D., Markakis, E. A., Willhoite, A. R., Safar, F. & Gage, F. H. Fibroblast growth factor-2 activates a latent neurogenic program in neural stem cells from diverse regions of the adult CNS. *J. Neurosci.* **19**, 8487–8497 (1999).
45. Zhao, M. *et al.* Evidence for neurogenesis in the adult mammalian substantia nigra. *Proc. Natl Acad. Sci. USA* **100**, 7925–7930 (2003).
46. Zhang, X., Klueber, K. M., Guo, Z., Lu, C. & Roisen, F. J. Adult human olfactory neural progenitors cultured in defined medium. *Exp. Neurol.* **186**, 112–123 (2004).
47. Consiglio, A. *et al.* Robust *in vivo* gene transfer into adult mammalian neural stem cells by lentiviral vectors. *Proc. Natl Acad. Sci. USA* **101**, 14835–14840 (2004).
48. Markakis, E. A., Palmer, T. D., Randolph-Moore, L., Rakic, P. & Gage, F. H. Novel neuronal phenotypes from neural progenitor cells. *J. Neurosci.* **24**, 2886–2897 (2004).
49. Toma, J. C., McKenzie, I. A., Bagli, D. & Miller, F. D. Isolation and characterization of multipotent skin-derived precursors from human skin. *Stem Cells* **23**, 727–737 (2005).
50. Messina, E. *et al.* Isolation and expansion of adult cardiac stem cells from human and murine heart. *Circ. Res.* **95**, 911–921 (2004).
51. Dontu, G. *et al.* *In vitro* propagation and transcriptional profiling of human mammary stem/progenitor cells. *Genes Dev.* **17**, 1253–1270 (2003).
52. Rietze, R. L. *et al.* Purification of a pluripotent neural stem cell from the adult mouse brain. *Nature* **412**, 736–739 (2001).
53. Capela, A. & Temple, S. LeX/sox-1 is expressed by adult mouse CNS stem cells, identifying them as non-ependymal. *Neuron* **35**, 865–875 (2002).
54. Kim, M. & Morshead, C. M. Distinct populations of forebrain neural stem and progenitor cells can be isolated using side-population analysis. *J. Neurosci.* **23**, 10703–10709 (2003).
55. Singh, S. K. *et al.* Identification of human brain tumour initiating cells. *Nature* **432**, 396–401 (2004). Shows that only CD133<sup>+</sup> human brain tumour cells are endowed with tumour-initiating capacity *in vivo*.
56. Ignatova, T. N. *et al.* Human cortical glial tumors contain neural stem-like cells expressing astroglial and neuronal markers *in vitro*. *Glia* **39**, 193–206 (2002).
57. Singh, S. K. *et al.* Identification of a cancer stem cell in human brain tumors. *Cancer Res.* **63**, 5821–5828 (2003).
58. Hemmati, H. D. *et al.* Cancerous stem cells can arise from pediatric brain tumors. *Proc. Natl Acad. Sci. USA* **100**, 15178–15183 (2003).
59. Corbeil, D., Roper, K., Weigmann, A. & Huttner, W. B. AC133 hematopoietic stem cell antigen: human homologue of mouse kidney prominin or distinct member of a novel protein family? *Blood* **91**, 2625–2626 (1998).
60. Tamaki, S. *et al.* Engraftment of sorted/expanded human central nervous system stem cells from fetal brain. *J. Neurosci. Res.* **69**, 976–986 (2002).
61. Galli, R. *et al.* Isolation and characterization of tumorigenic, stem-like neural precursors from human glioblastoma. *Cancer Res.* **64**, 7011–7021 (2004).
62. Tunic, P. *et al.* Genetic alterations and *in vivo* tumorigenicity of neurospheres derived from an adult glioblastoma. *Mol. Cancer* **3**, 25 (2004).
63. Yuan, X. *et al.* Isolation of cancer stem cells from adult glioblastoma multiforme. *Oncogene* **23**, 9392–9400 (2004).
64. Taylor, M. D. *et al.* Radial glia cells are candidate stem cells of ependymoma. *Cancer Cell* **8**, 323–335 (2005).
65. Merkle, F. T., Trumontin, A. D., Garcia-Verdugo, J. M. & Alvarez-Buylla, A. Radial glia give rise to adult neural stem cells in the subventricular zone. *Proc. Natl Acad. Sci. USA* **101**, 17528–17532 (2004).
66. Wechsler-Reya, R. & Scott, M. P. The developmental biology of brain tumors. *Annu. Rev. Neurosci.* **24**, 385–428 (2001).
67. Hopewell, J. W. & Wright, E. A. The importance of implantation site in cerebral carcinogenesis in rats. *Cancer Res.* **29**, 1927–1931 (1969).
68. Vick, N. A., Lin, M. J. & Bigner, D. D. The role of the subependymal plate in glial tumorigenesis. *Acta Neuropathol.* **40**, 63–71 (1977).
69. Zhu, Y. *et al.* Early inactivation of p53 tumor suppressor gene cooperating with NF1 loss induces malignant astrocytoma. *Cancer Cell* **8**, 119–130 (2005).
70. Holland, E. C. *et al.* Combined activation of Ras and Akt in neural progenitors induces glioblastoma formation in mice. *Nature Genet.* **25**, 55–57 (2000). Shows that cell-specific deregulation of oncogenic pathways leads to the development of glial tumours that arise from nestin-positive progenitors but not from differentiated astrocytes.
71. Holland, E. C., Hively, W. P., Gallo, V. & Varmus, H. E. Modeling mutations in the G1 arrest pathway in human gliomas: overexpression of CDK4 but not loss of INK4a-ARF induces hyperploidy in cultured mouse astrocytes. *Genes Dev.* **12**, 3644–3649 (1998).
72. Dai, C. *et al.* PDGF autocrine stimulation dedifferentiates cultured astrocytes and induces oligodendrogliomas and oligoastrocytomas from neural progenitors and astrocytes *in vivo*. *Genes Dev.* **15**, 1913–1925 (2001).
73. Bachoo, R. M. *et al.* Epidermal growth factor receptor and Ink4a/Arf: convergent mechanisms governing terminal differentiation and transformation along the neural stem cell to astrocyte axis. *Cancer Cell* **1**, 269–277 (2002).
74. Berger, F., Gay, E., Pelletier, L., Tropel, P. & Wion, D. Development of gliomas: potential role of asymmetrical cell division of neural stem cells. *Lancet Oncol.* **5**, 511–514 (2004).
75. Seaberg, R. M. & van der Kooy, D. Adult rodent neurogenic regions: the ventricular subependyma contains neural stem cells, but the dentate gyrus contains restricted progenitors. *J. Neurosci.* **22**, 1784–1793 (2002).
76. Bull, N. D. & Bartlett, P. F. The adult mouse hippocampal progenitor is neurogenic but not a stem cell. *J. Neurosci.* **25**, 10815–10821 (2005).
77. Frank, S. A. & Nowak, M. A. Cell biology: Developmental predisposition to cancer. *Nature* **422**, 494 (2003).
78. Huntly, B. J. & Gilliland, D. G. Leukaemia stem cells and the evolution of cancer-stem-cell research. *Nature Rev. Cancer* **5**, 311–321 (2005).
79. Mellingerhoff, I. K. *et al.* Molecular determinants of the response of glioblastomas to EGFR kinase inhibitors. *N. Engl. J. Med.* **353**, 2012–2024 (2005).
80. Kuhn, H. C., Winkler, J., Kempermann, G., Thal, L. J. & Gage, F. H. Epidermal growth factor and fibroblast growth factor-2 have different effects on neural progenitors in the adult rat brain. *J. Neurosci.* **17**, 5820–5829 (1997).
81. Craig, C. G. *et al.* *In vivo* growth factor expansion of endogenous subependymal neural precursor cell populations in the adult mouse brain. *J. Neurosci.* **16**, 2649–2658 (1996).
82. Potten, C. S., Booth, C. & Hargreaves, D. The small intestine as a model for evaluating adult tissue stem cell drug targets. *Cell Prolif.* **36**, 115–129 (2003).
83. Potten, C. S. & Loeffler, M. Stem cells: attributes, cycles, spirals, pitfalls and uncertainties. Lessons for and from the crypt. *Development* **110**, 1001–1020 (1990). Provides a fundamental introduction to the general concept of stem cells by describing the properties of the stem-cell compartment that is localized within the intestinal crypt.
84. Ross, E. A., Anderson, N. & Micklem, H. S. Serial depletion and regeneration of the murine hematopoietic system. Implications for hematopoietic organization and the study of cellular aging. *J. Exp. Med.* **155**, 432–444 (1982).
85. Hock, H. *et al.* Gfi-1 restricts proliferation and preserves functional integrity of haematopoietic stem cells. *Nature* **431**, 1002–1007 (2004).
86. Cairns, J. Mutation selection and the natural history of cancer. *Nature* **255**, 197–200 (1975).
87. Potten, C. S., Owen, G. & Booth, D. Intestinal stem cells protect their genome by selective segregation of template DNA strands. *J. Cell Sci.* **115**, 2381–2388 (2002).
88. Karpowicz, P. *et al.* Support for the immortal strand hypothesis: neural stem cells partition DNA asymmetrically *in vitro*. *J. Cell Biol.* **170**, 721–732 (2005).
89. Louis, D. N., Holland, E. C. & Cairncross, J. G. Glioma classification: a molecular reappraisal. *Am. J. Pathol.* **159**, 779–786 (2001).
90. Vescovi, A. L., Reynolds, B. A., Fraser, D. D. & Weiss, S. bFGF regulates the proliferative fate of unipotent (neural) and bipotent (neural/astroglial) EGF-generated CNS progenitor cells. *Neuron* **11**, 951–966 (1993).
91. Joy, A. *et al.* Nuclear accumulation of FGF-2 is associated with proliferation of human astrocytes and glioma cells. *Oncogene* **14**, 171–183 (1997).
92. Auguste, P. *et al.* Inhibition of fibroblast growth factor/fibroblast growth factor receptor activity in glioma cells impedes tumor growth by both angiogenesis-dependent and -independent mechanisms. *Cancer Res.* **61**, 1717–1726 (2001).
93. Purow, B. W. *et al.* Expression of Notch-1 and its ligands, Delta-like-1 and Jagged-1, is critical for glioma cell survival and proliferation. *Cancer Res.* **65**, 2353–2363 (2005).
94. Hitoshi, S. *et al.* Notch pathway molecules are essential for the maintenance, but not the generation, of mammalian neural stem cells. *Genes Dev.* **16**, 846–858 (2002).
95. Shen, Q. *et al.* Endothelial cells stimulate self-renewal and expand neurogenesis of neural stem cells. *Science* **304**, 1338–1340 (2004).
96. Molofsky, A. V. *et al.* Bmi-1 dependence distinguishes neural stem cell self-renewal from progenitor proliferation. *Nature* **425**, 962–967 (2003).
97. Bruggeman, S. W. *et al.* Ink4a and Arf differentially affect cell proliferation and neural stem cell self-renewal in Bmi-1-deficient mice. *Genes Dev.* **19**, 1438–1443 (2005).
98. Leung, C. *et al.* Bmi-1 is essential for cerebellar development and is overexpressed in human medulloblastomas. *Nature* **428**, 337–341 (2004).
99. Palma, V. *et al.* Sonic hedgehog controls stem cell behavior in the postnatal and adult brain. *Development* **132**, 335–344 (2005).
100. Goodrich, L. V., Milenkovic, L., Higgins, K. M. & Scott, M. P. Altered neural cell fates and medulloblastoma in mouse patched mutants. *Science* **277**, 1109–1113 (1997).

101. Pomeroy, S. L. *et al.* Prediction of central nervous system embryonal tumour outcome based on gene expression. *Nature* **415**, 436–442 (2002).
102. Baker, S. J. & McKinnon, P. J. Tumour-suppressor function in the nervous system. *Nature Rev. Cancer* **4**, 184–196 (2004).
103. Reya, T. & Clevers, H. Wnt signalling in stem cells and cancer. *Nature* **434**, 843–850 (2005).
104. Groszer, M. *et al.* Negative regulation of neural stem/progenitor cell proliferation by the *Pten* tumor suppressor gene *in vivo*. *Science* **294**, 2186–2189 (2001).
105. Li, L. *et al.* PTEN in neural precursor cells: regulation of migration, apoptosis, and proliferation. *Mol. Cell. Neurosci.* **20**, 21–29 (2002).
106. Rasheed, B. K., Wiltshire, R. N., Bigner, S. H. & Bigner, D. D. Molecular pathogenesis of malignant gliomas. *Curr. Opin. Oncol.* **11**, 162–167 (1999).
107. Chenn, A. & Walsh, C. A. Increased neuronal production, enlarged forebrains and cytoarchitectural distortions in  $\beta$ -catenin overexpressing transgenic mice. *Cereb. Cortex* **13**, 599–606 (2003).
108. Lie, D. C. *et al.* Wnt signalling regulates adult hippocampal neurogenesis. *Nature* **437**, 1370–1375 (2005).
109. Marino, S. Medulloblastoma: developmental mechanisms out of control. *Trends Mol. Med.* **11**, 17–22 (2005).
110. Roth, W. *et al.* Secreted Frizzled-related proteins inhibit motility and promote growth of human malignant glioma cells. *Oncogene* **19**, 4210–4220 (2000).
111. Dean, M., Fojo, T. & Bates, S. Tumour stem cells and drug resistance. *Nature Rev. Cancer* **5**, 275–284 (2005).
112. Shah, K. *et al.* Glioma therapy and real-time imaging of neural precursor cell migration and tumor regression. *Ann. Neurol.* **57**, 34–41 (2005).
113. Glass, R. *et al.* Glioblastoma-induced attraction of endogenous neural precursor cells is associated with improved survival. *J. Neurosci.* **25**, 2637–2646 (2005).
114. Benedetti, S. *et al.* Gene therapy of experimental brain tumors using neural progenitor cells. *Nature Med.* **6**, 447–450 (2000).  
**Shows that implantation in established glial tumours of neural stem/progenitor cells that have been engineered to secrete IL-4 elicits a strong anti-tumour effect.**
115. Ehteshami, M. *et al.* The use of interleukin 12-secreting neural stem cells for the treatment of intracranial glioma. *Cancer Res.* **62**, 5657–5663 (2002).
116. Kim, S. K. *et al.* PEX-producing human neural stem cells inhibit tumor growth in a mouse glioma model. *Clin. Cancer Res.* **11**, 5965–5970 (2005).
117. Aboody, K. S. *et al.* Neural stem cells display extensive tropism for pathology in adult brain: evidence from intracranial gliomas. *Proc. Natl Acad. Sci. USA* **97**, 12846–12851 (2000).  
**The first demonstration that distally implanted somatic neural stem cells can migrate considerable distances and target previously established tumours, including tumour cells that have infiltrated surrounding tissue.**
118. Zhang, Z. G. *et al.* Magnetic resonance imaging and neurosphere therapy of stroke in rat. *Ann. Neurol.* **53**, 259–263 (2003).
119. Tang, Y. *et al.* *In vivo* tracking of neural progenitor cell migration to glioblastomas. *Hum. Gene Ther.* **14**, 1247–1254 (2003).
120. Schmidt, N. O. *et al.* Brain tumor tropism of transplanted human neural stem cells is induced by vascular endothelial growth factor. *Neoplasia* **7**, 623–629 (2005).
121. Ehteshami, M. *et al.* Glioma tropic neural stem cells consist of astrocytic precursors and their migratory capacity is mediated by CXCR4. *Neoplasia* **6**, 287–293 (2004).

## Acknowledgements

We are grateful to S. Piccirillo for valuable help with the preparation of this manuscript and to R. Rietze and M. De Palma for their useful suggestions and comments.

## Competing interests statement

The authors declare competing financial interests: see web version for details.

## DATABASES

The following terms in this article are linked online to:

Entrez Gene: <http://www.ncbi.nlm.nih.gov/entrez/query.fcgi?db=gene>  
 BMI1 | CDKN2A | CXCR4 | DLK1 | EGF | EGFR | FGF2 | GFAP | GLI1 | GLI2 | GLI3 | IL-12 | IL-4 | JAG1 | Musashi 1 | Nf1 | PDGFR | PTEN | SHH | SOX2 | TGF $\alpha$  | Trp53 | VEGF  
 National Cancer Institute: <http://www.cancer.gov>  
 brain tumours

## FURTHER INFORMATION

International Society for Stem Cell Research: <http://www.isscr.org>

Access to this links box is available online.

# Sonic hedgehog controls stem cell behavior in the postnatal and adult brain

Verónica Palma<sup>1,\*†</sup>, Daniel A. Lim<sup>2,\*</sup>, Nadia Dahmane<sup>1,\*‡</sup>, Pilar Sánchez<sup>1,3,\*§</sup>, Thomas C. Brionne<sup>4,\*</sup>, Claudia D. Herzberg<sup>4,\*</sup>, Yorick Gitton<sup>1,¶</sup>, Alan Carleton<sup>4</sup>, Arturo Álvarez-Buylla<sup>2</sup> and Ariel Ruiz i Altaba<sup>1,3,\*\*</sup>

<sup>1</sup>The Skirball Institute, NYU School of Medicine, 540 First Avenue, New York, NY 10016, USA

<sup>2</sup>Neurosurgery Research, UCSF, 10 Kirkham Street, San Francisco, CA 94143, USA

<sup>3</sup>University of Geneva Medical School, 8242 CMU, 1 rue Michel Servet, 1211 Geneva 4, Switzerland

<sup>4</sup>Brain and Mind Institute, EPFL, Bat AAB, 1015 Lausanne, Switzerland

\*These authors contributed equally to this work

<sup>†</sup>Present address: Laboratorio de Biología del Desarrollo, Departamento de Biología, Universidad de Chile, Las Encinas 3370, Edificio Milenio piso 3, MACUL, Santiago, Chile

<sup>‡</sup>Present address: The Wistar Institute, 3601 Spruce Street, Philadelphia, PA 19104, USA

<sup>§</sup>Present address: Departament de Biologia Cel·lular, Universitat de València, Facultat de Ciències Biològiques, Ed B, 4 planta, c/Dr Moliner, s/n 46100 Burjassot, València, Spain

<sup>¶</sup>Present address: Ecole Normale Supérieure, 46 rue d'Ulm, 75230 Paris Cedex 05 Paris, France

\*\*Author for correspondence (e-mail: ariel.ruizaltaba@medecine.unige.ch)

Accepted 8 November 2004

Development 132, 335–344

Published by The Company of Biologists 2005

doi:10.1242/dev.01567

## Summary

Sonic hedgehog (Shh) signaling controls many aspects of ontogeny, orchestrating congruent growth and patterning. During brain development, Shh regulates early ventral patterning while later on it is critical for the regulation of precursor proliferation in the dorsal brain, namely in the neocortex, tectum and cerebellum. We have recently shown that Shh also controls the behavior of cells with stem cell properties in the mouse embryonic neocortex, and additional studies have implicated it in the control of cell proliferation in the adult ventral forebrain and in the hippocampus. However, it remains unclear whether it regulates adult stem cell lineages in an equivalent manner. Similarly, it is not known which cells respond to Shh signaling in stem cell niches. Here we demonstrate that Shh is required for cell proliferation in the mouse forebrain's subventricular zone (SVZ) stem cell niche and for the production of new olfactory interneurons *in vivo*. We

identify two populations of Gli1<sup>+</sup> Shh signaling responding cells: GFAP<sup>+</sup> SVZ stem cells and GFAP<sup>−</sup> precursors. Consistently, we show that Shh regulates the self-renewal of neurosphere-forming stem cells and that it modulates proliferation of SVZ lineages by acting as a mitogen in cooperation with epidermal growth factor (EGF). Together, our data demonstrate a critical and conserved role of Shh signaling in the regulation of stem cell lineages in the adult mammalian brain, highlight the subventricular stem cell astrocytes and their more abundant derived precursors as *in vivo* targets of Shh signaling, and demonstrate the requirement for Shh signaling in postnatal and adult neurogenesis.

Key words: Mouse, Stem cell, Brain, Hedgehog, Gli, Subventricular zone

## Introduction

Neurogenesis in the adult mammalian brain takes place in the subventricular zone (SVZ) of the lateral ventricular walls of the forebrain and in the subgranular layer of the dentate gyrus of the hippocampus (reviewed by Temple and Alvarez-Buylla, 1999; Taupin and Gage, 2002). In the adult SVZ, periventricular astrocytes (B cells) have been proposed to act as stem cells (Doetsch et al., 1999; Capela and Temple, 2002) and generate rapidly dividing transit amplifying (C) cells, which in turn generate migratory neuroblasts (A cells) which then join the rostral migratory stream to reach their final destination in the olfactory bulb where they differentiate into functional interneurons (Lois and Alvarez-Buylla, 1994; Doetsch et al., 1999; Alvarez-Buylla et al., 2002; Carleton et al., 2003).

The secreted factor Shh plays multiple roles in the formation

of the CNS, including the regulation of early ventral pattern in the neural tube (Jessell and Sanes, 2000) and of later precursor proliferation in the dorsal brain (Dahmane and Ruiz i Altaba, 1999; Weschler-Reya and Scott, 1999; Wallace, 1999; Dahmane et al., 2001) (reviewed by Ruiz i Altaba et al., 2002). This and the finding that Shh regulates the behavior of cells with stem cell properties in the developing embryonic neocortex (Palma and Ruiz i Altaba, 2004) led us to investigate its possible involvement in the control of stem cell lineages in the postnatal and adult forebrain SVZ, the best studied stem cell niche in the adult mammalian brain (Alvarez-Buylla et al., 2002).

Here we show that SVZ cells express *Shh* and *Gli1* and that blockage of hedgehog (Hh) signaling in adult and perinatal mice results in diminished expression of *Gli1* and deficits in SVZ cell proliferation *in vivo*. Our data are consistent with the

phenotype of conditional Shh signaling mutants (Machold et al., 2003) and with the increase in *Ptch1* expression observed after injection of Shh into the striatum (Charytoniuk et al., 2002). However, we further show that in vitro addition of Shh results in an increase in SVZ cell proliferation and in the number of cells with stem cell properties and resulting neurons, while blocking its function decreases their number. We provide evidence that Shh synergizes with EGF signaling in the modulation of SVZ cell proliferation. Moreover, cell-sorting and single-cell assays identify periventricular GFAP<sup>+</sup> astrocytes and GFAP<sup>+</sup> early precursors, but not ependymal cells or migrating neuroblasts, as *Gli1*<sup>+</sup> in vivo responders to endogenous Shh signaling. Our results thus show that Shh signaling is a critical mechanism for the maintenance of stem cell lineages and neurogenesis in the postnatal and adult brain. Together with the involvement of Shh signaling in the control of the behavior of stem cells in the embryonic neocortex (Palma and Ruiz i Altaba, 2004) and in the adult hippocampus (Lai et al., 2003; Machold et al., 2003), the present results demonstrate that Shh signaling regulates stem cell behavior in multiple brain niches throughout life. Moreover, we identify for the first time a cell type previously characterized as being a bona fide stem cell, the periventricular astrocyte (Doetsch et al., 1999), as an in vivo target of Shh signaling.

## Materials and methods

### Animals, dissections, cell-sorting and treatments

The SVZ of adult and postnatal mice were dissected and cultured as described (Lim et al., 2000; Lim and Alvarez-Buylla, 1999; Doetsch et al., 1999). For FACS, dissociated SVZ cells were prepared as previously described, and strained through a 40 µm nylon mesh (Beckton-Dickinson). All immunostaining incubations and washes were performed at 0–4°C: 1 × 10<sup>6</sup> SVZ cells were resuspended in 100 µl PBS-TR [PBS, 0.1% Tween-20 (Sigma), 100–200 units RNasin (Promega)] containing primary antibodies (biotinylated mCD24 antibody for ependymal (E) cells (PharMingen, 1:10); rabbit GFAP antibody for B cells (DAKO, 1:100) and incubated for 15 minutes. Cells were centrifuged in a tabletop centrifuge (Beckman). Cells were washed three times with 100 µl of PBS. Cells were then resuspended in 100 µl of PBS-TR containing streptavidin-Cy2 at 1:100 and anti-rabbit F(ab)<sub>2</sub> at 1:25 (Jackson) and incubated for 10 minutes. Cells were washed three times with PBS as before and resuspended in PBS at 500,000 cells/ml. Immunostained cells were isolated on a FACS Vantage (Beckton-Dickinson) cell-sorter. Neuroblasts (A cells) from postnatal animals were not sorted with antibodies; but were separated from type stem cell/transit amplifying precursor (B/C) cells by differential adhesion to poly-lysine treated plastic: type A cells do not stick to plastic, while B/C cells are tightly adherent. Anti-Shh (5E1) (Ericson et al., 1996) antibodies (used at 4 µg/ml) were purchased from the University of Iowa Hybridoma Bank. Recombinant octyl-modified Shh-N protein (used at 5 nM) was a kind gift from Curis.

### SVZ neurospheres

To make SVZ neurospheres (Reynolds and Weiss, 1992; Doetsch et al., 1999) the lateral walls of the lateral ventricle of postnatal or adult mice were dissected, collected in PBS, and incubated in PBS containing 0.3% activated papain (Worthington Biochemical). After 30 min incubation, ovomucoid inhibitor (Worthington Biochemical) and DNase (Sigma) were added in Neurobasal Medium (GIBCO) and the cells dissociated using a fire-polished pasteur pipette. After centrifugation, the cellular pellets were resuspended in neurosphere

medium [Neurobasal Medium (GIBCO) supplemented with N2 (GIBCO), 2 mM glutamine, 0.6% (w/v) glucose, 0.02 mg/ml insulin, antibiotics and 15 mM Hepes]. The cells were counted and plated in uncoated 25 ml culture flasks (1 × 10<sup>6</sup> cells per bottle) in the neurosphere medium containing 10 ng/ml epidermal growth factor (EGF; human recombinant, GIBCO). For passaging, neurospheres were centrifuged, triturated in 100 µl of medium with a P200 pipette and replated. For proliferation assays, neurospheres were plated at 4000 cells/well onto polyornithine/laminin-coated labtech chambers (Nunc) in the presence of 10 ng/ml EGF and grown for 1 week, unless otherwise indicated. For dose-response experiments, EGF was used at 1 ng/ml in combination with 5 and 0.5 nM Shh or 5 nM Shh with 5 and 0.5 µg/ml EGF. Clonal dilution assays were performed by plating at low cell densities documented to yield clonal cultures in one-third of conditioned media (Seaberg and van der Kooy, 2002).

### RNA, RT-PCR and in situ hybridization

RNA was isolated from whole SVZ dissections or from purified cells (Lim et al., 2000). 5000–10,000 selected cells were collected directly into RNeasy lysis buffer. Total RNA was isolated with RNeasy columns and concentrated by vacuum centrifugation to 12 µl; 9 µl of total RNA was combined with 1 µl of 100 mM T7LD3' primer, heated to 70°C for 5 minutes, then placed on ice. Forty units of RNasin, 4 µl of 5 × first strand buffer, 2 µl of 0.1 M DTT, 1 µl of 20 µM SMART III oligo (Clontech), and 1 µl of 10 mM dNTPs were added, and tubes were incubated at 42°C for 5 minutes. Four-hundred units of Superscript II was then added, and reactions incubated for another 60 minutes at 42°C. Two units of RNaseH were added and tubes incubated at 37°C for 20 minutes; 3 µl of total RNA was used in parallel reactions without Superscript as RT-minus controls. PCR was then performed for *Gli1*, *Gli2*, *Gli3*, *Shh*, *Ptch1* and *Hprt* as previously described (Dahmane and Ruiz i Altaba, 1999; Dahmane et al., 2001). In situ hybridizations with anti-sense digoxigenin-labeled anti-*Shh* or anti-*Gli1* probes were performed on fresh-frozen or perfused sections (Dahmane and Ruiz i Altaba, 1999; Dahmane et al., 2001).

### BrdU incorporation and immunohistochemical analyses

Incorporation of BrdU and immunochemical detection was performed as described (Lim et al., 2000; Dahmane et al., 2001) with anti-BrdU mouse monoclonal antibodies (Abs) (1:200; Roche). BrdU was added to cultures at 3 µM 16 hours prior to culture fixation except in the dose-response assays where 6-hour incubations were used. Neuronal phenotype was determined by immunolabeling with anti-beta III tubulin TuJ1 antibodies (1:1000; Babco). Nuclei were counterstained with Hoechst 33258 (Molecular Probes).

### Postnatal SVZ cell cultures

For the thymidine incorporation assay, 300,000 P3 SVZ cells were plated into uncoated wells into a 96-well plate in DMEM/F12/N2/B27/Gln/15 mM Hepes, pH 7.4 (Gibco) in the presence or absence of 5E1 or IgG (R&D systems) antibody at 4–5 µg/ml and cultured for a total of 44 hours. At this cell density, aggregates of SVZ cells form. At 27 hours, 2 µCi of [<sup>3</sup>H]-thymidine was added to each well. Cells were collected onto glass filters with a Tomtec 96 cell harvester, and [<sup>3</sup>H]-thymidine incorporation measured with a betaplate filter counter. Postnatal SVZ cultures for neurosphere growth were prepared as follows: 100,000 P7 SVZ cells were plated into 96-well plates in DMEM with 10% FCS for 3 days; at this point, cultures contain GFAP<sup>+</sup> and TuJ1<sup>+</sup> cells. The cultures were then washed and the medium changed to DMEM/F12/N2 (Gibco). In DMEM/F12/N2, these cultures proliferate to produce type A cells. After incubation with or without Shh, cultures were then washed with PBS three times, dissociated with papain (Lim and Alvarez-Buylla, 1999), and 30,000 cells cultured in neurosphere medium in six-well plates.

### In vivo and in vitro cyclopamine treatments

Cyclopamine (cyc, Toronto Research Biochemicals) was used at 1 mg/ml conjugated with 2-hydropropyl- $\beta$ -cyclodextrin [HBC (Sigma)]; prepared as a 45% solution in PBS (van den Brink et al., 2001). Five- to ten-week-old inbred C57Bl6/j mice were injected intraperitoneally for one week with HBC alone as control or cyc at 10 mg/kg/day. The day following the last injection, the mice were pulsed for 2 hours with BrdU (20 mg/kg, IP injection). Immunofluorescence of cryostat sections was as described (Dahmane et al., 2001). The stainings were digitally recorded using a cooled CCD camera-equipped Axiophot (Zeiss) and the BrdU<sup>+</sup>/DAPI<sup>+</sup> nuclei counted within the lateral wall of the lateral ventricles. For the in vivo cyc treatment followed by the preparation of neurospheres, P4 pups or adult animals were injected for 5 days with HBC alone or cyc at 10 mg/kg/day and neurospheres prepared as above from the SVZ of P9 or adult animals. Cyclopamine for in vitro use was dissolved in ethanol (10 mM) and used at 5  $\mu$ M final concentration.

For measurements in the olfactory bulb, ten (2 months old) C57Bl6/j mice were injected intraperitoneally for one week with HBC alone as control or cyc at 10 mg/kg/day (Palma and Ruiz i Altaba, 2004) and were injected intraperitoneally with BrdU (15 mg/ml dissolved in 0.7 mM NaOH with 0.9% NaCl; Sigma) at 100 mg/kg body weight, four times, two hours apart on the day before the last HBC or cyc injection. Mice were perfused 30 days later, first with saline (0.9% NaCl) containing heparin (5 units/ml) at 37°C then with 4% PFA in 0.1 M PB at 4°C. Brains were harvested and post-fixed for 48 hours in 4% PFA at 4°C then cut in 40  $\mu$ m coronal sections with a vibratome (Leica) and stored in 0.1 M PBS. Free-floating sections were washed in 0.1 M TBS with 0.1% Tween (TBST), pretreated in TBST with 0.7% H<sub>2</sub>O<sub>2</sub> and 0.1% Triton X-100, then pretreated in 2 M HCl in TBS to denature DNA, blocked with rabbit serum (10% in TBST; Vector) and incubated overnight at 4°C with rat monoclonal anti-BrdU antibody (1:600 in blocking solution; Accurate Scientific). Detection was performed with rabbit anti-rat biotinylated secondary antibody (1:200; Vector) followed by ABC kit (Vector) and revelation with DAB (175  $\mu$ g/ml; Sigma). Sections were mounted on slides and counterstained with cresyl violet acetate (0.5%; Sigma). One in three sections, 120  $\mu$ m apart, were selected for BrdU quantitation. An area of interest comprising the granule cell, internal plexiform and mitral cell layers was measured by computer-assisted microscopy (MicroBrightField). The number of BrdU-positive nuclei in this area of interest was related to its sectional volume to obtain a density per millimeter cubed.

### SVZ slice preparation and cell harvesting

C57Bl6/j mice (5-6 weeks old) were anesthetized by isoflurane inhalation before decapitation. The brain was rapidly removed and immediately placed in a 4°C normal artificial cerebrospinal fluid (ACSF) solution. The ACSF contained (mM): 124 NaCl, 3 KCl, 2 CaCl<sub>2</sub>, 1.3 MgSO<sub>4</sub>, 25 NaHCO<sub>3</sub>, 1.2 NaH<sub>2</sub>PO<sub>4</sub>, 10 D-glucose with pH=7.3 when bubbled with 95% O<sub>2</sub>-5% CO<sub>2</sub>. Coronal slices (150-200  $\mu$ m) were cut with a vibrating microslicer (Leica), kept in normal oxygenated ACSF at 34°C for about 20 min, and then stored at 20°C before the experiment. For cell harvesting, the slices were placed under a microscope in a chamber superfused with oxygenated ACSF warmed at 37°C. Cells close to the lateral ventricle were optically identified. Patch clamp pipettes filled with 6  $\mu$ l RNase free intracellular solution (in mM: 100 K-gluconate, 20 KCl, 10 HEPES, 4 ATP, 0.3 GTP, 10 phosphocreatine) were used to capture the cells. The seal of the pipette was monitored using a patch-clamp amplifier (Axoclamp 2B, Axon Instruments). The cell was then harvested from the tissue by applying negative pressure to the pipette and removing it from the tissue. The cell and pipette content were then expelled into a reaction tube.

### Primer design and multiplex single-cell RT-PCR

Primer design and single-cell RT-PCR were performed based on

methods described previously (Dulac, 1998; Toledo-Rodriguez et al., 2004; Wang et al., 2002). In brief, primers were designed using MacVector. Possible interactions between primers were then tested using Amplify 2.1. In addition, primers were subjected to a nucleotide database search to check for sequence specificity. To perform the reverse transcription, 5 pmol of each antisense primer, 0.3  $\mu$ l (40 U/ $\mu$ l) recombinant RNasin ribonuclease inhibitor (Promega, Madison/WI, USA), 1  $\mu$ l 6.15% NP-40, and RNase-free water were added to the cell content (final volume 12.3  $\mu$ l) and incubated for 3 minutes at 65°C. The tube was put on ice and the content spinned down. For a final volume of 20  $\mu$ l, 0.4  $\mu$ l ribonuclease inhibitor, 4  $\mu$ l X5 First-Strand Buffer, 2  $\mu$ l 0.1 M DTT (both Invitrogen), and 1  $\mu$ l (10 mM) dNTP mix were added. The mixture was incubated for 5 minutes at room temperature, placed at 42°C and 0.3  $\mu$ l (200 U/ $\mu$ l) SuperScript II RNase H<sup>-</sup> reverse transcriptase (Invitrogen) were added. After incubation for 1 hour at 42°C and 10 minutes at 65°C, the cDNA containing mix was aliquoted into 2  $\times$  10  $\mu$ l. One aliquot was kept at 4°C for a maximum of three days until use, the other one was stored at -20°C. The amplification and analysis of the single cell cDNA was performed in two distinct steps. For the first step, the ten cDNAs of interest were amplified in a single tube containing (in a final volume of 50  $\mu$ l): 10  $\mu$ l RT product, 0.2 mM dNTPs (Promega), 0.1  $\mu$ M of each primer, 1  $\times$  PCR buffer, 1  $\times$  solution Q, and 1.25 U HotStarTaq DNA polymerase (all Qiagen). As positive control 1 ng of whole brain total RNA was subjected to reverse transcription and 1/10 of the product was used for the first round of cDNA amplification; the negative control contained water. The first amplification consisted of 10 minutes hot start at 95°C followed by 28 cycles of (40 seconds 94°C, 40 seconds at 56°C, 1 minute at 72°C), 10 minutes at 72°C. The PCR was performed in a Mastercycler gradient (Eppendorf, Hamburg, Germany). The second round of PCR consisted of 3 minutes at 95°C followed by 35 cycles of (40 seconds at 95°C, 40 seconds at 56°C, 1 minute at 72°C), 10 minutes at 72°C. The amplification was performed in a total volume of 20  $\mu$ l containing water, 2  $\mu$ l first PCR product, 0.2 mM dNTPs, 1 M Betaine, 1  $\mu$ M of corresponding primer pair, 1  $\times$  ThermoPol Reaction buffer, and 1 U Taq DNA polymerase (both New England BioLabs). After amplification, the PCR products were analyzed on 1.5% agarose gels. Used primers were as follows: GAPDHsense: 5'-TGACATCAAGAGGTGGTGAAGC-3' and GAPDHantisense: 5'-CCCTGTTGCTGTAGCCGTATTC-3', amplifying a 203 bp fragment. GFAPsense: 5'-ATCCGCTCAGGTCATCTTACCC-3' and GFAPantisense: 5'-TGTCTGCTCAATGTCCTCCCTACC-3', amplifying a 287 bp fragment. Gli1sense: 5'-CAGCCTCTGTTTTCACATCATCC-3' and Gli1antisense: 5'-CGGTTTCTTCCCTCCCAAC-3', amplifying a 215 bp fragment.

## Results

### Expression of *Shh* and *Gli1* in the mouse postnatal and adult SVZ

To test whether *Shh* could have a role in SVZ neurogenesis in the adult brain, we first analyzed the expression of the *Shh* and *Gli1* genes, the latter being a consistent target and reliable marker of *Shh* signaling (Lee et al., 1997; Hynes et al., 1997; Bai et al., 2001). Both *Shh* and *Gli1* were detected by in situ hybridization at low levels in the lateral wall of the forebrain ventricles (Fig. 1A-H) where neurogenesis occurs. In this region expression was strongest ventrally. Expression was also found in the medial wall in a ventral domain (Fig. 1A,B,F,G), but it was absent from most of the medial wall of the lateral ventricle in more dorsal areas. Other brain regions around the SVZ were devoid of staining indicating the specificity of the hybridization (Fig. 1E). *Gli1* expression was very low or absent

in cells immediately adjacent to the ventricle, presumably the ependymal cells (Fig. 1D,H). Expression of these genes in the adult striatum and septum was detected at much lower levels in scattered cells (Fig. 1A,B). Other sites of *Shh* and *Gli1* expression in the perinatal and adult brain were observed, and have been documented elsewhere (Dahmane et al., 2001; Traiffort et al., 2001; Lai et al., 2003; Machold et al., 2003). Sense probes gave no signal (not shown).

### *Gli1*<sup>+</sup>/*GFAP*<sup>+</sup> cells are present in the SVZ stem cell niche

To attempt to identify the cells that express *Shh* and those that respond to it, dissociated and sorted postnatal (Lim and Alvarez-Buylla, 1999) and adult SVZ cells were used to perform RT-PCR assays testing for the expression of genes involved in Shh signaling (Fig. 2A). Like *Gli1*, the transcription of the gene encoding the Shh receptor *Ptch1* is Shh responsive. In contrast, *Gli2* activation by Shh is context dependent, whereas *Shh*/*Gli1* and *Gli3* often have an antagonistic relationship (e.g. Ruiz i Altaba, 1998). In the postnatal SVZ, all tested components are expressed. However, in neuroblasts (A cells), purified by differential adhesiveness to polylysine-coated plates, only expression of *Ptch1* and low levels of *Gli2* but not *Shh*, *Gli1* or *Gli3* were detected. The GFAP<sup>+</sup> fraction enriched in B and C cells [the GFAP<sup>+</sup> SVZ astrocytes (B cells) and the transit amplifying cells (C cells) that contaminate the pool] expressed *Shh*, *Gli2*, *Gli3*, *Ptch1*, and low levels of *Gli1* (not shown). In the adult, sorted mCD24<sup>+</sup> ependymal (E) cells expressed low levels of *Gli2* and *Ptch1*, but not *Gli1*, whereas the fraction containing B and C cells (labeled as B in Fig. 2), expressed high levels of *Gli1*, *Gli2* and *Ptch1*. We did not detect expression of *Gli3* in sorted adult GFAP<sup>+</sup> or mCD24<sup>+</sup> cells. To extend these findings, we analyzed gene expression in postnatal P7 SVZ neurospheres, stem cell-derived colonies, grown in standard media containing EGF. Cells in neurospheres express *Shh*, *Gli1*, *Gli2*, *Gli3* and *Ptch1* (Fig. 2C), further indicating that Shh signaling is active in SVZ stem cell lineages.

Since Shh normally acts through both *Gli1* and *Gli2*, and both *Gli1* and *Ptch1* are responsive to Shh (reviewed in Ruiz i Altaba et al., 2002), the data raises the possibility that adult SVZ stem (B) cells and/or early progenitor (C) cells respond to Shh signaling as they express *Gli1*, *Gli2* and *Ptch1*. While E cells express *Gli2* and *Ptch1*, their lack of *Gli1* expression suggests that they may not respond to Shh signaling. The absence of *Shh* expression in adult isolated B or E pools suggests that either other cells express it or that rare messages were lost during cell sorting and cDNA amplification, as *Shh* mRNA is indeed found in the adult and postnatal SVZ (Fig. 2A,B).

In order to confirm that B cells do indeed express *Gli1*, we performed single cell multiplex RT-PCR from single randomly collected SVZ cells with a patch-clamp pipette after recording their position (Fig. 3A). This method allows analysis of the expression of several genes at a single cell resolution. We

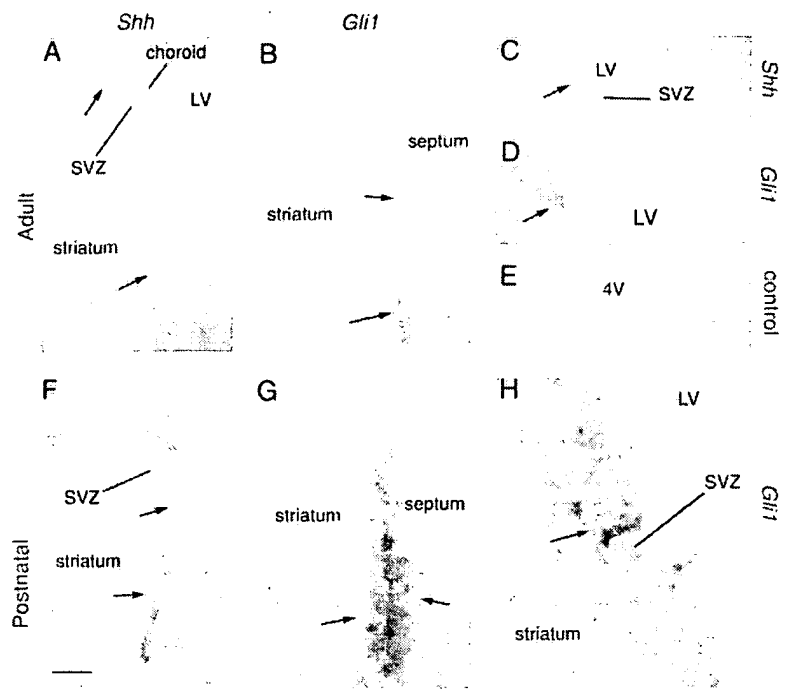


**Fig. 1.** *Gli1* and *Shh* gene expression in the SVZ. (A,C) Expression of *Shh* mRNA in the lateral wall of the lateral ventricles (LV) of adult mice. At high magnification, *Shh* expression is clearly detected in SVZ cells (C). (B,D,F-H) Expression of *Gli1* mRNA in the lateral wall of the lateral ventricle of adult (B,D) and postnatal (P3; G,H) mice. (E) Control section showing lack of hybridization of *Shh* antisense RNA probes in the fourth ventricle (4V) of an adult mouse. Sense probe controls gave no signal. (A-H) *In situ* hybridizations on cross sections. Arrows point to sites of expression. Dorsal is to the top. Scale bar in F: 400  $\mu$ m for A,F; 200  $\mu$ m for C-E; G, 150  $\mu$ m; H, 30  $\mu$ m.

found that 32.3% and 27.7% out of 65 sampled cells expressed *GFAP* and *Gli1*, respectively (Fig. 3B,C). Importantly, 17% of the cells co-expressed both genes, confirming that one population of *GFAP*<sup>+</sup> cells, known to be stem cells (Doetsch et al., 1999), express *Gli1* (Fig. 3C). Not all *GFAP*<sup>+</sup> cells expressed *Gli1*, possibly reflecting the choice of non-SVZ astrocytes in some cases, the existence of two subpopulations of *GFAP*<sup>+</sup> SVZ astrocytes or the activation by Shh of only a fraction of all SVZ B cell astrocytes at any one point. Moreover, many *Gli1*<sup>+</sup> cells did not express *GFAP*, suggesting that more abundant precursors (C cells) also respond, or may have recently responded, to Shh signaling as purified A or E cells do not express *Gli1* (Fig. 2).

### Inhibition of Shh signaling *in vivo* decreases cell proliferation in the intact SVZ

To investigate the requirement of Shh signaling *in vivo* we have used systemic injections of cyclopamine. Cyclopamine is a plant alkaloid that selectively inhibits Shh signaling (Incardona et al., 1998; Cooper et al., 1998). This drug was injected intraperitoneally, daily, into mice after its conjugation with cyclodextrin as carrier. This method does not injure the brain, a common unavoidable result of direct intracerebral injections. Injections of carrier alone were used as control. A 2-hour pulse of BrdU to label proliferating SVZ precursors was given before tissue harvesting ~12–24 hours after the last injection.



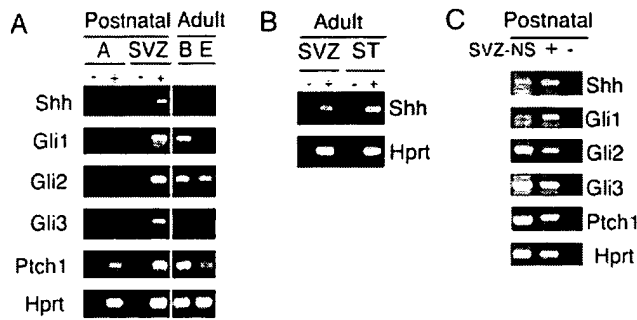


**Fig. 2.** Gene expression analyses in cell populations in the postnatal and adult SVZ. (A) RT-PCR analyses of postnatal (P5) and adult sorted cells. Postnatal whole SVZ is also shown as control. (B) RT-PCR analyses of *Shh* expression in the SVZ and adjacent striatum (ST) from the same animal. Note that *Shh* is expressed in the adult SVZ but it is not detected in either B or E sorted cells (see text). All samples were tested with (+) or without (–) reverse transcriptase to control for any possible signal resulting from contaminating genomic DNA. (C) RT-PCR analyses of gene expression in P7 SVZ neurospheres (SVZ-NS). As positive control (+), RNA from a P7 brain was used. As a negative control P7 SVZ RNA without reverse transcriptase was used (–). As control for RT-PCR, all genes were found to be expressed in dissected but non-cell-sorted SVZ pieces. As control for RNA recovery and amounts of cDNA, the levels of the housekeeping gene *Hprt* were measured.

Cyclopamine treatment of C57black adult mice for 7 days resulted in a marked decrease of BrdU incorporation in the SVZ as compared with the level of BrdU labeling in control injected siblings (Fig. 4A–D,G). Cyclopamine did not appear to affect the persistence or overall abundance of Nestin<sup>+</sup> or GFAP<sup>+</sup> cells (Fig. 4E,F). A decrease in BrdU incorporation, however, was accompanied by a decrease in *Gli1* and *Gli3* expression in tissue isolated ~4–6 hours following the last injection (Fig. 4H), indicating a correlation between lower *Gli1* expression levels, as a marker of a decrease in Shh pathway activity, and lower SVZ cell proliferation.

In order to study the consequences of reducing SVZ cell proliferation, we monitored changes in the number of olfactory bulb interneurons. We performed a 7 days' treatment with cyclopamine or vehicle alone followed by a pulse of BrdU during the treatment (see Fig. 5A). Animals were then killed 30 days later, which is the time necessary to obtain a fully functional interneuron (Carleton et al., 2003). As expected, reducing the proliferation in the SVZ led to a reduction of the number of BrdU<sup>+</sup> cells in the olfactory bulb granule cell layer (Fig. 5B–F), showing that no compensatory mechanisms were affecting the amount of newborn cells surviving. An overall 15% reduction ( $n=5$  mice for each group) was significantly observed after 30 days along the entire olfactory bulb (ANOVA,  $F=16.97$ ,  $P<0.0001$  and post-hoc Newman-Keuls test  $P<0.0002$ ). Treatments at higher doses and/or for longer periods might result in greater neuronal deficits.

#### Shh is a mitogen for SVZ precursors increasing the number of new neurons

To further test the role of Shh on SVZ cells, we plated dissociated postnatal day (P) 5 SVZ cells on a quiescent astrocytic monolayer in the absence of exogenous growth

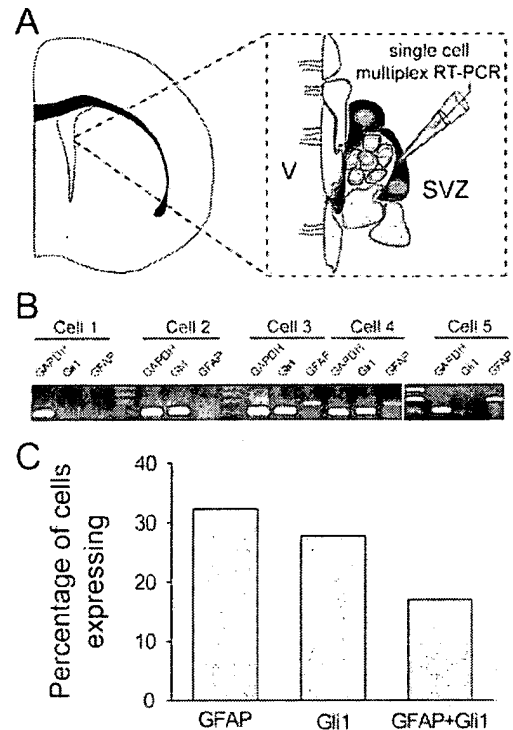


**Fig. 3.** Gene expression in single SVZ cells. (A) Schematic representation of the experimental procedure. Individual SVZ cells were randomly harvested with a patch-clamp pipette from fresh living slices, and were used for single cell multiplex RT-PCR. (B) Examples of RT-PCR assays showing gene expression in single SVZ cells. (C) Summary graph showing the expression of *GFAP*, *Gli1* or both in single cells, shown as percentage of the total number of collected cells ( $n=65$ ).

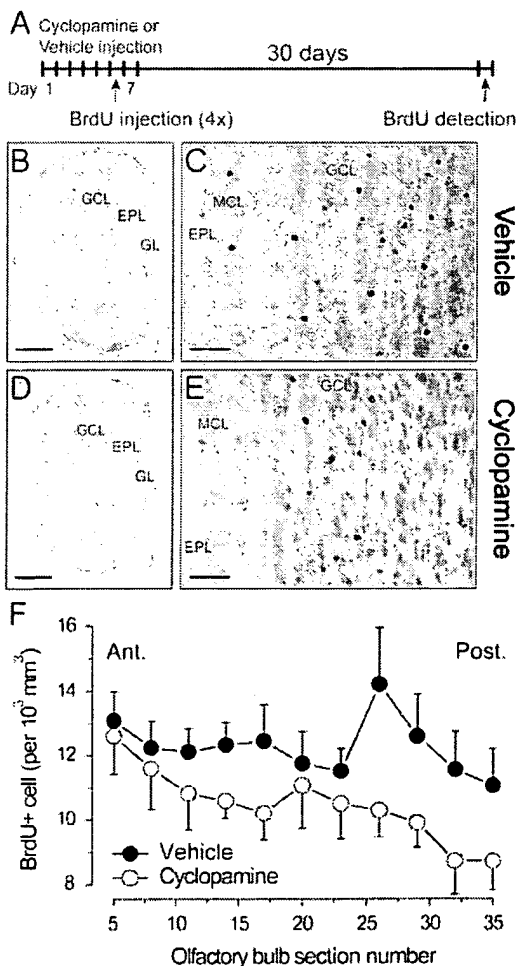
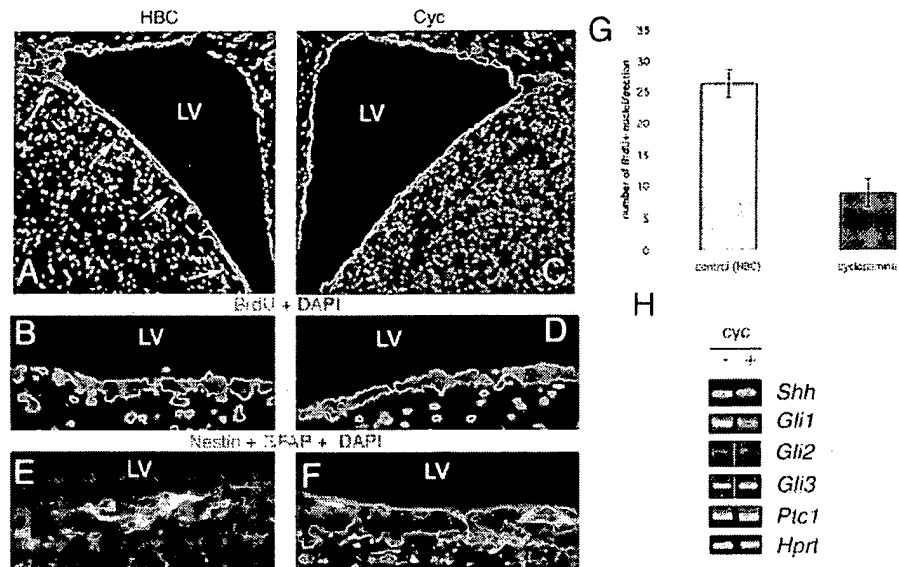
factors. These conditions recapitulate the large production of neurons observed in vivo from SVZ progenitors (Lim and Alvarez-Buylla, 1999; Lim et al., 2001). Addition of Shh (5 nM) doubled the number of BrdU<sup>+</sup> cells after five days (Fig. 6A) in these cultures. The requirement of Shh for SVZ cell proliferation in vitro was tested by making aggregates of dissociated postnatal SVZ cells in the absence of the astrocytic monolayer, and treating them with anti-Shh monoclonal antibody (4  $\mu$ g/ml) (Ericson et al., 1996) in the presence of [<sup>3</sup>H]-thymidine. Addition of anti-Shh antibody decreased proliferation by ~30% after two days, as compared to sibling cultures treated with an isotype-matched unrelated antibody at the same concentration (Fig. 6B).

We next tested the effects of Shh on the formation of neurons in SVZ cells plated onto astrocyte monolayers in a defined, serum-free medium. SVZ progenitors proliferate to form colonies of TuJ1<sup>+</sup> neuroblast (A) cells. In this assay, addition of Shh increased the number of newly born TuJ1<sup>+</sup> neurons, three-fold after 3 days and ten-fold after 7 days (Fig. 6C). Shh does not appear to increase neurogenesis by acting directly upon neuroblasts: Shh treatment of purified A cells did not increase their numbers as compared to controls (Fig. 6D).

The differences between control and Shh-treated samples are likely to reflect a cumulative effect of Shh on neurogenesis, as seen by the number of TuJ1<sup>+</sup>/BrdU<sup>+</sup> cells (Fig. 6E,F), derived



**Fig. 4.** Cyclopamine inhibits SVZ cell proliferation in vivo. (A,B,E) Cross section through the forebrain SVZ of an adult mouse showing normal BrdU incorporation (arrows in A,B) or the expression of GFAP and Nestin (E) following one week's injection of HBC carrier (cyclodextrin) alone. Animals were perfused ~12–24 hours after the last injection. (C,D,F) Decrease of BrdU<sup>+</sup> cells in adult mice treated with cyclopamine for one week (C,D) does not lead to the loss of Nestin<sup>+</sup> or GFAP<sup>+</sup> cells (F). (G) Quantification of the number of BrdU<sup>+</sup> cells in the SVZ of control and cyclopamine-treated adult mice. Counts are averaged and shown per section. Error bars=s.e.m.,  $n=13$  for control HBC-injected mice and  $n=18$  for cyclopamine-injected mice in four independent experiments pooled together. Out of 18 cyclopamine-injected mice, three animals did not respond, five animals decreased the number of BrdU<sup>+</sup> cells by ~50%, and ten animals reduced incorporation by ~100%. No reduction was observed in the HBC-injected mice. (H) RT-PCR of fresh SVZ tissue from adult control or cyclopamine-treated mice, dissected 4 hours after the last injection. *Hprt* levels are used as loading controls.



from a direct effect on early progenitors (B or C cells). Since Shh is added only at the beginning of the culture period, the observed increases in proliferation and neurogenesis after several days in vitro could be explained by an initial amplification of these early progenitors. A transient increase in stem/precursor cells by acute Shh treatment would explain the later increase in production of neuroblasts derived from such expanded progenitor pools.

### Exogenous Shh increases the number of SVZ neurospheres

To directly test for an effect of Shh on SVZ early progenitors, postnatal SVZ cell cultures (see Materials and methods) were grown with or without Shh (5 nM) for four days. Cells were then dissociated and washed, and equal numbers of cells cultured without additional Shh in the presence of EGF (10 ng/ml). This latter treatment induces the formation of neurospheres, floating colonies derived from single cells with stem cell properties exhibiting self-renewal and multipotentiality (Reynolds and Weiss, 1992). After 1 week in culture, the number of neurospheres was counted. Shh treatment was found to increase the number of neurospheres 2.5-fold over that obtained in untreated control samples (Fig. 7A,B).

**Fig. 5.** Reduced number of newborn interneurons in the adult olfactory bulb after cyclopamine treatment. (A) Experimental procedure. BrdU injections are done during cyclopamine or vehicle treatment. One month post-injection, the number of newborn neurons is quantified after BrdU staining. (B,C,D,E) Photographs of the BrdU staining in the olfactory bulb of vehicle- (B,C) or cyclopamine- (D,E) treated mice. (F) The number of BrdU<sup>+</sup> cells in the olfactory bulb of cyclopamine-treated mice (open circle,  $n=5$ ) is significantly reduced in comparison to vehicle-treated mice (filled circle,  $n=5$ ) along the antero-posterior axis. Error bars=s.e.m.

### Shh is a mitogen for adult SVZ cells able to form neurospheres

Recent data analyzing *Smo* and *Shh* null mice did not resolve whether SHH acts as a mitogen for adult SVZ cells (Machold et al., 2003). Here we have tested this possibility directly by treating adult SVZ neurospheres with different levels of Shh and diminished doses of EGF. Such modification derives from the observation that Shh and EGF synergize in the control of proliferation of neocortical cells with stem cell properties (Palma and Ruiz i Altaba, 2004). Indeed, in cultures of postnatal SVZ cells, Shh alone was unable to sustain

neurosphere growth and addition of Shh to neurosphere media containing standard saturating doses of EGF (10 ng/ml) was ineffective in increasing the number of neurospheres formed (not shown), consistent with previous data using embryonic or adult progenitors (Machold et al., 2003; Palma and Ruiz i Altaba, 2004).

At lower EGF concentrations, however, Shh had a synergistic effect on the proliferation of neurosphere cells.

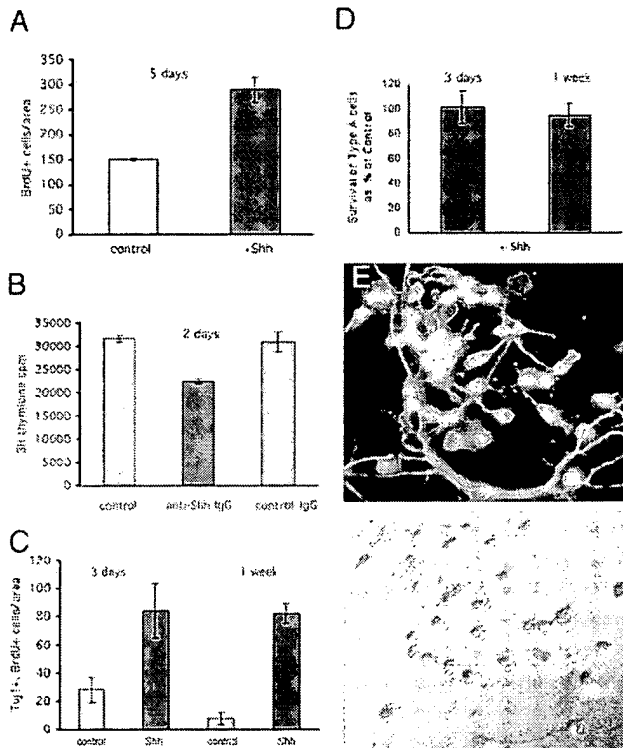


**Fig. 6.** Shh signaling regulates SVZ proliferation and neurogenesis. (A) Quantification of the effects of Shh on the proliferation of dissociated P5 SVZ cells plated on a quiescent astrocytic monolayer. BrdU incorporation was quantified by immunofluorescence. Under these conditions, SVZ precursors proliferate and generate new neurons, as they normally do in vivo. (B) Quantification of the effects of blocking anti-Shh monoclonal antibody (5E1) on the proliferation of P5 SVZ cells after dissociation and reaggregation. Cell proliferation was measured by radioactive thymidine incorporation. (C) Quantification of the effect of Shh on neurogenesis in dissociated adult SVZ cells plated on an astrocytic monolayer. Generation of new neurons was measured by co-labeling with Tuj1, identifying neurons, and anti-BrdU antibodies, identifying cells that replicated after BrdU addition. (D) Quantification of the effects of Shh on isolated type A SVZ neuroblasts. Type A cells were purified from P5 mice and cultured with or without Shh. At 3 and 7 days, the number of Tuj1+ cells in Shh-treated cultures were compared to control cultures. Error bars=s.e.m. (E) Immunocytochemistry of a 7-day SVZ cell culture on an astrocytic monolayer showing the labeling of neurons with Tuj1 (red) and recently divided cells with anti-BrdU (green) antibodies. Note the large number of doubly labeled (yellow) cells representing newly born neurons. (F) Nomarski optics image of the same panel shown in E.

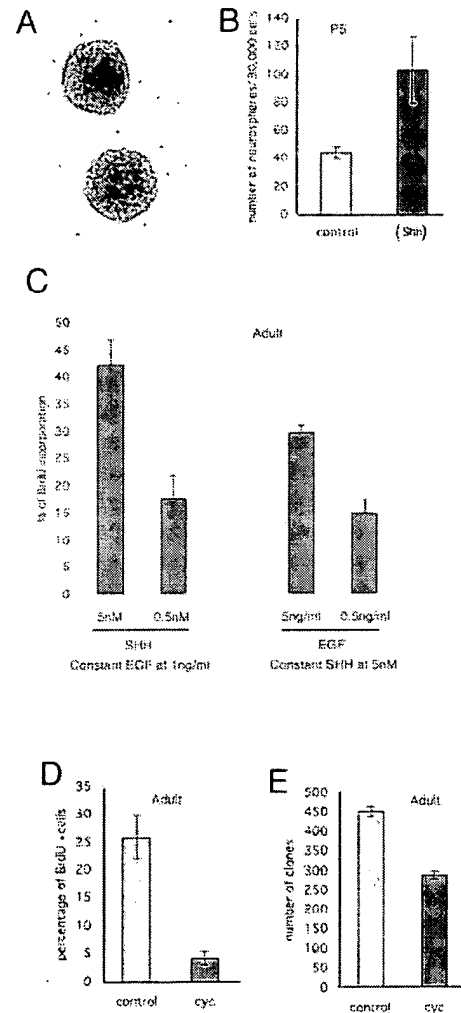


**Fig. 7.** Shh regulates proliferation and neurosphere formation in cooperation with EGF. (A) Image of neurospheres from adult SVZ cultures. (B) Quantification of the number of primary neurospheres formed from cultures of SVZ cells previously grown on astrocytic monolayers with or without exogenous Shh (5 nM). Shh was not added to the neurosphere cultures. (C) Synergism of Shh and EGF on neurosphere proliferation. The assay was done with a constant dose of EGF at 1 ng/ml, and varying doses of Shh at 5 or 0.5 nM (left) or with a constant dose of Shh at 5 nM and varying doses of EGF at 5 and 0.5 ng/ml (right). Treatments were for 48 hours. (D,E) Quantification of proliferation as measured by the percentage of BrdU+ cells (D) and the number of clones obtained in cloning assays (E) in adult SVZ neurospheres treated with cyclopamine (5  $\mu$ M) or treated with an equal dose of ethanol used as carrier for in vitro work. In all cases, error bars indicate s.e.m. of triplicate cultures.

Adult SVZ neurospheres were prepared by standard methods using 10 ng/ml EGF and passaged twice. Such neurospheres were then plated on an adhesive substrate in the presence of 1 ng/ml EGF plus 5 or 0.5 nM recombinant Shh. Analyses of BrdU incorporation after 48 hours showed enhanced proliferation with 5 versus 0.5 nM Shh (~2.5-fold; Fig. 7C). Conversely, adult neurospheres plated on adhesive substrate in the presence of 5 nM Shh plus 5 or 0.5 ng/ml EGF resulted in enhanced proliferation with 5 versus 0.5 ng/ml EGF (~2-fold; Fig. 7C). Interestingly, the percentage of BrdU incorporation was higher with 5 nM Shh plus 1 ng/ml EGF than with 5 nM Shh plus 5 ng/ml EGF. This difference suggests that higher doses of EGF negate any proliferative effects of Shh, explaining the lack of effect of Shh with full media containing 10 ng/ml EGF (not shown) (Machold et al., 2003; Palma and Ruiz i Altaba, 2004). Because Shh on its own, without EGF, is unable to sustain growth of neurospheres (not shown) (Machold et al., 2003; Palma and Ruiz i Altaba, 2004), our results suggest that Shh acts as a mitogenic cofactor when other growth factors are present. The lower synergistic effect of 5 ng/ml versus 1 ng/ml of EGF with Shh suggests that such synergism occurs within a limited concentration range, paralleling the effects we described with embryonic neocortical neurospheres (Palma and Ruiz i Altaba, 2004).

#### Inhibition of Shh signaling decreases SVZ cell proliferation and the number of neurosphere-forming stem cells

To directly test for the requirement of endogenous Shh signaling on adult SVZ cell proliferation and self-renewal using the neurosphere assay, we have utilized cyclopamine on floating neurosphere cultures. Treatment of adult SVZ neurospheres with cyclopamine (5  $\mu$ M) led to an inhibition of proliferation as measured by BrdU incorporation (Fig. 7D), showing that adult SVZ progenitors require Hh signaling for normal proliferation. In addition, cyclopamine treatment also decreased the number of neurospheres obtained in cloning assays (Fig. 7E), indicating that Hh signaling controls the number of neurosphere-forming adult SVZ cells. The lower relative decrease in clone number versus BrdU incorporation (Fig. 7D,E), together with the *in vivo* data, suggests a differential effect on two targets: *GFAP<sup>+</sup>/Gli1<sup>+</sup>* C cells (Fig. 3), and *GFAP<sup>+</sup>/Gli1<sup>+</sup>* B stem cells (Fig. 3) as the former account for the bulk of BrdU<sup>+</sup> cells while the latter can form neurospheres in clonogenic assays.

## Discussion

The results presented here demonstrate an involvement of Shh signaling in the regulation of SVZ stem cells, leading to sustained neurogenesis, in the postnatal and adult mouse brain. Taken together, the gene expression analyses and the *in vitro* and *in vivo* experiments indicate that Shh signaling is critical for the modulation of the number of cells with stem cell properties, for the proliferation of early precursors and consequently for the production of new neurons.

Our *in vivo* single cell analyses indicate that Shh acts directly on GFAP<sup>+</sup> periventricular astrocytes (B cells) and more abundant GFAP<sup>+</sup> early precursors (C cells). *In vitro* results are consistent with this conclusion, although responsiveness to Shh, present in stem (B) cells, could also be induced in

precursors *in vitro*. Indeed, transit amplifying precursors (C cells) can give rise to neurospheres *in vitro* under the influence of EGF, which may induce them to display stem cell properties (Doetsch et al., 2002). Ependymal (E) cells, which were also proposed to behave as stem cells (Johansson et al., 1999) (see Doetsch et al., 1999; Capela and Temple, 2002), and migrating neuroblasts (A cells) expressed *Gli2* and *Ptch1*, but not *Gli1*, suggesting that these cells do not show the canonical response to Shh if they respond at all. Consistently, A cells did not increase their proliferation *in vitro* in response to Shh.

In the developing cerebral cortex, Shh acts in cooperation with EGF but Shh on its own is not sufficient to alter neurosphere size or number (Palma and Ruiz i Altaba, 2004). We show here that Shh similarly has a proliferative effect on SVZ neurospheres in cooperation with low doses of EGF, demonstrating the conserved action of Shh as a mitogen that synergizes with EGF. The selective expression of EGFR in C cells (Doetsch et al., 2002), and thus the ability to respond to EGF, provides additional evidence that Shh and EGF synergize in the proliferation of these early precursors. Moreover, the inhibition of adult cell proliferation and neurosphere formation by cyclopamine further proves the requirement of Shh signaling in adult stem cell lineages.

In contrast to our results in the SVZ, Shh is sufficient to induce proliferation of hippocampal precursors (Lai et al., 1993). Such a difference could suggest the endogenous production of cofactors, such as EGF, by hippocampal cells at sufficient quantities *in vitro*. In addition here, and in contrast to other data (Machold et al., 2003), we show that Shh is sufficient to increase the number of neurospheres derived from SVZ cultures grown over quiescent astrocytes, indicating that in this case, such cultures may also produce sufficient levels of EGF or other cofactors. This difference might relate to the method used: it is possible that the astrocytes in the feeder layer produce enough cofactors but at low enough levels for Shh to act, whereas saturating levels of EGF mask the effects of Shh (Palma and Ruiz i Altaba, 2004).

Interestingly, our present data show that Shh and EGF synergize maximally within a narrow concentration range, in a manner similar to that we described in the embryonic neocortex (Palma and Ruiz i Altaba, 2004). It is therefore possible that in both cases, the range of effective Shh and EGF concentrations determines the neurogenic niche where stem cells exist and where the population of early precursors can expand.

The finding that *Shh* mRNA is detected in the walls of the lateral ventricles supports the idea that this molecule contributes to the definition of stem cell niches in the adult brain. However, since we have not yet been able to detect expression of Shh in sorted SVZ cell populations or in isolated single cells (not shown), it remains unclear which cells are the signaling cells. One can therefore not reject the possibility that Shh may be produced at a distance and transported through axonal terminals or dendritic arbors that reach the SVZ from afar. This possibility is also suggested, in part, by the finding that dopaminergic neurons in the ventral midbrain control SVZ cell proliferation at a distance (Höglinger et al., 2004). Whether these cells exert their action through the secretion of Shh remains to be determined. A similar scenario has been proposed for the control of cell proliferation in the hippocampal stem cell niche, where Shh has been proposed to

be transported from the septum to the subgranular layer (Lai et al., 1993). However, we note that there are cells that express *Shh* in the hilus (Dahmane et al., 2001), which could also exert a local effect. *Shh* has also been shown to be axonally transported in the fly visual system (Huang and Kunes, 1996), and it is possible that it is secreted from Purkinje cell dendrites to affect external germinal layer cell proliferation in the cerebellum (Dahmane and Ruiz i Altaba, 1999; Weschler-Reya and Scott, 1999; Wallace, 1999).

How *Shh* signaling is integrated with other niche factors, such as APP (Caillé et al., 2004), is not yet clear. For instance, BMP and *Shh* signaling show an antagonistic relationship in the neural tube patterning (Liem et al., 1995). In the postnatal brain SVZ, BMP signaling inhibits neurogenesis and promotes glial differentiation: ependymal cells secrete the BMP antagonist Noggin, thereby creating a favorable microenvironment for neurogenesis to occur (Lim et al., 2000). It is possible that in the postnatal and adult SVZ, as in the embryonic neural tube, BMP and *Shh* signaling act antagonistically, and inhibition of the former is necessary for the latter to act.

Our results showing that *Shh* is a niche factor that regulates the number of SVZ cells with stem cell properties and neurogenesis, parallel those in other CNS regions: *Shh* is expressed in the septum and the hilus of the hippocampus (Dahmane et al., 2001; Lai et al., 2003; Machold et al., 2003), it regulates cell proliferation in the subgranular layer (Lai et al., 2003; Machold et al., 2003), and is also involved in the control of stem cell behavior in the developing neocortex (Palma and Ruiz i Altaba, 2004). *Shh*-Gli signaling may thus be a general mechanism for the regulation of the number of stem cells and the number of precursors derived from primary progenitors. Moreover, it is interesting to propose that the control of the production of new adult neurons, from stem cell astrocytes in the SVZ and hippocampus (Doetsch et al., 1999; Seri et al., 2001), is largely regulated by already existing cells, located nearby or at a distance, through the action of *Shh* (see also Dahmane et al., 2001), providing a mechanism for the homeostatic regulation of neuronal number and perhaps a mechanism for response to injury and disease.

Finally, our findings also suggest a method for manipulating stem cell lineages for the generation of new neurons through the regulation of *Shh* signaling. Such a method may help develop new strategies for the treatment of neurodegenerative diseases, such as Parkinson's disease (reviewed by McKay et al., 2004), by expanding stem/precursor cell population in vitro, prior to reintroduction in vivo or by the activation of dormant endogenous stem cell activity in vivo.

We thank Barbara Stecca, Van Nguyen and Jozsef Kiss for discussion and comments on the manuscript and Mercedes Beyna for excellent technical assistance. This project was initiated by N.D. and A.R.A. in collaboration with D.A.L. and A.A.B. N.D. discovered expression of *Gli1* and *Shh* in the SVZ. D.A.L. and N.D. performed the in vitro culture and cell sorting assays. P.S., V.P. and Y.G. performed the in vivo HH blocking experiments with cyclopamine. V.P. performed neurosphere cultures. T.C.B., C.D.H. and A.C. in collaboration with P.S. and A.R.A. performed the single cell PCR assays and the quantification of new neurons after in vivo cyclopamine treatment. V.P. was a recipient of a Pew Latin American Fellowship. D.A.L. was supported by an MSTP grant from the NIH. P.S. was a recipient of an American Brain Tumor Foundation postdoctoral

fellowship. This work was supported by grants from the EPFL (to A.C.), the NIH-NINDS (to A.A.-B.) and from the NIH-NINDS, the Université de Genève and the Jeantet Foundation (to A.R.A.).

## References

- Alvarez-Buylla, A., Seri, B. and Doetsch, F. (2002). Identification of neural stem cells in the adult vertebrate brain. *Brain Res. Bull.* **57**, 751-758.
- Bai, C. B. and Joyner, A. L. (2001). Gli1 can rescue the in vivo function of Gli2. *Development* **128**, 5161-5172.
- Caillé, I., Allinquant, B., Dupont, E., Bouillot, C., Langer, A., Muller, U. and Prochiantz, A. (2004). Soluble form of amyloid precursor protein regulates proliferation of progenitors in the adult subventricular zone. *Development* **131**, 2173-2181.
- Capela, A. and Temple, S. (2002). LeX/ssea-1 is expressed by adult mouse CNS stem cells, identifying them as nonependymal. *Neuron* **35**, 865-875.
- Carleton, A., Petreanu, L. T., Lansford, R., Alvarez-Buylla, A. and Lledo, P. M. (2003). Becoming a new neuron in the adult olfactory bulb. *Nat. Neurosci.* **6**, 507-518.
- Charytoniuk, D., Traiffort, E., Hantraye, P., Hermel, J. M., Galdes, A. and Ruat, M. (2002). Intrastriatal sonic hedgehog injection increases Patched transcript levels in the adult rat subventricular zone. *Eur. J. Neurosci.* **16**, 2351-2357.
- Cooper, M. K., Porter, J. A., Young, K. E. and Beachy, P. A. (1998). Teratogen-mediated inhibition of target tissue response to *Shh* signaling. *Science* **280**, 1603-1607.
- Dahmane, N. and Ruiz i Altaba, A. (1999). Sonic hedgehog regulates the growth and patterning of the cerebellum. *Development* **126**, 3089-3100.
- Dahmane, N., Sanchez, P., Gitton, Y., Palma, V., Sun, T., Beyna, M., Weiner, H. and Ruiz i Altaba, A. (2001). The Sonic Hedgehog-Gli pathway regulates dorsal brain growth and tumorigenesis. *Development* **128**, 5201-5212.
- Doetsch, F., Caille, I., Lim, D. A., Garcia-Verdugo, J. M. and Alvarez-Buylla, A. (1999). Subventricular zone astrocytes are neural stem cells in the adult mammalian brain. *Cell* **97**, 703-716.
- Doetsch, F., Petreanu, L., Caille, I., Garcia-Verdugo, J. M. and Alvarez-Buylla, A. (2002). EGF converts transit-amplifying neurogenic precursors in the adult brain into multipotent stem cells. *Neuron* **36**, 1021-1034.
- Dulac, C. (1998). Cloning of genes from single neurons. *Curr. Top. Dev. Biol.* **36**, 245-258.
- Ericson, J., Morton, S., Kawakami, A., Roelink, H. and Jessell, T. M. (1996). Two critical periods of Sonic Hedgehog signaling required for the specification of motor neuron identity. *Cell* **87**, 661-673.
- Höglinger, G., Rizk, P., Muriel, M. P., Duyckaerts, C., Oertel, W. H., Caille, I. and Hirsch, E. C. (2004). Dopamine depletion impairs precursor cell proliferation in Parkinson disease. *Nat. Neurosci.* **7**, 726-735.
- Huang, Z. and Kunes, S. (1996). Hedgehog, transmitted along retinal axons, triggers neurogenesis in the developing visual centers of the *Drosophila* brain. *Cell* **86**, 411-422.
- Hynes, M., Stone, D. M., Dowd, M., Pitts-Meek, S., Goddard, A., Gurney, A. and Rosenthal, A. (1997). Control of cell pattern in the neural tube by the zinc finger transcription factor *Neuron* **19**, 15-26.
- Incardona, J. P., Gaffield, W., Kapur, R. P. and Roelink, H. (1998). The teratogenic Veratrum alkaloid cyclopamine inhibits sonic hedgehog signal transduction. *Development* **125**, 3553-3562.
- Jessell, T. M. and Sanes, J. R. (2000). Development. The decade of the developing brain. *Curr. Opin. Neurobiol.* **10**, 599-611.
- Johansson, C. B., Momma, S., Clarke, D. L., Risling, M., Lendahl, U. and Frisen, J. (1999). Identification of a neural stem cell in the adult mammalian central nervous system. *Cell* **96**, 25-34.
- Lai, K., Kaspar, B. K., Gage, F. H. and Schaffer, D. V. (2003). Sonic hedgehog regulates adult neural progenitor proliferation in vitro and in vivo. *Nat. Neurosci.* **6**, 21-27.
- Lee, J., Platt, K. A., Censullo, P. and Ruiz i Altaba, A. (1997). Gli1 is a target of Sonic hedgehog that induces ventral neural tube development. *Development* **124**, 537-552.
- Liem, K. F., Jr, Tremml, G., Roelink, H. and Jessell, T. M. (1995). Dorsal differentiation of neural plate cells induced by BMP-mediated signals from epidermal ectoderm. *Cell* **82**, 969-979.
- Lim, D. A. and Alvarez-Buylla, A. (1999). Interaction between astrocytes and adult subventricular zone precursors stimulates neurogenesis. *Proc. Natl. Acad. Sci. USA* **96**, 7526-7531.
- Lim, D. A., Tramontin, A. D., Trevejo, J. M., Herrera, D. G., Garcia-

- Verdugo, J. M. and Alvarez-Buylla, A. (2000). Noggin antagonizes BMP signaling to create a niche for adult neurogenesis. *Neuron* **28**, 713-726.
- Lois, C. and Alvarez-Buylla, A. (1994). Long-distance neuronal migration in the adult mammalian brain. *Science* **264**, 1145-1148.
- Machold, R., Hayashi, S., Rutlin, M., Muzumdar, M. D., Nery, S., Corbin, J. G., Gritti-Linde, A., Dellovade, T., Porter, J. A., Rubin, L. L. et al. (2003). Sonic hedgehog is required for progenitor cell maintenance in telencephalic stem cell niches. *Neuron* **39**, 937-950.
- McKay, R. D. (2004). Stem cell biology and neurodegenerative disease. *Philos. Trans. R. Soc. Lond. B Biol. Sci.* **359**, 851-856.
- Palma, V. and Ruiz i Altaba, A. (2004). Hedgehog-Gli signalling regulates the behavior of cells with stem cell properties in the developing neocortex. *Development* **131**, 337-345.
- Reynolds, B. A. and Weiss, S. (1992). Generation of neurons and astrocytes from isolated cells of the adult mammalian central nervous system. *Science* **255**, 1707-1710.
- Ruiz i Altaba, A. (1998). Combinatorial Gli gene function in floor plate and neuronal inductions by Sonic hedgehog. *Development* **125**, 2203-2212.
- Ruiz i Altaba, A., Palma, V. and Dahmane, N., (2002). Hedgehog-Gli signalling and the growth of the brain. *Nat. Rev. Neurosci.* **3**, 24-33.
- Seaberg, R. M. and van der Kooy, D. (2002). Adult rodent neurogenic regions: the ventricular subependyma contains neural stem cells, but the dentate gyrus contains restricted progenitors. *J. Neurosci.* **22**, 1784-1793.
- Seri, B., Garcia-Verdugo, J. M., McEwen, B. S. and Alvarez-Buylla, A. (2001). Astrocytes give rise to new neurons in the adult mammalian hippocampus. *J. Neurosci.* **21**, 7153-7160.
- Taupin, P. and Gage, F. H. (2002). Adult neurogenesis and neural stem cells of the central nervous system in mammals. *J. Neurosci. Res.* **69**, 745-749.
- Temple, S. and Alvarez-Buylla, A. (1999). Stem cells in the adult mammalian central nervous system. *Curr. Opin. Neurobiol.* **9**, 135-141.
- Toledo-Rodriguez, M., Blumenfeld, B., Wu, C., Luo, J., Attali, B., Goodman, P. and Markram, H. (2004). Correlation maps allow neuronal electrical properties to be predicted from single-cell gene expression profiles in Rat neocortex. *Cereb. Cortex* **14**, 1310-1327.
- Traiffort, E., Charytoniuk, D., Watroba, L., Faure, H., Sales, N. and Ruat, M. (1999). Discrete localizations of hedgehog signalling components in the developing and adult rat nervous system. *Eur. J. Neurosci.* **11**, 3199-3214.
- van den Brink, G. R., Hardwick, J. C., Tytgat, G. N., Brink, M. A., Ten Kate, F. J., van Deventer, S. J. and Peppelenbosch, M. P. (2001). Sonic hedgehog regulates gastric gland morphogenesis in man and mouse. *Gastroenterology* **121**, 317-328.
- Wang, Y., Gupta, A., Toledo-Rodriguez, M., Wu, C. Z. and Markram, H. (2002). Anatomical, physiological, molecular and circuit properties of nest basket cells in the developing somatosensory cortex. *Cereb. Cortex* **12**, 395-410.
- Wallace, V. A. (1999). Purkinje-cell-derived Sonic hedgehog regulates granule neuron precursor cell proliferation in the developing mouse cerebellum. *Curr. Biol.* **9**, 445-448.
- Wechsler-Reya, R. J. and Scott, M. P. (1999). Control of neuronal precursor proliferation in the cerebellum by Sonic Hedgehog. *Neuron* **22**, 103-114.

# Sonic hedgehog regulates adult neural progenitor proliferation *in vitro* and *in vivo*

Karen Lai<sup>1</sup>, Brian K. Kaspar<sup>2</sup>, Fred H. Gage<sup>2</sup> and David V. Schaffer<sup>1</sup>

<sup>1</sup> Department of Chemical Engineering and The Helen Wills Neuroscience Institute, 201 Gilman Hall, University of California, Berkeley, California 94720-1462, USA

<sup>2</sup> Laboratory of Genetics, Salk Institute for Biological Studies, Box 85800, San Diego, California 92186-5800, USA

Correspondence should be addressed to D.V.S. (schaffer@cchem.berkeley.edu)

Published online 2 December 2002; doi:10.1038/nn983

Neural stem cells exist in the developing and adult nervous systems of all mammals, but the basic mechanisms that control their behavior are not yet well understood. Here, we investigated the role of Sonic hedgehog (Shh), a factor vital for neural development, in regulating adult hippocampal neural stem cells. We found high expression of the Shh receptor Patched in both the adult rat hippocampus and neural progenitor cells isolated from this region. In addition, Shh elicited a strong, dose-dependent proliferative response in progenitors *in vitro*. Furthermore, adeno-associated viral vector delivery of *shh* cDNA to the hippocampus elicited a 3.3-fold increase in cell proliferation. Finally, the pharmacological inhibitor of Shh signaling cyclopamine reduced hippocampal neural progenitor proliferation *in vivo*. This work identifies Shh as a regulator of adult hippocampal neural stem cells.

Within the subventricular zone<sup>1–3</sup> and hippocampal regions<sup>4–6</sup> of the adult mammalian brain, neural precursors continually proliferate and differentiate into the three major cell lineages of the central nervous system. Furthermore, cells isolated from regions where neurogenesis is not observed show the capacity for multipotent neural differentiation *in vitro* and *in vivo*, indicating the presence of quiescent neural stem cell populations<sup>7,8</sup>. Several fundamental questions about the biology of these cells require further investigation. Progress has been made in establishing that newly born neurons are functional<sup>9</sup>, but further study will be needed to elucidate the biological purpose for their existence. Furthermore, the identities and characteristics of the stem cells that give rise to these functional neurons in different regions must be determined<sup>10–12</sup>. Finally, the environmental conditions and signaling molecules that regulate adult neural stem cell survival, proliferation, axonal guidance and differentiation must be fully investigated<sup>13–16</sup>.

Sonic hedgehog (Shh) is a soluble signaling protein that was first discovered and analyzed for its ability to pattern cell differentiation in the neural tube and limb bud<sup>17</sup>. Shh activity has subsequently been found to be crucial in regulating numerous other processes in the developing nervous system, including midbrain and ventral forebrain neuronal differentiation and neuronal precursor proliferation<sup>17–22</sup>. Although there has been significant progress in understanding Shh regulation during development, little is known about its normal role in adults.

Here we investigated the possibility that Shh regulation of neural cell behavior continues from development into adulthood. We have determined that Shh is a potent mitogen for neural progenitor cells of the adult hippocampus. Rat hippocampal progenitors proliferated when cultured in Shh, and

clonal populations that expanded in Shh retained their multipotency. Furthermore, delivery of Shh to the hippocampus through the use of an adeno-associated viral (AAV) vector led to significant increases in cell proliferation *in vivo*. We also found that cyclopamine, a pharmacological inhibitor of Shh and a potential treatment for medulloblastomas involving mutations in Shh signaling<sup>23</sup>, markedly reduced neural progenitor proliferation in the hippocampus. Finally, we posit that Shh may be transported to the hippocampus, where it regulates progenitor function. This work provides evidence that Shh is a regulator of adult neural progenitor proliferation.

## RESULTS

### Patched expression

To investigate the potential role for Shh in the regulation of adult neural progenitor cells, we immunohistochemically stained adult rat brain sections for Shh signaling components. The Shh receptor Patched (Ptc) was expressed in the hippocampal formation, particularly within the hilar region, and in pyramidal cells of CA1 through CA3 (Fig. 1a). Preincubation of the primary antibody with a blocking peptide eliminated all staining (data not shown). The commercially available antibodies against Shh or Smoothened (Smo), a cellular transducer of Shh signaling, did not yield specific staining. However, the Ptc immunohistochemistry is consistent with reported *in situ* hybridization results, which detected both *ptc* and *smo* mRNA in the adult dentate gyrus, and to a lesser extent in CA1–CA3 (ref. 24).

We next addressed whether Shh could regulate hippocampal neural progenitors, previously isolated and expanded in fibroblast growth factor 2 (FGF-2; ref. 8). All cells that expressed nestin, a marker for immature neural cells<sup>25</sup>, also expressed Patched with

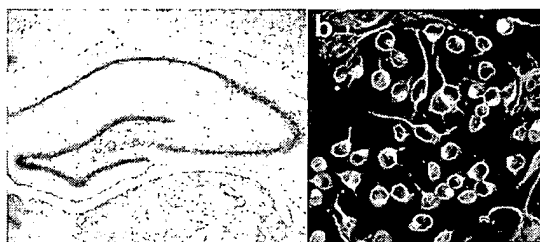


**Fig. 1.** Expression of Patched *in vitro* and *in vivo*. (a) Patched immunostaining in the adult rat hippocampus. (b) Progenitor cells were stained for Patched (red) and nestin (green), with nuclear counterstaining using DAPI (blue).

an apparent cell-surface localization (Fig. 1b). These results corroborate earlier work that used reverse transcription polymerase chain reaction (RT-PCR) to show that progenitor cell populations express *Ptc* and *Smo*<sup>26</sup>. To further confirm *Ptc* expression, we cloned rat *Ptc* and *Smo* by RT-PCR from progenitor cell total RNA. The full-length *ptc* cDNA sequence, which has not previously been reported, encodes a 1,434 amino acid protein with 99.1% identity to mouse and 95% identity to human *Ptc* protein (see Supplementary Fig. 1 online).

#### Shh-dependent cell proliferation *in vitro*

To further investigate a potential role for Shh in regulating progenitor cell function, progenitor cells were cultured in recombinant Shh, and preliminary work indicated that it stimulated cell proliferation. To further characterize this effect, cells were incubated in a range of concentrations. Cultures in 5–50 nM Shh proliferated robustly throughout the 8-day experiment, expanding by a factor of 170 at the highest concentration. In contrast, cells at 0 or 1 nM Shh did not expand (Fig. 2). The cell doubling time was 44 hours at 50 nM, though saturation was not yet reached at this dosage, a result that is in agreement with a reported EC<sub>50</sub> value of 18.5 nM for N-terminal Shh in cerebellar granule cell precursors<sup>21</sup>. By comparison, the doubling time in 20 ng/ml of FGF-2 was 28 hours (data not shown). The relatively high concentration needed for Shh may be due to the fact that recombinant Shh produced in bacteria is not as potent as the native, lipid-modified form. From these data, we conclude that Shh directly promotes progenitor proliferation *in vitro*.

#### Multipotency of clonal populations expanded in Shh

Although these results establish Shh as a mitogen for a population of cells derived from progenitors, it is unclear whether this factor expands multipotent cells or those that are already committed to a specific lineage. We therefore expanded individual cells into clonal populations for differentiation analysis. Individual cells were sorted into 96-well plates by flow cytometry, with approximately 60% cell viability just after sorting. FGF-2 requires an autocrine cofactor, a glycosylated form of cystatin C, for stimulating neural stem cell proliferation, particularly at low density where this factor becomes limiting<sup>16</sup>. To determine whether progenitors grown in Shh share a similar requirement, both fresh media and media previously conditioned for 24 hours by high-density cultures growing in Shh were used for the expansion of the clones. Out of 30 possible clones, no progenitors survived in the absence of recombinant Shh. However, individual cells cultured solely with 50 nM Shh, in either fresh or conditioned media, were able to survive and proliferate into clonal

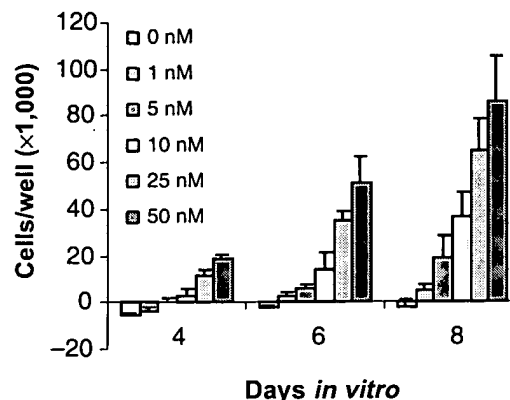


**Fig. 2.** Shh induction of neural progenitor cell proliferation *in vitro*. Cells were expanded at the concentrations and times indicated, and the final cell number per well is plotted. Each value represents the average of three points compared to the standard curve, with error bars representing standard deviations.

populations. From a total of 96 wells, 19 clones expanded and were stored for further study.

To assess multipotency, 7 of the 19 clonal populations were exposed to differentiating conditions and immunofluorescently stained for the presence of lineage-specific markers<sup>27</sup>. Nearly all (6 of 7) developed into neurons and glia, as indicated by the expression of the neuronal antigen  $\beta$ III-tubulin and the astrocytic marker glial fibrillary acidic protein (GFAP; Fig. 3a and b). Parallel stains for the marker O4 indicated that the Shh-expanded cells were also capable of differentiating into an oligodendrocyte lineage (Fig. 3c). These results established that clones expanded in Shh plus fresh or conditioned media (Fig. 3a–e) maintained their multipotency and also indicated that Shh activity toward progenitor cells does not seem to require a cofactor.

#### Mitogenic effect of Shh *in vivo*

The expression of *Ptc* in the dentate gyrus of adult rats suggests that Shh may regulate progenitor proliferation *in vivo* as well as *in vitro*. To test this possibility, cDNA encoding the N-terminal active fragment of rat Shh was inserted into a recombinant AAV vector, which was produced at a titer of  $4 \times 10^{12}$  particles/ml. In contrast to adenoviral vectors, AAV vectors are gutted of all viral genes and lead to highly efficient gene delivery with essentially no toxicity, immunogenicity or other aberrant effects on cell function<sup>28,29</sup>. To confirm that cells infected with this virus produced Shh, human embryonic kidney (HEK-293) cells were infected with rAAV-Shh or rAAV-GFP virus containing green fluorescent protein (GFP) cDNA also at a titer of  $4 \times 10^{12}$  particles/ml. Subsequent western blotting analysis of cell lysate and media showed that the 20 kDa Shh was present only in cultures infected with the Shh virus (data not shown).

Next, rAAV-Shh, or rAAV-GFP as a control, was stereotactically injected into the dentate gyrus of adult rats ( $n = 8$ ). After a two-week period for viral genome processing<sup>28,29</sup>, two animals were killed to confirm GFP and Shh expression. rAAV-GFP injection into the hippocampus resulted in high levels of transgene expression, confirming the high titer of the virus and the fact that the injection site was within the hilar region of the dentate gyrus (Fig. 4a). As commercially available Shh antibodies do not yield specific immunohistochemical staining<sup>30</sup>, we used RT-PCR to

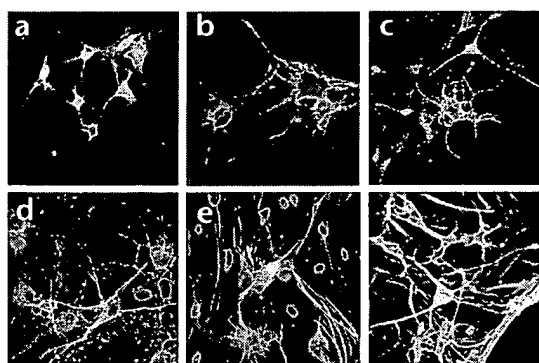


**Fig. 3.** Differentiation of clonal cell populations expanded in Shh. Cells from a differentiated clonal population were stained to detect (a) ̢III-tubulin, a neuronal marker (green), (b) GFAP antibody, an astrocytic marker (red) and (c) O4, an oligodendrocytic marker (green). Nuclei were counterstained with TO-PRO3 (blue). Results from three additional individual clones were simultaneously stained to detect ̢III-tubulin (green), GFAP (red) and TO-PRO3 (blue). (d) A clonal population expanded in Shh-conditioned media with 50 nM Shh. (e, f) Clonal populations expanded in fresh media with 50 nM Shh.

detect a viral message (Fig. 4b). With primers flanking the ̢-globin intron, amplification from single- or double-stranded viral genomic DNA generates a 1,400 base pair (bp) product encompassing the intron and the *shh* cDNA, whereas mRNA that has been processed to excise the intron yields a smaller 800 bp product. As indicated by the presence of an 800 bp band in lane 2, rAAV injection into the hippocampus yielded recombinant *shh* mRNA. In contrast, RT-PCR of tissue from the cerebellum of the same animal, as well as from the hippocampus and cerebellum of control animals injected with rAAV-GFP, did not yield a product. Also, PCR of mRNA that had not undergone reverse transcription did not generate a product in any samples. These results indicate that rAAV injection into the hippocampus leads to recombinant *shh* mRNA transcription.

The remaining animals ( $n = 6$ ) were injected with the mitotic marker bromo-deoxyuridine (BrdU) for 8 days and killed on the ninth. Tissue sections (40  $\mu$ m) were then stained for BrdU and NeuN by immunofluorescence and analyzed by fluorescence confocal microscopy. Both animal groups had significant numbers of cells that had undergone mitosis within the subgranular zone of the dentate gyrus, consistent with earlier results<sup>4–6</sup> (Fig. 4d and e). However, whereas rAAV-GFP animals had an average of  $15.6 \pm 3.0$  BrdU-positive nuclei per section, animals injected with rAAV-Shh had  $52.1 \pm 9.1$  cells, a robust 3.33-fold increase in cell proliferation ( $P < 0.01$ ; Fig. 4c).

To determine the long-term fate of proliferating cells, a second group of animals ( $n = 6$ ) was treated as described above, but were killed three weeks after the last BrdU injection. The average number of BrdU<sup>+</sup> cells per section dropped significantly over this time period to  $16.3 \pm 4.5$  in rAAV-Shh animals and to  $8.9 \pm 1.0$  in AAV-GFP animals, and the 1.8-fold higher value in the Shh animals was statistically significant ( $P < 0.05$ ). Tissue sections stained for BrdU and NeuN showed that a significant number of cells that divided during the course of the BrdU injection subsequently migrated into the granule cell layer and differentiated into NeuN<sup>+</sup> neurons (Fig. 5a and b). The average number of BrdU<sup>+</sup>/NeuN<sup>+</sup> cells per section was  $7.1 \pm 0.7$  and  $2.2 \pm 0.7$  for Shh and GFP, respectively, a three-fold difference ( $P < 0.01$ ;

Fig. 5c). The fractions of BrdU<sup>+</sup> cells that differentiated into neurons were 43% for AAV-Shh and 25% for AAV-GFP, although these percentages were not statistically different ( $P = 0.063$ ). These results confirm that Shh is a mitogen for adult hippocampal neural progenitors *in vivo* as well as *in vitro*.

### Inhibition of Shh

We next assessed whether inhibiting this potential endogenous Shh signaling in the hippocampus would reduce the proliferation of neural progenitor cells. Two micrograms of cyclopamine, a pharmacological inhibitor of Shh signaling<sup>23</sup>, were complexed with the vehicle cyclodextrin (HBC) and injected into the hippocampus. HBC has been used extensively to increase the solubility of hydrophobic compounds for delivery to the brain and hippocampus, with no observed side effects<sup>22,31</sup>. After injection with cyclopamine or vehicle alone, followed by 3 days of BrdU injections, hippocampal sections adjacent to the injection site were analyzed. BrdU counts were high, probably owing to the twice-daily injections. Cyclopamine reduced the proliferation of neural progenitor cells in the dentate gyrus to half of that in animals injected with vehicle (Fig. 6). Furthermore, addition of 1  $\mu$ g/ml cyclopamine to progenitor cells in culture reduced their proliferation in response to 50 nM Shh by more than nine-fold, as compared to the vehicle control (data not shown).

Shh protein, but not mRNA, has been detected in the hippocampus. However, Shh is expressed at high levels in the basal forebrain<sup>24,30</sup>, which projects to the hippocampus via the fornix. Furthermore, anterograde axonal transport of both *Drosophila* Hedgehog (Hh) and Shh has been detected<sup>30,32</sup>. To address whether the anterograde transport of Shh via the fornix may regulate progenitor proliferation, BrdU uptake in the hippocampus was analyzed in animals receiving fimbria-fornix lesions. Progenitor proliferation was significantly reduced in lesioned animals, and the injection of cyclopamine into lesioned animals did not further reduce progenitor proliferation in these animals (Fig. 6).

### DISCUSSION

In the present study, we have shown that Sonic hedgehog regulates the proliferation of progenitor cells of the adult rat hippocampus *in vitro* and *in vivo*. Although its numerous and important functions during development have been investigated, little is known about Shh's role in adults. We observed that the Shh receptor Patched is expressed in the dentate gyrus and Ammon's horn of the hippocampal formation of adult rats (Fig. 1), in agreement with *in situ* hybridization that showed high levels of Patched message in the granule cells, and, to a lesser extent, in the pyramidal cell layers<sup>24</sup>. In addition, progenitor cells isolated from the hippocampus, which apparently derive from the subgranular zone of the dentate gyrus<sup>6</sup>, also express Patched. We also cloned and sequenced rat Patched from progenitor cell cultures, a sequence not previously reported in its entirety.

Although Shh signal transducers were clearly present in adult hippocampal progenitor cells, Shh activity could have a variety of potential effects in these cells. In different contexts during development, Shh regulates neural stem cell differentiation, survival and proliferation. In the spinal cord, Shh governs progenitor cell differentiation into floor plate cells, motor neurons and interneurons in a dose-dependent fashion<sup>33</sup>. It also regulates midbrain and forebrain dopaminergic and serotonergic neuronal differentiation<sup>20,34</sup>. In other contexts, however, Shh promotes differentiation into oligodendrocytes<sup>35</sup> and astroglia<sup>36</sup>. In addition to regulating differentiation, Shh is a mitogen for



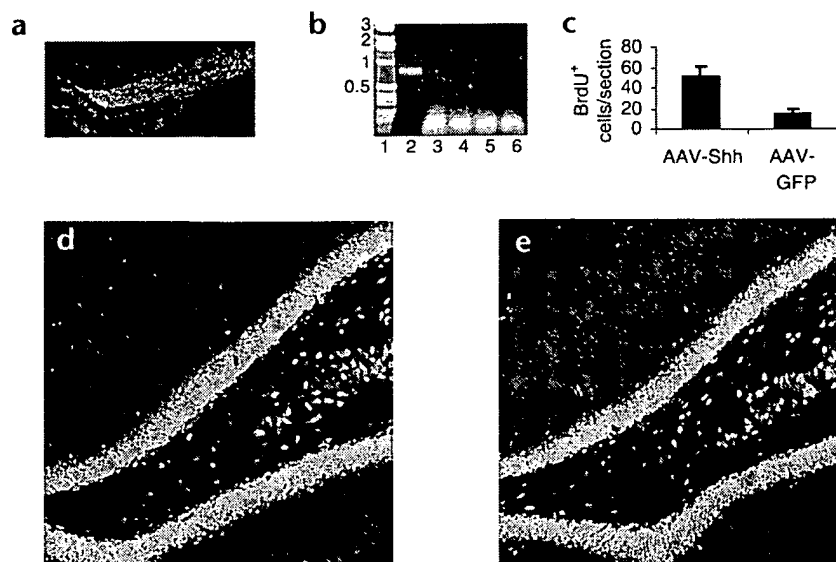


**Fig. 4.** Shh induction of progenitor proliferation *in vivo*. (a) Direct GFP fluorescence in the hilar region of the dentate gyrus after injection of rAAV-GFP. (b) RT-PCR analysis of rAAV-Shh transcription. Lane 1, DNA standard, with sizes indicated in kilobases; lane 2, hippocampal mRNA of an animal injected with rAAV-Shh; lane 3, hippocampal mRNA of an animal injected with rAAV-Shh, with no reverse transcription; lane 4, hippocampal mRNA of an animal injected with rAAV-GFP; lane 5, hippocampal mRNA of an animal injected with rAAV-GFP, with no reverse transcription; lane 6, cerebellar mRNA of an animal injected with rAAV-Shh. (c) The average number of cells in the hilus per section in which BrdU was detected in each animal group (total  $n = 6$ ) is plotted. The asterisk indicates the values are significantly different ( $P < 0.05$ ). Representative images of BrdU (red) and NeuN (green) staining within the dentate gyrus are shown for an animal injected with (d) rAAV-Shh or (e) rAAV-GFP.

cerebellar granule neurons and neocortical and spinal precursors during development<sup>17,37</sup>.

Addition of recombinant Shh to adult hippocampal progenitor cells elicited potent time- and dose-dependent proliferation, whereas cells died in the absence of Shh (Fig. 2). The target of Shh activity was a multipotent neural progenitor cell, as clonal populations still had the capacity for differentiation into the three major CNS cell lineages (Fig. 3). This finding establishes Shh as the first known factor capable of clonal expansion of adult hippocampal neural progenitor cells in the absence of autocrine factors in conditioned media. Furthermore, adeno-associated viral vector delivery of *shh* cDNA to the rat hippocampus led to a greater than three-fold increase in the number of newly born cells in the dentate gyrus of adult rats (Fig. 4). Finally, progenitor cells that divided after rAAV-Shh injection later underwent differentiation into granule cell neurons (Fig. 5). There was a three-fold higher number of NeuN<sup>+</sup>/BrdU<sup>+</sup> cells in the Shh animals as compared to the GFP controls; however, the fraction of cells that differentiated into neurons in each case was not statistically different, indicating that Shh does not bias cells toward a neuronal lineage.

Whereas the addition of exogenous Shh stimulated neural progenitor proliferation *in vitro* and *in vivo*, this result does not address the question of whether endogenous Shh is normally involved in regulating hippocampal progenitor function. Cyclopamine, a natural inhibitor of Shh signaling, has been used to elucidate Shh's role in a number of processes, including early brain expansion and medulloblastoma growth<sup>22,23</sup>. We found that the introduction of cyclopamine into the hippocampus repressed cell proliferation in the subgranular zone by a factor of two, indicating that endogenous Shh signaling is involved in adult progenitor expansion (Fig. 6). Furthermore, this finding

reveals a potential side effect for the recently proposed use of Shh in the treatment of medulloblastoma<sup>23</sup>.

Shh could induce progenitor proliferation by a number of intracellular mechanisms. Binding of Shh to Ptc releases this receptor's repression of Smo, which then transduces the signal by acting on the transcription factors of the Gli family. The transcriptionally activating Gli forms then upregulate Shh targets, including *ptc*, *gli1*, *gli2* and *shh* itself<sup>17</sup>. Shh signaling may directly regulate the cell cycle, as it can upregulate the expression of G1-phase cyclins of type D and E, and Patched can act directly on the G2-phase cyclin B<sup>17</sup>. Alternatively, Shh activity may activate other signaling systems that control cell proliferation. Gli1 upregulates platelet-derived growth factor receptor  $\alpha$  (PDGFR $\alpha$ ) expression to promote basal cell carcinoma expansion<sup>38</sup>. Moreover, *igf-2* is a known Shh transcriptional target, and Shh could therefore act upstream of this family of growth factors to induce cell proliferation<sup>14,39</sup>.

Shh's proliferative effect in adult hippocampal neural stem cells is analogous to its regulation of cerebellar granule cell precursors during development, but with several distinctions. First, in contrast to the hippocampus, neurogenesis does not occur in the adult cerebellum. Second, Shh acts upon granule neuron precursors in the cerebellum, whereas adult hippocampal progenitors are multipotent. Further work is required, however, to identify the precise cellular target of Shh within the hippocampus<sup>11</sup>. Finally, although defects in Shh signaling have led to medulloblastomas, we did not find tumors in the hippocampus. This could indicate that in regions with ongoing adult neurogenesis, cell proliferation is balanced by signals that regulate differentiation and death.

We also probed the potential cellular source of Shh in the hippocampus. Shh is expressed in the dentate gyrus of E15 mice for an unknown function<sup>40</sup>, but its transcripts are not present

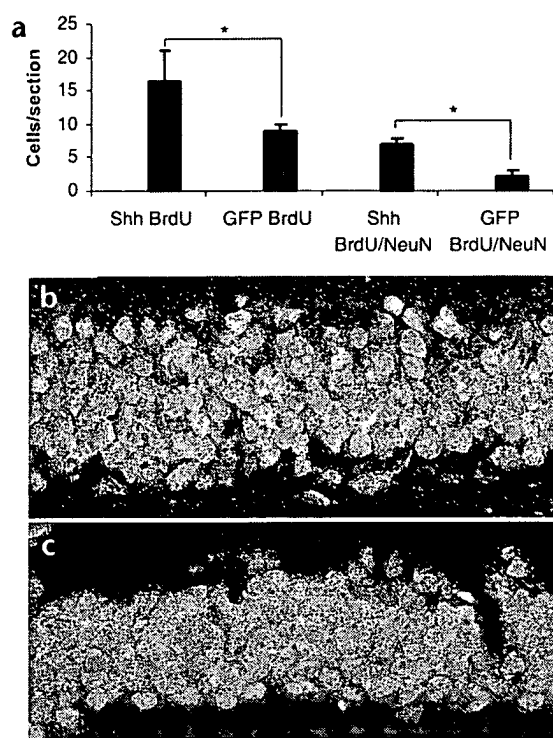


**Fig. 5.** Progenitor cell differentiation. (a) Quantification of the average number of cells in the dentate gyrus and hilar region per section that are BrdU<sup>+</sup> and BrdU<sup>+</sup>/NeuN<sup>+</sup> three weeks after the completion of BrdU injections (\**P* < 0.05). Representative images of the granule cell layer in animals injected with (b) AAV-Shh and (c) AAV-GFP, stained for the analysis of BrdU uptake (red) and differentiation into NeuN<sup>+</sup> neurons (green).

at detectable levels in the adult hippocampus<sup>24</sup>. In contrast, Shh is expressed at high levels in several structures of the adult basal forebrain<sup>24</sup> that are known to project to the dentate gyrus<sup>41</sup>. In addition, like the neurotrophins BDNF and NT-3, *Drosophila* Hh and Shh can undergo anterograde axonal transport along projections from the retina to the brain<sup>30,32,42</sup>. Finally, Shh protein is present in the adult hamster hippocampus<sup>30</sup>. These considerations collectively raise the intriguing possibility that the basal forebrain may regulate adult neurogenesis by transporting Shh to the hippocampus. In support of this possibility, we found that a lesion of the fimbria-fornix, which would block such Shh transport, significantly reduced neural progenitor proliferation, and that the introduction of cyclopamine into the hippocampus of lesioned animals did not further inhibit this proliferation (Fig. 6). Although this lesion disrupts both basal forebrain and other hippocampal inputs, these results support the hypothesis that Shh transport into the hippocampus regulates adult neural progenitor expansion.

Relatively few factors are known to regulate adult neural stem cell function. Conditions such as an enriched environment and exercise upregulate hippocampal neurogenesis<sup>13,43</sup>. At the molecular level, FGF-2 was first used to expand progenitors, and its required autocrine cofactor, cystatin C, was recently discovered<sup>16</sup>. In addition, peripheral administration of IGF-1 stimulates hippocampal progenitor proliferation<sup>14</sup>, and heparin-binding EGF apparently mediates increased neurogenesis in response to

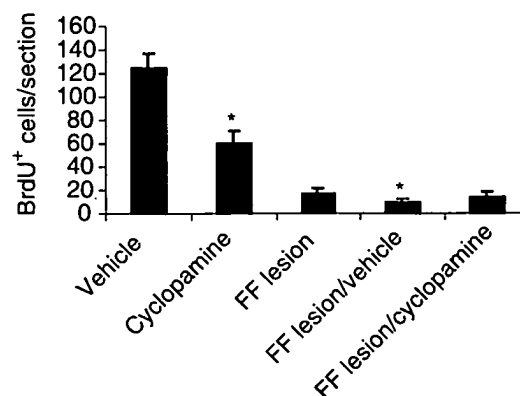


**Fig. 6.** Inhibition of Shh. BrdU uptake was analyzed in animals injected with cyclopamine or vehicle, in some cases after fimbria-fornix (FF) lesion. The average number of cells in the hilar region per section in which BrdU was detected under each condition (*n* = 3 animals each; \**P* < 0.05).

ischemia<sup>44</sup>, whereas glucocorticoids downregulate neurogenesis<sup>45</sup>. By comparison, EGF and ephrins induce the proliferation of adult stem cells from the subventricular zone<sup>3,46</sup>. Whether Shh also regulates subventricular zone progenitor proliferation will require additional study.

The fact that multiple factors modulate neural stem and/or progenitor cell proliferation raises the possibility that they act in concert to regulate distinct steps in the progression of the cell to a terminally differentiated phenotype. For example, we propose a model in which FGF-2 is a general survival factor and mitogen for early, immature neural stem cells<sup>8,16</sup>. Additional factors such as Shh and IGF-1 may support the survival and proliferation of these cells and prepare them for differentiative instructions, such as neurotrophins for a neuronal fate or Notch for an astrocytic fate<sup>27,47</sup>. In addition to regulating sequential steps in the progenitor cell life cycle, these multiple factors could offer several points of either local or distant control over stem cell proliferation and neurogenesis. It is known that neurotrophins that undergo anterograde transport are released from presynaptic terminals in an activity-dependent manner to modulate synaptic properties<sup>42</sup>. In the basal forebrain, Shh appears to be expressed primarily by GABAergic neurons<sup>24</sup>. One possibility is that the activity-dependent synthesis or secretion of Shh into the hippocampus by these cells may be a mechanism for regulating neurogenesis, and thus modulates the processing of memories within these two structures.

In summary, we found that Shh, a signaling molecule that is well known for its control of numerous processes during development, regulates the proliferation of adult hippocampal neural stem cells *in vitro* and *in vivo*. To our knowledge, this represents the first known normal function of Shh in the adult nervous system and one of the few demonstrated functions of Shh in adult organisms<sup>48</sup>. Furthermore, the transport of signaling factors to neurogenic zones may represent a new mechanism for the control and regulation of adult neurogenesis. Finally, as few factors are known to directly stimulate neural progenitor proliferation in culture and *in vivo*, this finding of a proliferative effect of Shh in the adult nervous system may have therapeutic implications for regeneration of neural tissue in neurodegenerative disorders.

## METHODS

**Neural progenitor cell isolation and culture.** Neural progenitors were isolated and cultured from the hippocampi of adult female Fischer 344 rats as previously described<sup>8</sup>. Cells were propagated on culture plates (Becton Dickinson, Franklin Lakes, New Jersey) that were coated with poly-ornithine (Sigma-Aldrich, St. Louis, Missouri) and mouse laminin (Invitrogen, Carlsbad, California) in HAMS F-12/DMEM media with N2 supplement and 20 ng/ml of FGF-2 (Invitrogen). Animal protocols were approved by the UCB Animal Care and Use Committee in accordance with NIH guidelines.

**Recombinant Shh growth assay and clonal expansion.** Recombinant rat Shh encompassing amino acids 25–198 was produced in *E. coli*. Progenitors were plated at a density of 500 cells/well in coated 96-well plates (Becton Dickinson). Recombinant Shh at a range of 0–50 nM was added to the cells, which were then incubated for a period of 8 d with an 80% media change every other day. Cell proliferation was assayed using the WST-1 reagent (Roche, Pleasanton, California) following the manufacturer's instructions and using a Bio-Tek Instruments spectrophotometer.

For clonal expansion, progenitor cultures were first expanded for 6 d in 1 µg/ml (50 nM) of Shh and then individually sorted into coated 96-well plates by flow cytometry (Becton Dickinson). These single cells were then expanded in 1 µg/ml Shh in either fresh N2 medium or a 50:50 mixture of fresh and N2 + Shh media previously conditioned by high-density progenitor cultures. Surviving clones were expanded by a factor of 10<sup>6</sup> before cryopreservation. For differentiation studies, cells were plated at a density of 2,500 cells/cm<sup>2</sup> onto coated 8-well chamber slides (Becton Dickinson). After 24–48 h in Shh-supplemented media, cells were switched into 0.2 µM retinoic acid, 5 µM forskolin (Biomol, Plymouth Meeting, Pennsylvania) and 0.5% fetal bovine serum (BioWhittaker, Walkersville, Maryland) to induce cell differentiation<sup>27</sup> for 10–14 d.

**Immunofluorescent staining.** Cells were fixed in 4% paraformaldehyde (Sigma-Aldrich), dissolved in phosphate-buffered saline (PBS), and blocking and staining were performed in Tris-buffered saline containing 0.3% Triton X-100 and 5% donkey serum (Santa Cruz Biotechnology, Santa Cruz, California). The following primary antibodies were used: mouse anti-β-tubulin III (1:500; Sigma-Aldrich), guinea pig anti-glial fibrillary acidic protein (1:1,000; Advanced Immunochemical, Long Beach, California), mouse anti-O4 (1:2; gift from O. Boegler), mouse anti-nerfin (1:1,000; Becton Dickinson) and goat anti-Patched (1:500; Santa Cruz Biotechnology). Detection of primary antibodies was performed with Alexa fluorochrome-conjugated secondary antibodies (Molecular Probes, Eugene, Oregon) at a dilution of 1:250. Nuclei were stained with the nuclear marker TO-PRO3 (Molecular Probes). Images were captured by fluorescent confocal microscopy (Leica Microsystems, Wetzlar, Germany). Sections of adult rat brains, which had been previously generated as described below, were stained for the presence of Patched using anti-Patched antibody (1:1,000; Santa Cruz) and biotinylated anti-goat IgG (Jackson ImmunoResearch, West Grove, Pennsylvania), with diaminobenzidine as a chromagen as described<sup>13</sup>. Images were analyzed on a Nikon Eclipse microscope (Nikon, Melville, New York).

**Adeno-associated viral vector production.** Recombinant AAV-2 using the CMV promoter to drive expression of the enhanced GFP (Becton Dickinson) or rat *shh* cDNA encoding the N-terminal active polypeptide with secretion signal peptide was produced. Virus was generated by calcium phosphate transient transfection of the vector plasmid and pAAV/Ad8 helper plasmid<sup>49</sup> into HEK-293 cells (ATCC, Manassas, Virginia), followed by infection with adenovirus dl312 (MOI 2.0). Purification and titering were conducted as previously described<sup>28,29</sup>. HEK-293 cells were infected with adeno-associated virus carrying the Shh cDNA (rAAV-Shh) at a multiplicity of infection of 10, and after two days, western blotting was performed on cell lysates and cell culture media to detect the presence of recombinant Shh protein using anti-Shh primary (Santa Cruz), anti-goat IgG HRP (Jackson) and ECL detection (Amersham-Pharmacia, Piscataway, New Jersey).

**Animal surgeries and immunohistochemistry.** Recombinant AAV was stereotactically injected into the hippocampus (anteroposterior axis, −3.5; mediolateral axis, ±3.0; dorsoventral axis, −3.9 from skull, with nose bar at 3 mm up) of anesthetized female Fischer-344 rats (150–165 g). After two weeks, rats were administered a daily, intraperitoneal injection of BrdU (50 mg/kg, Sigma-Aldrich) for 8 d. Either the next day, or three weeks later, animals were perfused (4% paraformaldehyde), and the brains were excised, stored in fixative overnight, and transferred to 30% sucrose. Coronal sections (40 µm) were cut on a sliding microtome, and GFP fluorescence was visualized directly. Sections were processed for BrdU immunohistochemical staining as previously described<sup>13</sup> and stained using rat anti-BrdU (1:400; Accurate, Harlan Sera-Lab, Loughborough, England), biotinylated donkey anti-rat IgG (Jackson), and streptavidin-Cy3 (Jackson) in addition to mouse anti-NeuN (1:20; from R. J. Mullen, University of Utah) and FITC-labeled donkey anti-mouse IgG (Jackson). In some samples, staining was also conducted for GFAP (Advanced Immunochemical). Results were analyzed for statistical significance using the ANOVA test and are reported with standard deviations.

Animals received a lesion of the fimbria-fornix as previously described<sup>50</sup>. Cyclopamine (Toronto Research Chemicals, Toronto, Canada) was dissolved in 45% (w/v) 2-hydroxypropyl-β-cyclodextrin (HBC, Sigma-Aldrich) in PBS. Two groups received a 2 µl injection of either cyclopamine or HBC vehicle into the hippocampus as described above. After 24 h, animals were injected with BrdU (50 mg/kg) every 12 h for the next 72 h.

**RT-PCR.** Animals (*n* = 2) received hippocampal rAAV-Shh or rAAV-GFP injections as described above. After two weeks, hippocampi were excised using RNase-free materials and reagents. Reverse transcription was performed as described previously<sup>29</sup>. The 5' primer (GTGGATCCTGA-GAACTTCAG), homologous to the 5' untranslated region of the rAAV-Shh transcript, and the 3' primer (GCCGCCAGATTGGCCGC-CACGGAGT), homologous to Shh, flank a human β-globin intron that is spliced from the mRNA. For Patched cloning, RNA from progenitor cells was subjected to RT-PCR using primers based on the known mouse sequence (GenBank #6679518). The products of three independent RT-PCR reactions were cloned and sequenced.

*Note: Supplementary information is available on the Nature Neuroscience website.*

## Acknowledgments

We thank L. Hinh, D. Chui, N. Sherkat, L. Frost and M. Lucero for technical assistance. We also thank M.L. Gage for critical reading of the manuscript. This work was initiated with National Institutes of Health NRSA support to D.S. It was funded by an Office of Naval Research Young Investigator Grant to D.S. and a National Science Foundation graduate fellowship to K.L.

## Competing interests statement

The authors declare that they have no competing financial interests.

RECEIVED 30 SEPTEMBER; ACCEPTED 13 NOVEMBER 2002

1. Reynolds, B.A. & Weiss, S. Generation of neurons and astrocytes from isolated cells of the adult mammalian central nervous system. *Science* 255, 1707–1710 (1992).
2. Lois, C. & Alvarez-Buylla, A. Proliferating subventricular zone cells in the adult mammalian forebrain can differentiate into neurons and glia. *Proc. Natl. Acad. Sci. USA* 90, 2074–2077 (1993).
3. Weiss, S. *et al.* Is there a neural stem cell in the mammalian forebrain? *Trends Neurosci.* 19, 387–393 (1996).
4. Altman, J. & Das, G.D. Autoradiographic and histological evidence of postnatal hippocampal neurogenesis in rats. *J. Comp. Neurol.* 124, 319–335 (1965).
5. Kaplan, M.S. & Hinds, J.W. Neurogenesis in the adult rat: electron microscopic analysis of light radioautographs. *Science* 197, 1092–1094 (1977).
6. Gage, F.H., Kempermann, G., Palmer, T.D., Peterson, D.A. & Ray, J. Multipotent progenitor cells in the adult dentate gyrus. *J. Neurobiol.* 36, 249–266 (1998).

7. Weiss, S. *et al.* Multipotent CNS stem cells are present in the adult mammalian spinal cord and ventricular neuroaxis. *J. Neurosci.* 16, 7599–7609 (1996).
8. Palmer, T.D., Markakis, E.A., Willhoite, A.R., Safar, F. & Gage, F.H. Fibroblast growth factor-2 activates a latent neurogenic program in neural stem cells from diverse regions of the adult CNS. *J. Neurosci.* 19, 8487–8497 (1999).
9. van Praag, H. *et al.* Functional neurogenesis in the adult hippocampus. *Nature* 415, 1030–1034 (2002).
10. Doetsch, F., Caille, L., Lim, D.A., Garcia-Verdugo, J.M. & Alvarez-Buylla, A. Subventricular zone astrocytes are neural stem cells in the adult mammalian brain. *Cell* 97, 703–716 (1999).
11. Seri, B., Garcia-Verdugo, J.M., McEwen, B.S. & Alvarez-Buylla, A. Astrocytes give rise to new neurons in the adult mammalian hippocampus. *J. Neurosci.* 21, 7153–7160 (2001).
12. Hitoshi, S., Tropepe, V., Ekker, M. & van der Kooy, D. Neural stem cell lineages are regionally specified, but not committed, within distinct compartments of the developing brain. *Development* 129, 233–244 (2002).
13. Kempermann, G., Kuhn, H.G. & Gage, F.H. More hippocampal neurons in adult mice living in an enriched environment. *Nature* 386, 493–495 (1997).
14. Aberg, M.A., Aberg, N.D., Hedbacker, H., Oscarsson, J. & Eriksson, P.S. Peripheral infusion of IGF-I selectively induces neurogenesis in the adult rat hippocampus. *J. Neurosci.* 20, 2896–2903 (2000).
15. Lim, D.A. *et al.* Noggin antagonizes BMP signaling to create a niche for adult neurogenesis. *Neuron* 28, 713–726 (2000).
16. Taupin, P. *et al.* FGF-2-responsive neural stem cell proliferation requires CCG, a novel autocrine/paracrine cofactor. *Neuron* 28, 385–397 (2000).
17. Ruiz, I.A.A., Palma, V. & Dahmane, N. Hedgehog-Gli signalling and the growth of the brain. *Nat. Rev. Neurosci.* 3, 24–33 (2002).
18. Chiang, C. *et al.* Cyclopia and defective axial patterning in mice lacking Sonic hedgehog gene function. *Nature* 383, 407–413 (1996).
19. Ericson, J. *et al.* Sonic Hedgehog induces the differentiation of ventral forebrain neurons: a common signal for ventral patterning within the neural tube. *Cell* 81, 747–756 (1995).
20. Hynes, M. *et al.* Induction of midbrain dopaminergic neurons by Sonic Hedgehog. *Neuron* 15, 35–44 (1995).
21. Wechsler-Reya, R.J. & Scott, M.P. Control of neuronal precursor proliferation in the cerebellum by Sonic Hedgehog. *Neuron* 22, 103–114 (1999).
22. Britto, L., Tannahill, D. & Keynes, R. A critical role for Sonic hedgehog signaling in the early expansion of the developing brain. *Nat. Neurosci.* 5, 103–110 (2002).
23. Berman, D. M. *et al.* Medulloblastoma growth inhibition by Hedgehog pathway blockade. *Science* 297, 1559–1561 (2002).
24. Traiffort, E. *et al.* Discrete localizations of Hedgehog signalling components in the developing and adult rat nervous system. *Eur. J. Neurosci.* 11, 3199–3214 (1999).
25. Lendahl, U., Zimmerman, L.B. & McKay, R.D. CNS stem cells express a new class of intermediate filament protein. *Cell* 60, 585–595 (1990).
26. Sakurada, K., Ohshima-Sakurada, M., Palmer, T.D. & Gage, F.H. Nurrl, an orphan nuclear receptor, is a transcriptional activator of endogenous tyrosine hydroxylase in neural progenitor cells derived from the adult brain. *Development* 126, 4017–4026 (1999).
27. Palmer, T.D., Takahashi, J. & Gage, F.H. The adult rat hippocampus contains primordial neural stem cells. *Mol. Cell. Neurosci.* 8, 389–404 (1997).
28. Kaspar, B.K. *et al.* Adeno-associated virus effectively mediates conditional gene modification in the brain. *Proc. Natl. Acad. Sci. USA* 99, 2320–2325 (2002).
29. Kaspar, B.K. *et al.* Targeted retrograde gene delivery for neuronal protection. *Mol. Ther.* 5, 50–56 (2002).
30. Traiffort, E., Moya, K.L., Faure, H., Hassig, R. & Ruat, M. High expression and anterograde axonal transport of aminoterminal Sonic Hedgehog in the adult hamster brain. *Eur. J. Neurosci.* 14, 839–850 (2001).
31. Uekama, K., Hirayama, F. & Irie, T. Cyclodextrin drug carrier systems. *Chem. Rev.* 98, 2045–2076 (1998).
32. Huang, Z. & Kunes, S. Signals transmitted along retinal axons in *Drosophila*: Hedgehog signal reception and the cell circuitry of lamina cartridge assembly. *Development* 125, 3753–3764 (1998).
33. Jessell, T.M. Neuronal specification in the spinal cord: inductive signals and transcriptional codes. *Nat. Rev. Genet.* 1, 20–29 (2000).
34. Ye, W., Shimamura, K., Rubenstein, J.L., Hynes, M.A. & Rosenthal, A. FGF and Shh signals control dopaminergic and serotonergic cell fate in the anterior neural plate. *Cell* 93, 755–766 (1998).
35. Poncet, C. *et al.* Induction of oligodendrocyte progenitors in the trunk neural tube by ventralizing signals: effects of notochord and floor plate grafts, and of Sonic Hedgehog. *Mech. Dev.* 60, 13–32 (1996).
36. Dahmane, N. & Ruiz-i-Altaba, A. Sonic Hedgehog regulates the growth and patterning of the cerebellum. *Development* 126, 3089–3100 (1999).
37. Rowitch, D.H. *et al.* Sonic Hedgehog regulates proliferation and inhibits differentiation of CNS precursor cells. *J. Neurosci.* 19, 8954–8965 (1999).
38. Xie, J. *et al.* A role of PDGFR $\alpha$  in basal cell carcinoma proliferation. *Proc. Natl. Acad. Sci. USA* 98, 9255–9259 (2001).
39. Hahn, H. *et al.* Patched target Igf2 is indispensable for the formation of medulloblastoma and rhabdomyosarcoma. *J. Biol. Chem.* 275, 28341–28344 (2000).
40. Dahmane, N. *et al.* The Sonic Hedgehog-Gli pathway regulates dorsal brain growth and tumorigenesis. *Development* 128, 5201–5212 (2001).
41. Amaral, D.G. & Kurz, I. An analysis of the origins of the cholinergic and noncholinergic septal projections to the hippocampal formation of the rat. *J. Comp. Neurol.* 240, 37–59 (1985).
42. Altar, C.A. & DiStefano, P.S. Neurotrophin trafficking by anterograde transport. *Trends Neurosci.* 21, 433–437 (1998).
43. van Praag, H., Kempermann, G. & Gage, F.H. Running increases cell proliferation and neurogenesis in the adult mouse dentate gyrus. *Nat. Neurosci.* 2, 266–270 (1999).
44. Jin, K. *et al.* Heparin-binding epidermal growth factor-like growth factor: hypoxia-inducible expression *in vitro* and stimulation of neurogenesis *in vitro* and *in vivo*. *J. Neurosci.* 22, 5365–5373 (2002).
45. Gould, E., McEwen, B.S., Tanapat, P., Galea, L.A. & Fuchs, E. Neurogenesis in the dentate gyrus of the adult tree shrew is regulated by psychosocial stress and NMDA receptor activation. *J. Neurosci.* 17, 2492–2498 (1997).
46. Conover, J.C. *et al.* Disruption of Eph/ephrin signaling affects migration and proliferation in the adult subventricular zone. *Nat. Neurosci.* 3, 1091–1097 (2000).
47. Tanigaki, K. *et al.* Notch1 and Notch3 instructively restrict bFGF-responsive multipotent neural progenitor cells to an astroglial fate. *Neuron* 29, 45–55 (2001).
48. Pola, R. *et al.* The morphogen Sonic Hedgehog is an indirect angiogenic agent upregulating two families of angiogenic growth factors. *Nat. Med.* 7, 706–711 (2001).
49. Samulski, R.J., Chang, L.S. & Shenk, T. Helper-free stocks of recombinant adeno-associated viruses: normal integration does not require viral gene expression. *J. Virol.* 63, 3822–3828 (1989).
50. Rosenberg, M.B. *et al.* Grafting genetically modified cells to the damaged brain: restorative effects of NGF expression. *Science* 242, 1575–1578 (1988).

# Adrenal Hormones Suppress Cell Division in the Adult Rat Dentate Gyrus

Elizabeth Gould, Heather A. Cameron, Deborah C. Daniels, Catherine S. Woolley and Bruce S. McEwen

Laboratory of Neuroendocrinology, The Rockefeller University, New York, New York 10021

The rat dentate gyrus is unusual among mammalian brain regions in that it shows cell birth well into adulthood. During development, dentate gyrus cell birth is regulated by adrenal steroids. However, it is presently unknown whether cell division in the adult is also mediated by these same factors. In order to determine whether this is the case, we combined adrenalectomy, with or without corticosterone (CORT) replacement, and  $^3\text{H}$ -thymidine autoradiography, Nissl staining, and immunohistochemistry for the glial cell markers vimentin and glial fibrillary acidic protein (GFAP) as well as for the neuronal marker neuron-specific enolase. Removal of circulating adrenal steroids resulted in a greater density of both GFAP-immunoreactive and vimentin-immunoreactive cells compared to sham-operated animals; CORT replacement prevented increases in both of these cell types. The increase in the density of vimentin-immunoreactive cells probably resulted from an increase in the birth of these cells, as adrenalectomized rats showed greater numbers of  $^3\text{H}$ -thymidine-labeled vimentin-positive cells compared to sham rats. In contrast, no changes in the number of  $^3\text{H}$ -thymidine-labeled GFAP-positive cells were observed with adrenalectomy, indicating that the increase in this cell type probably does not involve cell birth. In addition, the density of  $^3\text{H}$ -thymidine-labeled cells that were not immunoreactive for either glial cell marker and that showed neuronal characteristics was dramatically increased with adrenalectomy. These results suggest that adrenal hormones normally suppress the birth of both glia and neurons in the adult rat dentate gyrus.

The dentate gyrus is unique in the mammalian brain in that it shows many processes, such as cell birth, death, and migration, into adulthood that are typically observed in other brain regions only during discrete developmental periods. Several studies have shown that the adult rat dentate gyrus continues to produce a small but steady number of both neurons and glia up until at least a year (Kaplan and Hinds, 1977; Kaplan and Bell, 1984). The presence of a low but predictable number of pyknotic cells in the granule cell layer (Gould et al., 1990a) suggests that cell death is an ongoing process in adults as well. Migration has also been demonstrated to occur in the adult rat dentate gyrus; newly

born cells typically arise from the hilar region and travel to the granule cell layer as rapidly as 24 hr following DNA synthesis (Cameron et al., 1991).

In most brain regions, radial glia are present only during development when they presumably guide migrating neurons to their appropriate destinations (Rakic, 1981). After this neuronal migration has been completed, radial glia are believed to differentiate into mature astrocytes (Pixley and de Vellis, 1984). Unlike the majority of neural systems, the rat dentate gyrus retains radial glia into adulthood (Kosaka and Hama, 1986; Rickmann et al., 1987). Although mature astrocytes exist in the adult granule cell layer, their numbers are low compared to other brain regions (Kosaka and Hama, 1986). This unique pattern of glial cell distribution is intriguing in that it may be related to the unusual neuronal characteristics of the adult dentate gyrus. For example, it is likely that radial glia persist into adulthood in order to provide guidance for newly born migrating granule cells.

An understanding of the factors that permit the persistence of typically developmental features, that is, cell birth, death, and the presence of radial glia, in the adult rat dentate gyrus is of considerable interest in our attempt to identify the cues that normally terminate these characteristics in other systems once development is complete. Since cell birth, death, and migration are generally considered to be developmental processes, it is likely that factors that regulate their occurrence during development continue to do so in adulthood. Several lines of evidence suggest that adrenal steroids mediate cell birth, survival, and migration in the dentate gyrus during development. First, maximal cell birth, death, and migration in the developing dentate gyrus occur during a time, called the stress hyperresponsive period, when adrenal steroid levels are naturally low (Schlessinger et al., 1975; Rickmann et al., 1987; Gould et al., 1991a; compare with Sapolsky and Meaney, 1986). Second, increasing the levels of adrenal steroids during the stress hyporesponsive period decreases the rate of cell birth (Bohn, 1980; Gould et al., 1991c), cell death (Gould et al., 1991b), and possibly cell migration in the dentate gyrus (see Gould et al., 1991b,c, for commentary). Third, adrenalectomy toward the end of the stress hyporesponsive period, when adrenal steroids begin to rise naturally, increases the rate of both hippocampal cell division (Yehuda et al., 1989) and dentate gyrus cell death (Gould et al., 1991b).

Recent findings suggest that the survival of adult dentate gyrus cells depends on adrenal steroids (Sloviter et al., 1989; Gould et al., 1990a), indicating that these hormones continue to regulate certain developmental processes throughout adulthood. It is presently unknown precisely what types of dentate gyrus cells require adrenal steroids for their survival and whether cell birth

Received Nov. 11, 1991; revised Apr. 9, 1992; accepted Apr. 17, 1992.

This research was supported by NRSA Postdoctoral Fellowship NS08804 to E.G., NRSA Training Grant GM07524-15 to H.A.C. and C.S.W., and NIMH grant MH41256 to B.S.M.

Correspondence should be addressed to Elizabeth Gould, Ph.D., Laboratory of Neuroendocrinology, The Rockefeller University, 1230 York Avenue, New York, NY 10021.

Copyright © 1992 Society for Neuroscience 0270-6474/92/123642-09\$05.00/0

in the adult dentate gyrus is also regulated by these hormones. In order to determine whether dentate gyrus neurons, glia, or both require adrenal steroids for their survival and whether the birth of dentate gyrus cells is mediated by adrenal hormones, we performed  $^3\text{H}$ -thymidine autoradiography, Nissl staining, and immunohistochemistry for the glial cell markers vimentin and glial fibrillary acidic protein (GFAP) as well as for the neuronal marker neuron-specific enolase (NSE), on brain tissue from control and hormonally manipulated adult rats.

## Materials and Methods

**Experiment 1: to determine whether the density of GFAP- and vimentin-immunoreactive cells changes with ADX and whether ADX-induced pyknotic cells are GFAP, vimentin, or NSE immunoreactive**

**Animal treatments and histology.** Adult (3 months) male Sprague-Dawley rats (Charles River) were group housed and provided with unlimited access to food and water. These rats were subjected to one of the following treatments: (1) sham operation, (2) bilateral adrenalectomy, or (3) bilateral adrenalectomy with corticosterone (CORT) replacement in the drinking water (25  $\mu\text{g}/\text{ml}$ ). This dose results in blood levels of CORT that are within the lower range of normal levels (Gould et al., 1990a). All surgery was performed using aseptic procedures under Metofane anesthesia. Adrenalectomized rats were provided with 0.9% NaCl in the drinking water to maintain salt balance. Seven days following surgery, these rats were deeply anesthetized with Metofane and perfused with 120 ml of 4.0% paraformaldehyde in 0.1 M phosphate buffer with 1.5% (v/v) picric acid. The brains were dissected from the skulls and postfixed overnight in the perfusion solution. Brain sections 40  $\mu\text{m}$  thick were cut on a Vibratome into a bath of PBS and reacted for either vimentin, GFAP, or NSE immunohistochemistry as described previously (Gould et al., 1990b). Briefly, the sections were placed in a solution of mouse monoclonal antibodies to vimentin (Boehringer Mannheim, diluted 1:50 in PBS), mouse monoclonal antibodies to GFAP (Boehringer Mannheim, diluted 1:50 in PBS), or rabbit polyclonal antibodies to NSE (Polysciences, diluted 1:2000 in PBS) overnight. The sections were then rinsed in PBS and transferred to a solution containing anti-mouse or anti-rabbit secondary antibodies (Vector Laboratories, diluted 1:50 in PBS with horse or goat normal serum, respectively) for 2 hr. The sections were again rinsed in PBS and incubated for 2 hr in avidin-biotin-HRP (Vector Laboratories, diluted 1:50 in PBS). Following this, the sections were rinsed in PBS and reacted in a solution containing diaminobenzidine, hydrogen peroxide, and PBS for 15 min. After a final rinse in PBS, the sections were mounted onto gelatinized slides, dried, rinsed in distilled water, dehydrated, cleared in HistoClear, and coverslipped under Permount. Prior to dehydration, some sections were counterstained for Nissl using cresyl violet. As immunohistochemical controls, the above procedures were performed with omission of the primary antibody incubation. Examination of this control tissue revealed no nonspecific staining of the secondary antibody. In an effort to maximize the reliability of comparisons within and between animals, vimentin, GFAP, and NSE immunohistochemistry were performed simultaneously on tissue from brains of all treatment groups.

**Data analysis.** The slides were coded prior to the analysis, and the code was not broken until the analysis was complete. For each brain, a minimum of six each of vimentin-immunostained and GFAP-immunostained sections were analyzed. Selected sections were located in the middle portion of the dentate gyrus. At this level, the dentate gyrus is located horizontally beneath the corpus callosum and the suprapyramidal and infrapyramidal blades are joined at the crest. The numbers of GFAP- and vimentin-immunoreactive cell bodies in the granule cell layer were counted by use of a light microscope (400 $\times$ ). Included in these counts were immunoreactive cells with somata in the subgranular zone (the border between the granule cell layer and the hilus) and processes extending into the granule cell layer. The granule cell layer was then traced by use of a camera lucida drawing tube (32 $\times$ ), and the cross-sectional area of the layer was determined with a Zeiss Interactive Digitizing Analysis System (ZIDAS). The data were expressed as the number of immunoreactive cell bodies per  $10^6 \mu\text{m}^2$ . Means of these variables were determined for each animal, and the data were subjected to one-way ANOVA followed by Tukey HSD post hoc comparisons.

The percentages of pyknotic cells immunoreactive for vimentin, GFAP, and NSE were also determined by counting the numbers of immunoreactive and nonimmunoreactive pyknotic cells from a minimum of four sections for each antigen from each brain. Pyknotic cells were characterized by the lack of a nuclear membrane, light or absent cytoplasm, and the presence of darkly stained circular condensed chromatin (see Sengelaub and Finlay, 1982; Gould et al., 1991a, for examples).

**Experiment 2: to determine whether ADX alters the density of  $^3\text{H}$ -thymidine-labeled cells and whether these  $^3\text{H}$ -thymidine-labeled cells are GFAP, vimentin, or NSE immunoreactive**

**Animal treatments and histology.** Adult (4 months) male Sprague-Dawley rats (Charles River) were group housed and provided unlimited access to food and water. These rats were subjected to one of the following treatments: (1) sham operation or (2) bilateral adrenalectomy. All surgical procedures were performed using aseptic techniques under Metofane anesthesia. Adrenalectomized animals were provided with 0.9% NaCl in the drinking water. On days 2, 4, and 6 following surgery, these rats received an intraperitoneal injection of 5.0  $\mu\text{Ci}/\text{gm}$  body weight  $^3\text{H}$ -thymidine in water (New England Nuclear; specific activity, 80 Ci/mmol). Twenty-four hours following the last injection, the rats were deeply anesthetized with Metofane and transcardially perfused as described for experiment 1. This last survival interval was selected because it provides enough time for the uptake of thymidine and the completion of mitosis by granule cell neuroblasts (Lewis, 1978). The brains were dissected from the cranial cavities and processed for vimentin, GFAP, and NSE immunohistochemistry as described above. After mounting onto gelatinized slides, the reacted sections were dried, rinsed in distilled water, and dipped in photographic emulsion (Kodak, NTB-2). The slides were stored in the dark at 4°C for 6 weeks. The slides were then developed (Kodak, Dektol), rinsed in distilled water, fixed (Kodak, Ektaflo), rinsed in running tap water, counterstained for Nissl using cresyl violet, dehydrated, cleared in HistoClear, and coverslipped under Permount.

**Data analysis.** The slides were coded prior to quantitative analysis, and the code was not broken until the analysis was finished. For each brain, a minimum of four sections each of vimentin-immunoreactive, GFAP-immunoreactive, and NSE-immunoreactive tissue were analyzed for this experiment. As indicated above, selected sections were located in the middle portion of the dentate gyrus. For each section, the numbers of immunoreactive and nonimmunoreactive  $^3\text{H}$ -thymidine-labeled cells were determined. These counts included cells with somata in the subgranular zone but not the hilus itself. The cross-sectional area of the granule cell layer was determined as described above, and these values were expressed as number of cells per  $10^6 \mu\text{m}^2$ . Means of these variables were determined for each animal, and the data were subjected to two-tailed Student's *t* tests. In order to confirm the results of experiment 1, the percentages of pyknotic cells immunoreactive for GFAP, vimentin, and NSE were also determined.

**Experiment 3: to determine whether ADX affects the density of  $^3\text{H}$ -thymidine-labeled cells with glial and neuronal morphologies and to determine whether ADX alters the density of healthy cells**

**Animal treatments and histology.** Adult (5 months) male Sprague-Dawley rats (Charles River) were group housed and provided unlimited access to food and water. These rats received either sham operation or bilateral adrenalectomy using aseptic procedures under Metofane anesthesia. Adrenalectomized rats received 0.9% NaCl in the drinking water. All rats involved in this study received a single injection of 5.0  $\mu\text{Ci}/\text{gm}$  body weight of  $^3\text{H}$ -thymidine (New England Nuclear; specific activity, 80 Ci/mmol) 6 d after surgery. Twenty-four hours after this injection, the rats were transcardially perfused as described above. This survival interval between injection and perfusion was selected because it provides adequate time for the uptake of thymidine by dividing cells and the completion of mitosis by granule cell neuroblasts (Lewis, 1978). After postfixation, these brains were placed in 30% sucrose in PBS until they sank. The brains were then frozen on dry ice, and sections 18  $\mu\text{m}$  thick were cut on a cryostat and thaw mounted onto gelatinized slides. The slides were then dipped in photographic emulsion, incubated, and developed as described for experiment 2. The slides were Nissl stained using cresyl violet, dehydrated, cleared in HistoClear, and coverslipped under Permount.

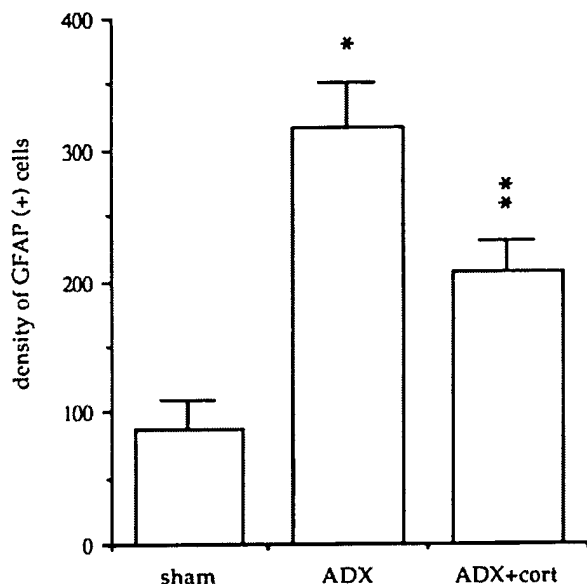


**Figure 1.** The density of GFAP-immunoreactive cell bodies (mean + SEM) in the granule cell layer of sham-operated, ADX, and ADX+CORT rats ( $n = 6$  for each group). Single asterisk represents significant difference ( $p < 0.05$ , one-way ANOVA followed by Tukey HSD post hoc comparisons) from both sham and ADX+CORT. Double asterisk represents significant difference ( $p < 0.05$ ) from sham and ADX.

**Data analysis.** The slides were coded prior to light microscopic analysis, and the code was not broken until the analysis was complete. For each brain, a minimum of four sections were analyzed. In order to avoid the necessity of correcting for twice-counted cells, the selected sections were at least  $36 \mu\text{m}$  apart. For each selected section, the number of  $^3\text{H}$ -thymidine-labeled cells was determined. Each  $^3\text{H}$ -thymidine-labeled

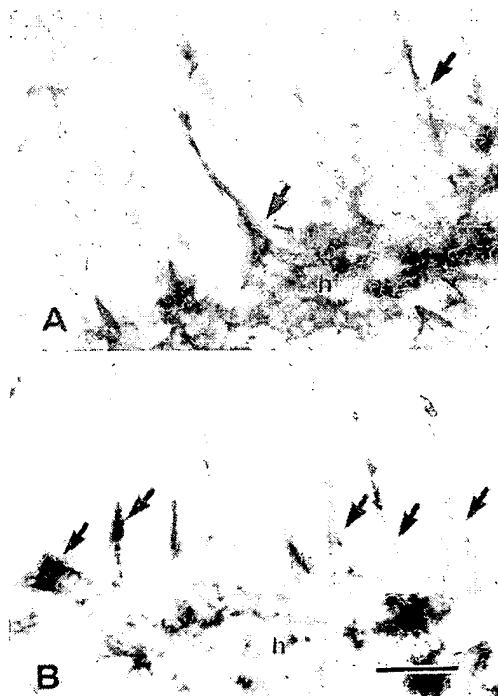


**Figure 2.** Photomicrographs of representative vimentin-immunoreactive cells (arrows) in the granule cell layer of sham-operated (A) and ADX rats (B). The density of these cells is greater in B than A. Scale bar,  $30 \mu\text{m}$  for both A and B.

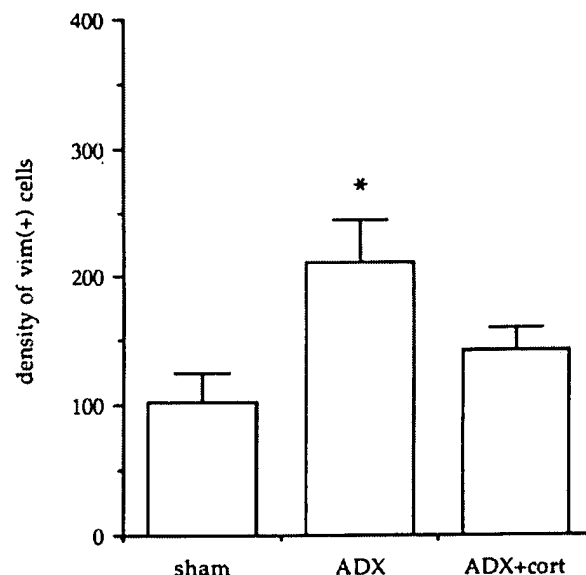


**Figure 3.** The density of vimentin-immunoreactive cell bodies (mean + SEM) in the granule cell layer of sham operated, ADX, and ADX+CORT rats ( $n = 6$  for each group). Asterisk represents significant difference ( $p < 0.05$ , one-way ANOVA followed by Tukey HSD post hoc comparisons) from both sham and ADX+CORT.

cell was rated as showing either glial morphology, i.e., small ( $< 70 \mu\text{m}^2$  cross-sectional cell body area) irregularly shaped cell bodies, or neuronal morphology, i.e., medium-sized ( $> 70 \mu\text{m}^2$  cross-sectional cell body area) round or oval shaped cell bodies. These criteria are likely to underestimate the number of neurons because newly born neurons may be smaller than mature ones and may be elongated during migration. In addition, the numbers of pyknotic and of healthy cells, that is, not pyknotic, within the granule cell layer were counted. A cell was counted as healthy if it showed a distinct boundary and appeared to be whole; cell fragments were not included in the analysis. The cross-sectional area of the granule cell layer was determined as described above, and the data were expressed as number of cells per  $10^6 \mu\text{m}^2$ . Means of the above-described variables were determined for each animal, and the data were subjected to two-tailed Student's  $t$  tests.

## Results

### Experiment 1

Examination of the dentate gyrus from control brains revealed low numbers of GFAP-immunoreactive astrocytes in the granule cell layer compared to the surrounding regions. Quantitative analysis of the density of GFAP-immunoreactive cells in the granule cell layer revealed significant increases with adrenalectomy ( $p < 0.05$ ; Fig. 1). CORT replacement to adrenalectomized rats prevented this increase in the density of GFAP-immunoreactive cells (Fig. 1).

Light microscopic examination of the dentate gyrus of control rats revealed vimentin-immunoreactive cells that appeared to be radial glia, that is, small cell bodies with radial processes (Fig. 2). The cell bodies of these glia were usually located in the subgranular zone, and their processes extended into the granule cell layer. Quantitative analysis of the density of vimentin-immunoreactive cell bodies in the dentate gyrus across treatment groups revealed significant overall differences ( $p < 0.05$ ; Fig. 3). Specifically, adrenalectomy resulted in a significant increase in the number of vimentin-immunoreactive cells compared to sham operation (Figs. 2, 3). CORT replacement to adrenalectomized rats prevented this increase in vimentin-immunoreactive cells (Fig. 3).

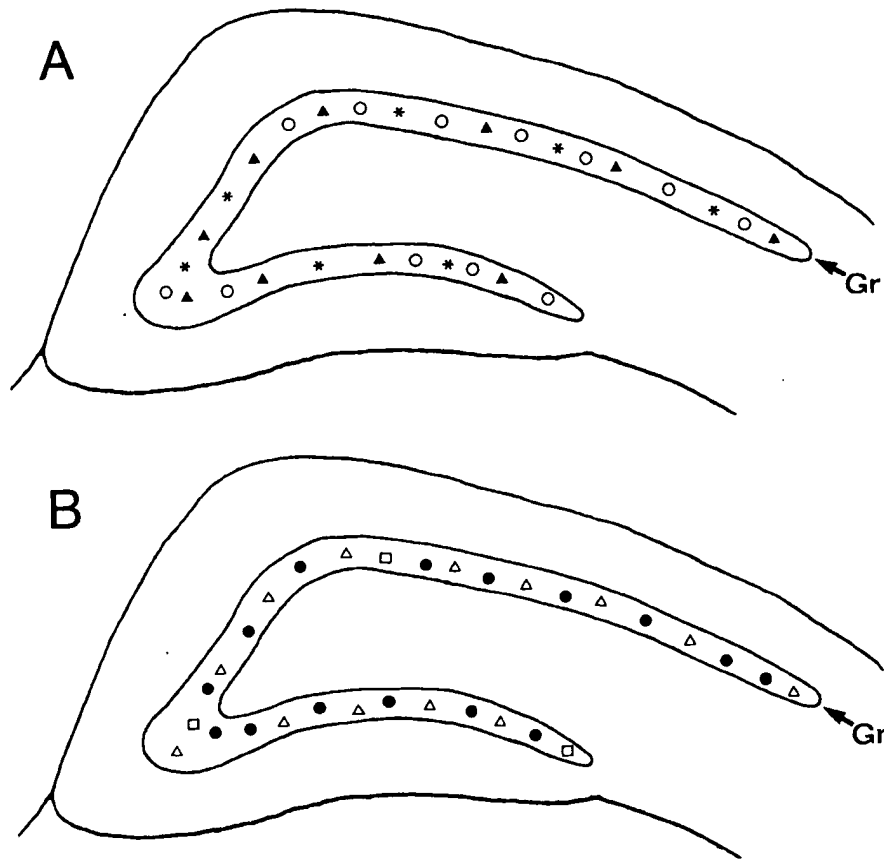


**Figure 4.** Templates showing the cellular identity and distribution of pyknotic cells (*A*) and  $^3\text{H}$ -thymidine-labeled cells (*B*) in the granule cell layer (*Gr*) of ADX rats. Solid triangles represent vimentin-immunoreactive pyknotic cells, asterisks represent NSE-immunoreactive pyknotic cells, open circles represent nonimmunoreactive pyknotic cells (1 symbol = 5 pyknotic cells). Open triangles represent vimentin-immunoreactive  $^3\text{H}$ -thymidine-labeled cells, open squares represent GFAP-immunoreactive  $^3\text{H}$ -thymidine-labeled cells, solid circles represent nonimmunoreactive  $^3\text{H}$ -thymidine-labeled cells (1 symbol = 1  $^3\text{H}$ -thymidine-labeled cell). These values represent the mean number of each cell type for a single section.

As previously reported (see Gould et al., 1990a), quantitative analysis of the density of pyknotic cells revealed a large increase with adrenalectomy that was prevented with CORT treatment (mean number of pyknotic cells/ $10^6 \mu\text{m}^2 = 3.8 \pm 1.0$  for sham,  $519.4 \pm 189.6$  for ADX,  $4.9 \pm 0.7$  for ADX + CORT). In addition, a general relationship between the magnitude of pyknosis and the density of GFAP- and vimentin-positive cells was observed. The brains that showed the greatest density of pyknotic cells were the brains that showed the greatest density of GFAP- and vimentin-immunoreactive cells. Examination of immunoreactive tissue from adrenalectomized rats counterstained for Nissl revealed some pyknotic cells that were immunoreactive for vimentin (approximately 35% of the total number of pyknotic cells), some pyknotic cells that were immunoreactive for NSE (approximately 25% of the total number of pyknotic cells), and no examples of GFAP-immunoreactive pyknotic cells (Fig. 4).

#### Experiment 2

In control brains, a small but significant number of vimentin-immunoreactive  $^3\text{H}$ -thymidine-labeled cells that appeared to be radial glia were observed in the dentate gyrus (Figs. 5, 6). Quantitative analysis of vimentin-immunoreactive  $^3\text{H}$ -thymidine-labeled cells revealed a significant increase with adrenalectomy ( $p < 0.05$ ; Fig. 6). The distribution of  $^3\text{H}$ -thymidine-labeled vimentin-immunoreactive cells was no different from that observed for non-thymidine-labeled vimentin-immunoreactive cells; cell bodies were typically located in the subgranular zone with processes extending through the granule cell layer.

Moreover, despite the dramatic increase in  $^3\text{H}$ -thymidine-labeled cells with adrenalectomy, no difference in the distribution of these cells was observed with treatment. The number of  $^3\text{H}$ -thymidine-labeled cells in these same sections that were not immunoreactive for vimentin determined from these same sections also increased with adrenalectomy ( $p < 0.05$ ; Figs. 5, 6). In contrast, no change in the number of GFAP-immunoreactive  $^3\text{H}$ -thymidine-labeled cells was observed with adrenalectomy ( $p > 0.1$ ; Fig. 7). The number of  $^3\text{H}$ -thymidine-labeled cells that were not immunoreactive for GFAP increased appreciably with adrenalectomy ( $p < 0.05$ ; Fig. 7). In addition, as seen for experiment 1, the number of GFAP-immunoreactive cells that were not labeled with  $^3\text{H}$ -thymidine was much greater in brains of adrenalectomized rats compared to controls.

Light microscopic examination of NSE-immunoreactive  $^3\text{H}$ -thymidine-labeled tissue revealed no double labeled cells in the dentate gyrus of either sham-operated or adrenalectomized animals. However, many  $^3\text{H}$ -thymidine-labeled cells showed neuronal characteristics and were not immunoreactive for glial cell markers (Fig. 5). The numbers of these profiles increased with adrenalectomy (Fig. 4).

As shown for experiment 1, no GFAP-immunoreactive pyknotic cells were observed in brains of either sham operated or adrenalectomized rats but many of the pyknotic cells in the latter treatment group were vimentin immunoreactive (approximately 35%) or NSE immunoreactive (approximately 25%) (Fig. 4). Although an occasional  $^3\text{H}$ -thymidine-labeled cell was pyknotic, no change in these profiles was observed with adrenalectomy. In no instance were vimentin-, NSE-, or GFAP-immunoreactive  $^3\text{H}$ -thymidine-labeled pyknotic cells observed.



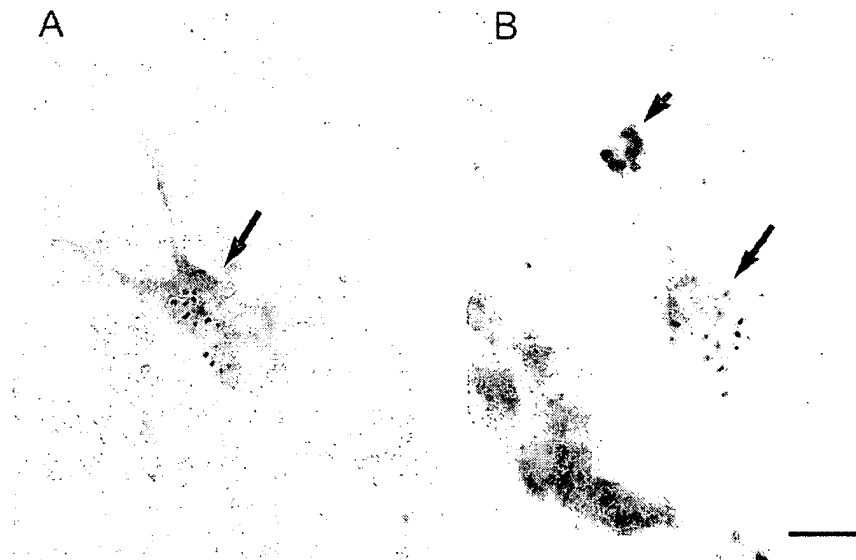


**Figure 5.** Photomicrographs of representative  $^3\text{H}$ -thymidine-labeled cells (long arrows) that are vimentin-positive (*A*) and vimentin-negative (*B*) from the adult rat dentate gyrus. Short arrow in *B* indicates a pyknotic cell. Scale bar, 20  $\mu\text{m}$  for both *A* and *B*.

### Experiment 3

Light microscopic examination of  $^3\text{H}$ -thymidine-labeled Nissl-stained thin sections revealed labeled cells scattered throughout the dentate gyrus. The majority of these labeled cells were located in the subgranular zone, with fewer seen in the hilus or the granule cell layer itself. In sham-operated brains, approximately 65% of all labeled cells showed glial morphologies, that is, small, irregularly shaped cell bodies, whereas the remaining  $^3\text{H}$ -thymidine-labeled cells (approximately 35%) showed neuronal characteristics, that is, medium sized round or oval cell bodies (Fig. 8). The density of  $^3\text{H}$ -thymidine-labeled cells increased with adrenalectomy ( $p < 0.05$ ; Fig. 9). Despite this observation, no change in the proportion of labeled cells with neuronal versus glial morphologies was observed. In addition, the number of healthy cells showed a slight but significant decrease with adrenalectomy ( $p < 0.05$ ; Fig. 10). The results of experiments 1–3 are summarized in Table 1.

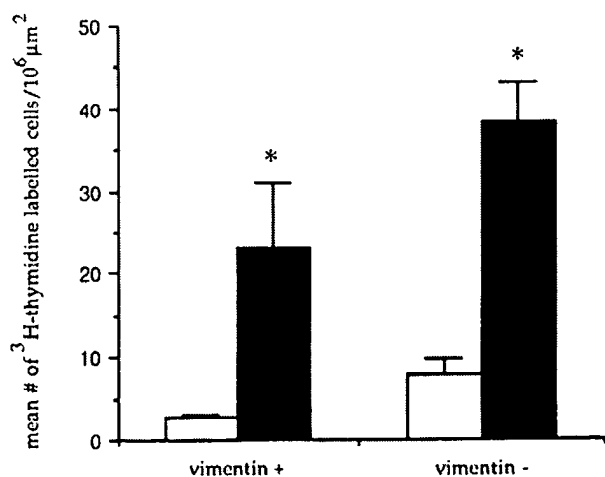


**Figure 6.** Density of  $^3\text{H}$ -thymidine-labeled cells (mean  $\pm$  SEM) that are immunoreactive for vimentin and  $^3\text{H}$ -thymidine-labeled cells that are vimentin-negative in the dentate gyrus of sham-operated (open bar) and ADX (solid bar) rats ( $n = 5$  for each group). Asterisks represent significant difference ( $p < 0.05$ , Student's *t* tests) from sham value for same cell type.

### Discussion

The results of this study show that removal of adrenal hormones results in numerous cellular changes in the adult rat dentate gyrus. Adrenalectomy results in an increase in the density of GFAP- and vimentin-immunoreactive cells; this effect can be prevented by providing CORT replacement. Adrenalectomy also results in an increase in the numbers of both degenerating cells and newly born cells in the dentate gyrus; these populations are probably comprised of both glia and neurons (see Table 1 for summary).

#### Identity of pyknotic cells in the adult dentate gyrus

The results of this report indicate that the population of cells that degenerates with adrenalectomy comprises neurons and glia, but not mature astrocytes. Our previous studies have shown that adrenalectomy results in a dramatic increase in the density

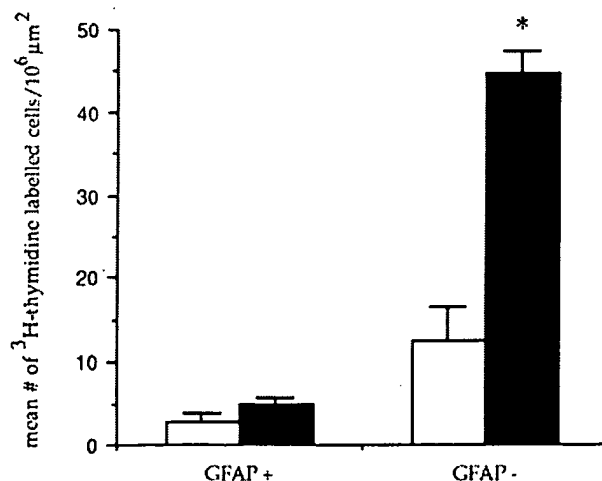


**Figure 7.** Density of  $^3\text{H}$ -thymidine-labeled cells (mean  $\pm$  SEM) that are GFAP-positive and  $^3\text{H}$ -thymidine-labeled cells that are GFAP-negative in the dentate gyrus of sham-operated (open bar) and ADX (solid bar) rats ( $n = 5$  for each group). Asterisk represents significant difference ( $p < 0.05$ , Student's *t* tests) from sham value for same cell type.

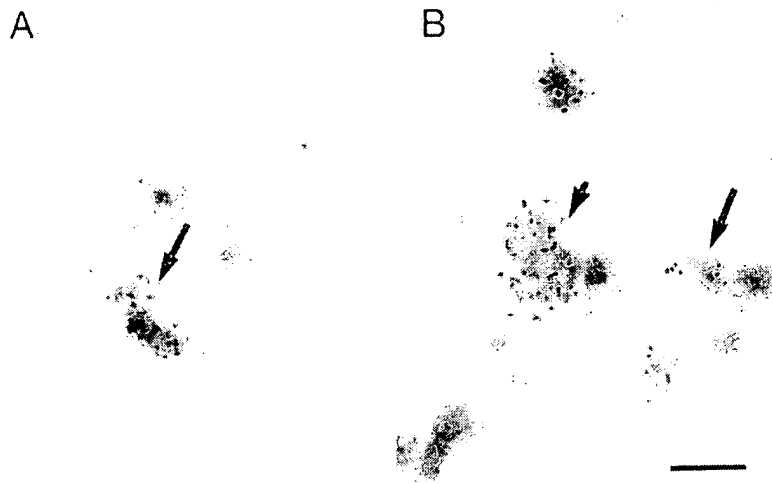


Figure 8. Photomicrographs of representative  $^3\text{H}$ -thymidine-labeled Nissl-stained cells showing morphology characteristic of glia (long arrows) and neurons (short arrow). Scale bar, 20  $\mu\text{m}$  for both A and B.

of pyknotic cells in the granule cell layer (Gould et al., 1990a; Woolley et al., 1991). Although these degenerating cells were observed in the granule cell layer, a region that contains a relatively low density of glial cells (Kosaka and Hama, 1986), it was unknown whether these pyknotic cells were glial or neuronal. A single-section Golgi study indicating that adrenalectomy results in a decrease in the number of dendritic branch points and cell body area of granule cells (Gould et al., 1990a) suggests that neurons are in fact degenerating. The results of the present study showing that some pyknotic cells express NSE provides direct evidence to support this contention. The data reported here showing that adrenalectomy results in a net increase in GFAP-immunoreactive and vimentin-immunoreactive cells and a net decrease in total cells also support the notion that most degenerating cells are neurons. However, the presence of a large proportion of vimentin-immunoreactive pyknotic cells (approximately 35% of all pyknotic cells) indicates that many glial cells are dying as well. It is likely that the vimentin-im-

munoreactive cells that are degenerating represent a separate population of glial cells from those that are dividing in response to adrenalectomy since no examples of vimentin-immunoreactive  $^3\text{H}$ -thymidine-labeled pyknotic cells were observed. Although many pyknotic cells appear to be vimentin immunoreactive or NSE immunoreactive, a large proportion of these degenerating cells were not immunoreactive for either antigen. Although the identity of these pyknotic cells is unknown, it is likely that cells become nonimmunoreactive for antigens they previously expressed as degeneration proceeds.

#### Identity of $^3\text{H}$ -thymidine labeled cells in the adult dentate gyrus

The results of this study indicate that the population of  $^3\text{H}$ -thymidine-labeled cells in the adult rat dentate gyrus comprises both glia and neurons. Since GFAP has been shown to be a marker for mature astrocytes (Pixley and de Vellis, 1984), it is

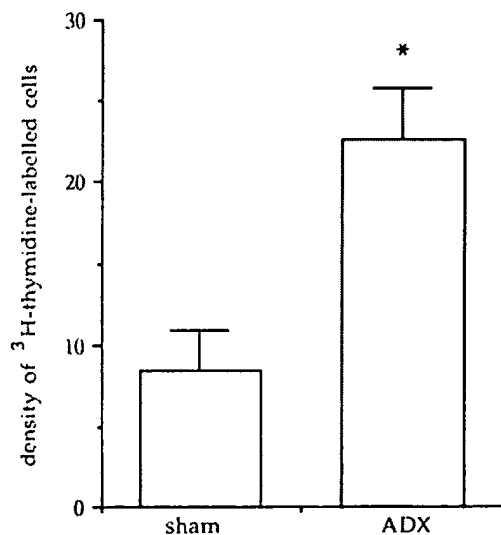


Figure 9. Density of  $^3\text{H}$ -thymidine-labeled cells (mean + SEM) in the granule cell layer of Nissl-stained tissue from sham-operated and ADX rats ( $n = 5$  for each group). Asterisk represents significant difference ( $p < 0.05$ , Student's  $t$  test) from sham.

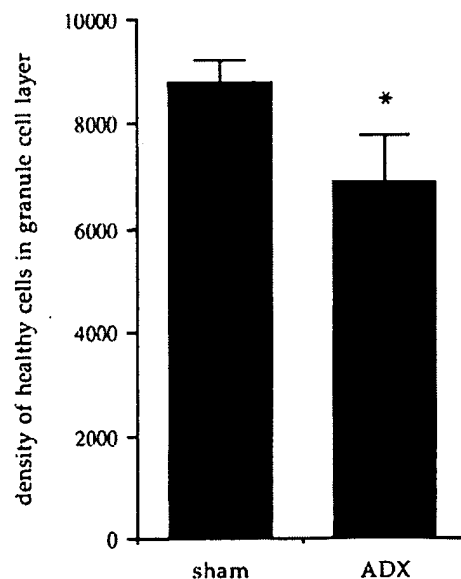


Figure 10. Density of healthy cells (mean + SEM) in the granule cell layer of Nissl-stained tissue from sham-operated and ADX rats ( $n = 5$  for each group). Asterisk represents significant difference ( $p < 0.05$ , Student's  $t$  test) from sham.

Table 1. Summary of changes in different cell types with ADX

	Vimentin stained		GFAP stained		NSE stained		Nissl stained
	+	-	+	-	+	-	
Healthy cells	↑	*	↑	*	*	*	↓
<sup>3</sup> H-thymidine-labeled cells	↑	↑	→	↑	0	↑	↑
Pyknotic cells	↑	↑	0	↑	↑	↑	↑

Arrows pointing up indicate increases and arrows pointing down indicate decreases in the density of this cell type with ADX. Horizontal arrows indicate no change in this cell type with ADX. Zeros indicate no cells of this particular type observed, and asterisks represent no data collected for this cell type.

likely that the small number of GFAP-immunoreactive <sup>3</sup>H-thymidine-labeled cells observed in this study are glia. Vimentin has been shown to be a marker for immature glial cells (Pixley and de Vellis, 1984). The majority of <sup>3</sup>H-thymidine-labeled vimentin-immunoreactive cells observed in our study possessed radial glial morphologies: small cell bodies with thin processes radiating through the granule cell layer. Recent studies performed in the neural pathways mediating canary bird song have led to the suggestion that radial glia differentiate into neurons (see Alvarez-Buylla, 1990, for commentary). Future time course studies will be required in order to determine whether decreases in the number of <sup>3</sup>H-thymidine-labeled radial glia coincide with increases in the number of <sup>3</sup>H-thymidine-labeled neurons in the adult rat dentate gyrus.

Although it is likely that the <sup>3</sup>H-thymidine-labeled cells that are immunoreactive for GFAP and vimentin are glial cells, it is not clear what population of cells is represented by the <sup>3</sup>H-thymidine-labeled nonimmunoreactive cells. It is likely that a substantial proportion of the <sup>3</sup>H-thymidine-labeled GFAP-negative cells represent vimentin-immunoreactive cells. However, it is not likely that a substantial proportion of the dividing vimentin-negative cells represent GFAP-immunoreactive cells because the number of vimentin-negative <sup>3</sup>H-thymidine-labeled cells dramatically increased with adrenalectomy whereas the number of GFAP-immunoreactive <sup>3</sup>H-thymidine-labeled cells remained very low.

Previous studies have shown that neurons are generated in the adult rat dentate gyrus (Kaplan and Hinds, 1977; Kaplan and Bell, 1984). In the normal adult rat dentate gyrus, <sup>3</sup>H-thymidine-labeled cells have been shown to possess synapses (Kaplan and Hinds, 1977; Kaplan and Bell, 1984) and to extend axons into target sites (Trice and Stanfield, 1986). Since many of the <sup>3</sup>H-thymidine-labeled nonimmunoreactive cells observed in the present study are relatively large and show neuronal morphologies, it is likely that at least some of these cells are neurons. It is possible that the low level of neurogenesis that normally occurs in the rat dentate gyrus is increased by adrenalectomy. Although the absence of any NSE-immunoreactive <sup>3</sup>H-thymidine-labeled cells in this experiment weighs against this hypothesis, it is important to note that, during development, neurons do not express NSE until migration is complete and mature synaptic connections are formed (Schmechel et al., 1980). Since the longest interval between <sup>3</sup>H-thymidine injection and perfusion in this study was less than 1 week, it is likely that more time is required for newly born neurons to express this protein in this system. Indeed, preliminary evidence from our laboratory suggests that by 1 month following <sup>3</sup>H-thymidine injection

many <sup>3</sup>H-thymidine-labeled cells in the normal adult rat dentate gyrus are NSE immunoreactive (H. A. Cameron and E. Gould, unpublished observation). Whether a similar time lag exists for NSE expression in the adrenalectomized rat dentate gyrus remains to be determined.

#### Functional significance of changes in GFAP-immunoreactive cells

Since adrenalectomy results in degeneration of cells in the granule cell layer (Gould et al., 1990a), it is possible that the increase in the density of GFAP-immunoreactive cells that we noted in this brain region is an astrocytic reaction to neuronal death. Astrocytes have been shown to migrate, hypertrophy, and/or divide in response to neuronal damage (Smith et al., 1986). The reaction of astrocytes in response to neuronal damage is thought to be an important step in the removal of cellular debris. The timing of adrenalectomy-induced increases in GFAP mRNA is consistent with this possibility; the onset of increased pyknosis in the granule cell layer precedes the increase in hippocampal GFAP mRNA (Gould et al., 1990a; compare with Nichols et al., 1990). It is unlikely that the increase in GFAP-immunoreactive cells is due to the division of astrocytes since we found no increase in the number of <sup>3</sup>H-thymidine-labeled GFAP-immunoreactive cells with adrenalectomy. However, the possibility exists that these cells either migrate into the dentate gyrus or express higher levels of GFAP in response to neuronal damage.

Alternatively, there is some evidence to suggest that the increase in GFAP-immunoreactive cells is independent of neuronal damage. In brain regions that do not show an increase in the density of pyknotic cells with adrenalectomy, that is, the cerebellum (see McEwen and Gould, 1990), GFAP and GFAP mRNA levels are elevated by adrenalectomy (O'Callaghan et al., 1989; Nichols et al., 1990). Future studies will be required in order to determine whether the increase in density of GFAP-immunoreactive cell bodies observed in the dentate gyrus after adrenalectomy occurs independently of neuronal damage.

#### Functional significance of changes in vimentin-immunoreactive cells

Vimentin is expressed by radial glia and other immature glial cells that will, in most cases, differentiate into mature astrocytes with time (Pixley and de Vellis, 1984). Unlike most other brain regions, the dentate gyrus retains radial glia into adulthood. The cell bodies of these glia reside in the subgranular zone and their radial processes extend into the granule cell layer (Kosaka and Hama, 1986; Rickmann et al., 1987). A number of studies have shown that granule cells are born in the subgranular zone during adulthood (Kaplan and Hinds, 1977; Kaplan and Bell, 1984; Crespo et al., 1986). Although the function of radial glia in the adult dentate gyrus is presently unknown, it is likely that they subserve a similar function in adulthood as observed developmentally: to provide a substrate for the migration of newly born granule cells (Rickmann et al., 1987).

The results of this study show that the adrenalectomy-induced increase in the number of vimentin-immunoreactive radial glia is due to an increase in the birth of these cells. It is possible that the adrenalectomy-induced increase in the density of radial glia observed in this study is related to an increase in the birth of new granule cells. This hypothesis is supported by the fact that, during development, the appearance of a new set of radial glia usually precedes each period of increased neurogenesis in the

dentate gyrus (Rickmann et al., 1987). Furthermore, developmental studies have shown that administration of adrenal steroids inhibits the birth of granule cells (Bohn, 1980; Gould et al., 1991c), suggesting that these hormones may suppress granule cell birth in adulthood as well. The observations of the present study that the density of cells with granule neuron morphology that are not immunoreactive for glial cell markers increases in response to adrenalectomy support this possibility. Studies aimed at positively identifying as neurons this third population of  $^3\text{H}$ -thymidine-labeled cells, that is, those that are not immunoreactive for GFAP or vimentin, are ongoing in our laboratory.

#### *The relationship between cell birth and cell death in the adult rat dentate gyrus*

The rat dentate gyrus shows ongoing cell birth and death into adulthood (Kaplan and Hinds, 1977; Kaplan and Bell, 1984; Gould et al., 1990a). Both newly born cells and pyknotic cells appear most commonly in the subgranular zone of the dentate gyrus (Crespo et al., 1986; Gould et al., 1990a), raising the possibility that they represent the same population of cells. If these cells simply turn over, it would follow that cell birth and death in the adult rat dentate gyrus do not affect the total number of granule cells. However, studies of granule cells during adult life have shown that these neurons increase in number up until at least 12 months of life (Bayer et al., 1982; Bayer, 1982; but see Boss et al., 1985), indicating that cell birth normally outweighs cell death in this region. The results of this study show that removal of circulating adrenal hormones upsets this relationship; adrenalectomy results in a slight but significant net decrease in healthy granule cells after 7 d, indicating that cell death outweighs cell birth.

Developmental studies have shown that even small numbers of pyknotic cells usually reflect a high magnitude of cell loss due to rapid clearing of cellular debris. Given the magnitude of the pyknosis observed in this and our previous studies (Gould et al., 1990a; Woolley et al., 1991), it is surprising that a greater decrease in the number of healthy cells was not observed. This study indicates that the slight decrease observed probably reflects a compensatory increase in the rate of cell birth that partially offsets the increased cell death. The results of Sloviter et al. (1989) showed that adrenalectomy can result in complete obliteration of the granule cell layer at 3–4 months following surgery. This suggests that, with time, the discrepancy between cell death and cell birth continues such that by 3–4 months, neuroblasts would no longer be able to replace dead granule cells. Future studies will be necessary to determine the rate of cell death and birth at different times after adrenalectomy.

#### *The role of adrenal hormones in the suppression of cell death and cell survival*

The results of this study and previous studies (Gould et al., 1990a; Woolley et al., 1991) show that the increase in pyknotic cells and GFAP-immunoreactive and vimentin-immunoreactive cells with adrenalectomy is due to the removal of circulating adrenal steroids and not due to the removal of catecholamines. Replacement of CORT in the drinking water of adrenalectomized rats prevents the increase in density of pyknotic cells and GFAP-immunoreactive and vimentin-immunoreactive cells in the dentate gyrus. We have previously shown that type 1 adrenal steroid receptors are involved in the adrenalectomy-induced pyknosis; replacement with the type 1 receptor agonists CORT or aldosterone prevent this effect, whereas replacement with the

type 2 receptor agonist RU28362 does not prevent this effect (Woolley et al., 1991). Although it is likely that the adrenalectomy-induced increase in  $^3\text{H}$ -thymidine-labeled vimentin-immunoreactive cells is dependent on activation of the type 1 receptor, that is, because low doses of CORT prevented the increase in vimentin-immunoreactive cells, it is unknown whether activation of the type 1 receptor will block the increase in nonimmunoreactive  $^3\text{H}$ -thymidine-labeled cells. Future studies will be required to determine which adrenal hormone and receptor type normally prevents division of cells that do not express vimentin in the intact rat.

Under normal circumstances, the adult rat dentate gyrus shows a slow but steady level of cell birth and cell death. Bilateral removal of the adrenal glands results in markedly increased rates of both of these processes (Gould et al., 1990a; present results), suggesting that cell birth and death are normally suppressed by adrenal hormones. This contention is consistent with developmental findings that postnatal cell birth and death in the rat dentate gyrus are maximal at a time when adrenal hormone levels are exceedingly low (Schlessinger et al., 1975; Bayer, 1980; Gould et al., 1991a; compare with Sapolsky and Meaney, 1986). Experimentally induced increases in adrenal hormones during this postnatal period diminish both cell birth and cell death (Bohn, 1980; Gould et al., 1991b,c). As the adrenal gland matures and circulating levels of its hormones rise, the rates of cell birth and cell death taper off. The findings of this report show that developmental levels of both cell birth and cell death can be reinitiated by removing the adrenal glands. This suggests that adrenal hormones are the natural signal for the inhibition of developmental processes, such as cell birth and death in adult rat dentate gyrus.

## References

- Alvarez-Buylla A (1990) Mechanism of neurogenesis in adult avian brain. *Experientia* 46:948–955.
- Bayer SA (1980) Development of the hippocampal region in the rat. I. Neurogenesis examined with  $^3\text{H}$ -thymidine autoradiography. *J Comp Neurol* 190:87–114.
- Bayer SA (1982) Changes in the total number of dentate granule cells in juvenile and adult rats: a correlated volumetric and  $^3\text{H}$  thymidine autoradiographic study. *Exp Brain Res* 46:315–323.
- Bayer SA, Yackel JW, Puri PS (1982) Neurons in the rat dentate gyrus granular layer substantially increase during juvenile and adult life. *Science* 216:890–892.
- Bohn MC (1980) Granule cell genesis in the hippocampus of rats treated neonatally with hydrocortisone. *Neuroscience* 5:2003–2012.
- Boss BD, Peterson GM, Cowan WM (1985) On the number of neurons in the dentate gyrus of the rat. *Brain Res* 338:144–150.
- Cameron HA, Gould E, Daniels DC, McEwen BS (1991) Evidence for rapid migration of newly born cells in the adult rat dentate gyrus. *Soc Neurosci Abstr* 17:205.
- Crespo D, Stanfield BB, Cowan WM (1986) Evidence that late-generated granule cells do not simply replace earlier formed neurons in the rat dentate gyrus. *Exp Brain Res* 62:541–548.
- Gould E, Woolley CS, McEwen BS (1990a) Short-term glucocorticoid manipulations affect neuronal morphology and survival in the adult dentate gyrus. *Neuroscience* 37:367–375.
- Gould E, Frankfurt M, Westlind-Danielsson A, McEwen BS (1990b) Developing forebrain astrocytes are sensitive to thyroid hormone. *Glia* 3:283–292.
- Gould E, Woolley CS, McEwen BS (1991a) Naturally occurring cell death in the developing dentate gyrus of the rat. *J Comp Neurol* 304:408–418.
- Gould E, Woolley CS, McEwen BS (1991b) Adrenal steroids regulate postnatal development of the rat dentate gyrus. I. Effects of glucocorticoids on cell death. *J Comp Neurol* 313:479–485.
- Gould E, Woolley CS, Cameron HA, Daniels DC, McEwen BS (1991c)

- Adrenal steroids regulate postnatal development of the rat dentate gyrus. II. Effects of glucocorticoids and mineralocorticoids on cell birth. *J Comp Neurol* 313:486–493.
- Kaplan MS, Bell DH (1984) Mitotic neuroblasts in the 9 day old and 11 month old rodent hippocampus. *J Neurosci* 4:1429–1441.
- Kaplan MS, Hinds JW (1977) Neurogenesis in the adult rat: electron microscopic analysis of light radioautographs. *Science* 197:1092–1094.
- Kosaka T, Hama K (1986) Three-dimensional structure of astrocytes in the rat dentate gyrus. *J Comp Neurol* 249:242–260.
- Lewis PD (1978) Kinetics of cell proliferation in the postnatal rat dentate gyrus. *Neuropathol Appl Neurobiol* 4:191–195.
- McEwen BS, Gould E (1990) Adrenal steroid influences on the survival of hippocampal neurons. *Biochem Pharmacol* 40:2393–2402.
- Nichols NR, Osterburg HH, Masters JN, Millar SL, Finch CE (1990) Messenger RNA for glial fibrillary acidic protein is decreased in rat brain following acute and chronic corticosterone treatment. *Mol Brain Res* 7:1–7.
- O'Callaghan JP, Brinton RE, McEwen BS (1989) Glucocorticoids regulate the concentration of glial fibrillary acidic protein throughout the brain. *Brain Res* 494:159–161.
- Pixley SKR, de Vellis J (1984) Transition between immature radial glia and mature astrocytes studied with a monoclonal antibody to vimentin. *Dev Brain Res* 15:201–209.
- Rakic P (1981) Neuronal-glial interaction during brain development. *Trends Neurosci* 4:184–187.
- Rickmann M, Amaral DG, Cowan WM (1987) Organization of radial glial cells during the development of the rat dentate gyrus. *J Comp Neurol* 264:449–479.
- Sapolsky RM, Meaney MJ (1986) Maturation of the adrenocortical stress response: neuroendocrine control mechanisms and the stress hyporesponsive period. *Brain Res Rev* 11:65–76.
- Schlessinger AR, Cowan WM, Gottlieb DI (1975) An autoradiographic study of the time of origin and the pattern of granule cell migration in the dentate gyrus of the rat. *J Comp Neurol* 159:149–176.
- Schmechel DE, Brightman MW, Marangos PJ (1980) Neurons switch from non-neuronal enolase to neuron-specific enolase during differentiation. *Brain Res* 190:195–214.
- Sengelaub DR, Finlay BL (1982) Cell death in the mammalian visual system during normal development. I. Retinal ganglion cells. *J Comp Neurol* 204:311–317.
- Sloviter RS, Valiquette G, Abrams GM, Ronk EC, Sollas AI, Paul LA, Neubort SL (1989) Selective loss of hippocampal granule cells in the mature rat brain after adrenalectomy. *Science* 243:535–538.
- Smith GM, Miller RH, Silver J (1986) Changing role of forebrain astrocytes during development, regenerative failure and induced regeneration upon transplantation. *J Comp Neurol* 251:23–43.
- Trice JE, Stanfield BB (1986) Evidence for the generation in the adult rat dentate gyrus of neurons that extend axonal projections. *Ann Neurol* 20:392.
- Woolley CS, Gould E, Sakai RR, Spencer RL, McEwen BS (1991) Effects of aldosterone or RU28362 treatment on adrenalectomy-induced cell death in the dentate gyrus of the adult rat. *Brain Res* 554:312–314.
- Yehuda R, Fairman KR, Meyer JS (1989) Enhanced brain cell proliferation following early adrenalectomy in rats. *J Neurochem* 53:241–248.



# Diabetes impairs hippocampal function through glucocorticoid-mediated effects on new and mature neurons

Alexis M Stranahan<sup>1,2</sup>, Thiruma V Arumugam<sup>2,4</sup>, Roy G Cutler<sup>2</sup>, Kim Lee<sup>2</sup>, Josephine M Egan<sup>3</sup> & Mark P Mattson<sup>2</sup>

Many organ systems are adversely affected by diabetes, including the brain, which undergoes changes that may increase the risk of cognitive decline. Although diabetes influences the hypothalamic-pituitary-adrenal axis, the role of this neuroendocrine system in diabetes-induced cognitive dysfunction remains unexplored. Here we demonstrate that, in both insulin-deficient rats and insulin-resistant mice, diabetes impairs hippocampus-dependent memory, perforant path synaptic plasticity and adult neurogenesis, and the adrenal steroid corticosterone contributes to these adverse effects. Rats treated with streptozocin have reduced insulin and show hyperglycemia, increased corticosterone, and impairments in hippocampal neurogenesis, synaptic plasticity and learning. Similar deficits are observed in *db/db* mice, which are characterized by insulin resistance, elevated corticosterone and obesity. Changes in hippocampal plasticity and function in both models are reversed when normal physiological levels of corticosterone are maintained, suggesting that cognitive impairment in diabetes may result from glucocorticoid-mediated deficits in neurogenesis and synaptic plasticity.

As a result of high-calorie diets and sedentary lifestyles, diabetes is rapidly becoming more prevalent in Western societies<sup>1</sup>. In addition to its well known adverse effects on the cardiovascular and peripheral nervous systems, diabetes also appears to negatively affect the brain, increasing the risk of depression and dementia<sup>2,3</sup>. Human subjects with either type 1 (caused by insulin deficiency) or type 2 (mediated by insulin resistance) diabetes typically show impaired cognitive function compared to age-matched nondiabetic subjects<sup>3,4</sup>. Cognitive deficits have also been documented in studies of rodent models of diabetes. For example, rats rendered diabetic by treatment with the pancreatic  $\beta$ -cell toxin streptozocin (STZ) a model of type 1 diabetes, show impaired performance in tests of spatial learning ability<sup>5,6</sup>. Similar deficits have been reported in the *db/db* mouse<sup>7</sup>, a model of type 2 diabetes in which obesity, hyperglycemia and elevations in circulating corticosterone arise from a mutation that inactivates the leptin receptor<sup>8</sup>. However, the mechanism(s) responsible for cognitive dysfunction in diabetes has not been established.

Within the hippocampus, changes in the strength of synapses between groups of neurons are critical in certain types of learning and memory. At the level of the dentate gyrus, regulation of synaptic connectivity extends beyond changes in the number and strength of synapses to the *de novo* addition of new neurons in adulthood<sup>9</sup>. Data from studies of animal models suggest impairment of both synaptic

plasticity and adult neurogenesis in diabetes. Long-term potentiation (LTP) of synaptic transmission, believed to be a cellular mechanism of learning and memory, is impaired in the dentate gyrus of rats with streptozocin-induced diabetes<sup>10</sup>. Diabetic rodents also show lower rates of adult neurogenesis<sup>11</sup>, whereas exercise and dietary energy restriction, which have antidiabetic effects, can enhance synaptic plasticity<sup>12,13</sup> and neurogenesis<sup>12,14,15</sup>. Because cognitive ability is impaired in subjects with either type 1 or type 2 diabetes and in animal models of both types of diabetes, it is unlikely that global changes in insulin concentrations are directly responsible for impaired neuronal plasticity.

Humans with poorly controlled diabetes show hyperactivation of the hypothalamic-pituitary-adrenal (HPA) axis, resulting in elevated circulating cortisol<sup>2,4</sup>. Similarly, adrenal glucocorticoids are elevated in rodents with experimental diabetes<sup>16–20</sup>. The specific mechanism by which diabetes results in hyperactivation of the HPA axis is unknown, but it is apparently not the result of the hyperglycemia *per se*<sup>17</sup>. Although it is not known whether glucocorticoids are involved in cognitive dysfunction in diabetes, elevated cortisol has been associated with poor cognitive ability in humans subjected to psychosocial stress<sup>21</sup>, during normal aging<sup>22</sup> and in Alzheimer's disease<sup>23</sup>. Studies of rodents have provided evidence that elevated adrenal glucocorticoids mediate deficits in cognitive function caused by chronic stress<sup>24,25</sup>. In addition, chronic stress and high corticosterone can impair synaptic

<sup>1</sup>Psychology Department, Princeton University, Green Hall Washington Road, Princeton, New Jersey 08544, USA. <sup>2</sup>Laboratory of Neurosciences, Cellular and Molecular Neurosciences Section and <sup>3</sup>Laboratory of Clinical Investigation, Diabetes Section, National Institute on Aging Intramural Research Program, 5600 Nathan Shock Drive, Baltimore, Maryland 21224, USA. <sup>4</sup>Present address: Department of Pharmaceutical Sciences, School of Pharmacy, Texas Tech University Health Sciences Center, Amarillo, Texas 79430, USA. Correspondence should be addressed to M.P.M. ([mattsonm@grc.nia.nih.gov](mailto:mattsonm@grc.nia.nih.gov)).

Received 13 December 2007; accepted 24 January 2008; published online 17 February 2008; doi:10.1038/nn2055

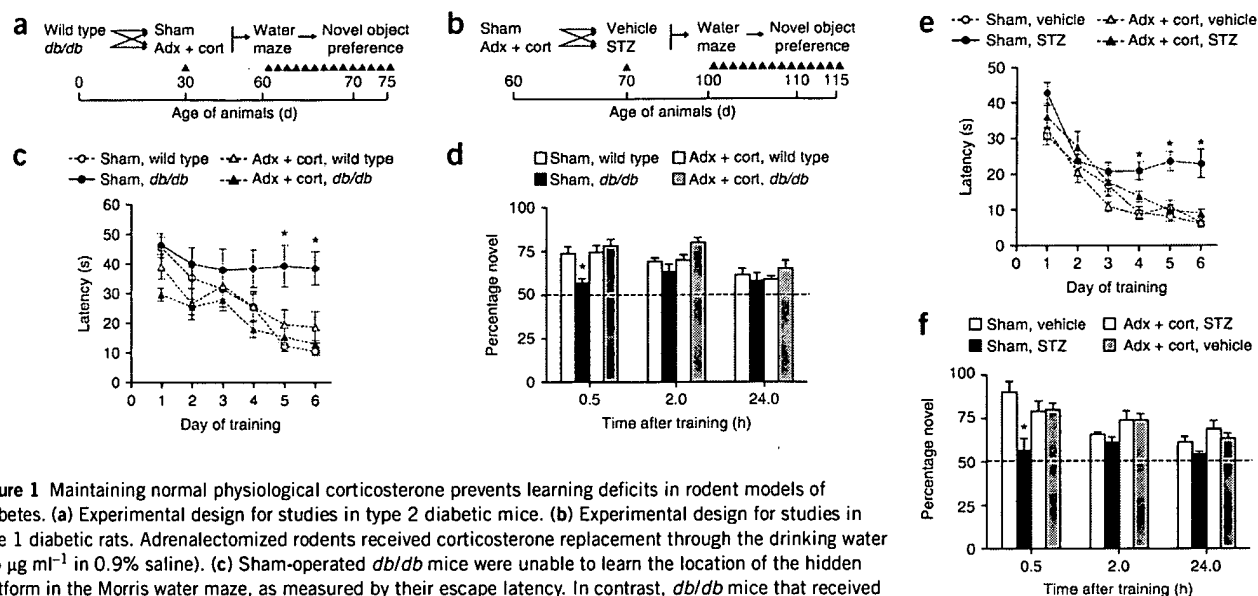


**Figure 1** Maintaining normal physiological corticosterone prevents learning deficits in rodent models of diabetes. **(a)** Experimental design for studies in type 2 diabetic mice. **(b)** Experimental design for studies in type 1 diabetic rats. Adrenalectomized rodents received corticosterone replacement through the drinking water ( $25 \mu\text{g ml}^{-1}$  in 0.9% saline). **(c)** Sham-operated  $db/db$  mice were unable to learn the location of the hidden platform in the Morris water maze, as measured by their escape latency. In contrast,  $db/db$  mice that received adrenalectomy and corticosterone replacement learned the location of the platform as effectively as nondiabetic mice. Shorter latencies on the first day of training in adrenalectomized  $db/db$  mice were attributable to performance on successive trials, as escape latencies were similar during the first trial (see Results). **(d)**  $db/db$  mice with intact adrenal glands showed impaired object recognition, while  $db/db$  mice with corticosterone 'clamped' through adrenalectomy and corticosterone replacement showed preference for the novel object that was similar to wild-type controls. **(e)** Learning was impaired in insulin-deficient diabetic rats experiencing elevated corticosterone, but not in diabetic rats that received adrenalectomy and corticosterone replacement. **(f)** Novel object preference was reduced in sham-operated diabetic rats, but preserved in diabetic rats with normal levels of corticosterone. Adx + cort., adrenalectomized with  $25 \mu\text{g ml}^{-1}$  corticosterone replacement. Error bars, s.e.m.

plasticity<sup>26–29</sup>. Moreover, concentrations of corticosterone characteristic of stress inhibit neurogenesis in the hippocampus of adult rats<sup>30</sup>, and corticosterone concentrations during the course of aging are correlated with age-related declines in neurogenesis and memory<sup>31</sup>. It is therefore possible that elevated corticosterone in diabetes may mediate central impairment of neuronal structure and function.

Here we provide direct evidence that elevated glucocorticoids contribute to the impairment of synaptic plasticity and neurogenesis, and to associated learning and memory deficits, in rodent models of both insulin-resistant and insulin-deficient diabetes. These findings support a role for HPA axis hyperactivity in diabetes-induced cognitive impairment, and suggest new approaches for improving cognitive function in subjects with diabetes.

## RESULTS

### Lowering corticosterone reverses learning deficits

To evaluate whether elevated corticosterone is accompanied by alterations in hippocampus-dependent learning in diabetic animals, we tested cognitive function in diabetic and nondiabetic mice and rats that had been adrenalectomized and administered low-dose corticosterone replacement<sup>30</sup> or had been sham-operated (Fig. 1a,b). Adrenalectomized rodents received corticosterone replacement through the drinking water ( $25 \text{ mg ml}^{-1}$  in 0.9% saline). This intervention has previously been used to both lower and normalize corticosterone after stress<sup>32</sup>. First we evaluated performance in the hippocampus-dependent version of the water maze task. In both  $db/db$  mice and STZ-treated rats, sham-operated diabetic animals had longer escape latencies and took a less direct route to the hidden platform (Fig. 1; Supplementary Fig. 1a,b online). These findings concur with previous reports<sup>5–7</sup>. Both of these deficits were reversed in diabetic mice and rats with normal physiological levels of corticosterone (escape latency in  $db/db$  mice,  $F_{1,32} = 4.91$ ,  $P = 0.03$ ; in STZ-treated rats,

$F_{1,46} = 7.19$ ,  $P = 0.01$ ; path length in  $db/db$  mice,  $F_{1,33} = 4.52$ ,  $P = 0.04$ ; path length in STZ-treated rats,  $F_{1,31} = 13.62$ ,  $P = 0.001$ ). There was no effect of adrenalectomy and corticosterone replacement in nondiabetic mice and rats. Additionally, there were no significant differences in swimming speed across diabetic and nondiabetic mice and rats with different levels of corticosterone ( $db/db$  mice,  $F_{1,33} = 1.42$ ,  $P = 0.24$ ; STZ-treated rats,  $F_{1,43} = 0.14$ ,  $P = 0.71$ ). Although  $db/db$  mice that had received adrenalectomy and corticosterone replacement had shorter escape latencies and path lengths on the first day of training (Fig. 1c, Supplementary Fig. 1a), this was primarily due to improvements during the successive trials, as latency and path length during trial 1 were not different from other groups (data not shown).

In a probe trial conducted 24 h after the last session of acquisition training, sham-operated STZ-diabetic rats spent less time searching in the target quadrant, relative to nondiabetic, sham-operated rats ( $F_{1,27} = 5.07$ ,  $P = 0.03$ ; Supplementary Fig. 1d). This contrasts with the results of the probe trial in the  $db/db$  mice, where we observed no significant effect of diabetes or adrenalectomy on the percentage of time spent searching in the target quadrant ( $F_{1,33} = 0.85$ ,  $P = 0.36$ ; Supplementary Fig. 1c). Performance in the visible-platform version of the Morris water maze, which is not hippocampus dependent, was similar across conditions in both models ( $db/db$  mice,  $F_{1,33} = 0.001$ ,  $P = 0.96$ ; STZ-treated rats,  $F_{1,28} = 0.57$ ,  $P = 0.45$ ; data not shown).

Next we tested recognition memory in the novel object preference test. This task takes advantage of the natural bias for novelty in rodents and, unlike the water maze, does not depend on aversive motivation. In both models, nondiabetic mice and rats showed robust preference for the novel object, particularly at the shortest post-training interval. However, sham-operated diabetic mice and rats showed less of a preference for the novel object ( $db/db$  mice,  $F_{1,26} = 10.52$ ,  $P = 0.003$ ; STZ-treated rats,  $F_{1,11} = 11.68$ ,  $P = 0.006$ , Fig. 1d,f). In contrast, diabetic mice and rats that had received adrenalectomy and

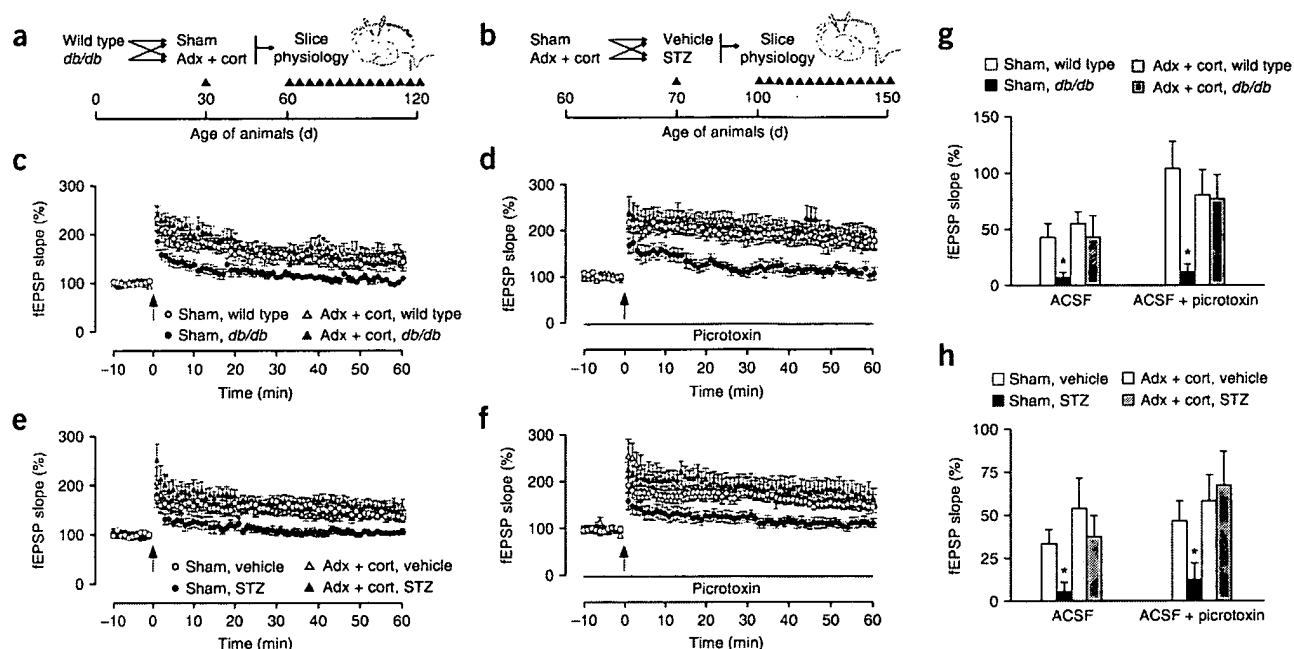


**Figure 2** Lowering corticosterone regulates synaptic plasticity in diabetic rodents. (a) Design for studies in type 2 diabetic mice. (b) Design for studies in type 1 diabetic rats. (c) Sham-operated *db/db* mice showed reduced dentate gyrus LTP, but *db/db* mice with normal physiological corticosterone were not impaired. (d) Insulin-resistant mice that had been sham-operated also showed impaired LTP in the presence of picROTOXIN, which decreases local inhibition and also blocks GABAergic excitation on new neurons<sup>34,35</sup>. In contrast, insulin-resistant mice with normal physiological corticosterone showed control levels of LTP under these conditions. (e) Sham-operated insulin-deficient rats showed reduced LTP; preventing elevation of corticosterone before induction of experimental diabetes restored LTP. (f) STZ-diabetic rats with intact adrenal glands showed reduced LTP in the presence of picROTOXIN. Lowering corticosterone also reversed the effect of diabetes on LTP under these conditions. (g,h) Comparison of the amount of potentiation in slices from diabetic and nondiabetic mice (g) and rats (h) with different levels of corticosterone, recorded in ACSF and in ACSF with picROTOXIN. Error bars, s.e.m.; Adx + cort., adrenalectomized with 25  $\mu\text{g ml}^{-1}$  corticosterone replacement; fEPSP, field excitatory postsynaptic potential.

corticosterone replacement preferred to explore the novel object, with biases that were similar to those of nondiabetic rodents. We also recorded the latency to begin exploring and the total time spent exploring both objects during each trial (novel + familiar/duration of behavioral observation; see **Supplementary Methods** online). In the *db/db* mouse model, diabetic mice spent more time exploring the objects ( $F_{1,28} = 22.78$ ,  $P = 0.001$ ; **Supplementary Fig. 2a** online), and latency to approach either object was not different across groups (**Supplementary Fig. 2b**). In the STZ-treated rat model, there were no differences in the amount of time spent exploring the objects (**Supplementary Fig. 2c**), but sham-operated diabetic rats waited longer before approaching the objects, and adrenalectomized diabetic rats waited less ( $F_{1,12} = 6.14$ ,  $P = 0.001$ ; **Supplementary Fig. 2d**). The parameters surrounding object exploration are difficult to interpret, because neither total time exploring nor the latency to explore was significantly correlated with preference for the novel object (data not shown). However, together with the water maze results, these data suggest that untreated diabetes exerts pervasive negative effects on hippocampus-dependent memory, and that these effects can be reversed by lowering corticosterone.

### Normalizing corticosterone restores LTP

We further examined the role of corticosterone in the diabetes-induced impairment of hippocampal learning by measuring synaptic plasticity at perforant path–dentate gyrus synapses in acute slices from another group of adrenalectomized or sham-operated diabetic and nondiabetic rodents (Fig. 2a,b). In agreement with previous studies<sup>6,7</sup>, both *db/db* mice and STZ-diabetic rats showed reduced LTP at medial perforant

path synapses in the dentate gyrus when recordings were made in the presence of the GABA<sub>A</sub> receptor antagonist picROTOXIN (100  $\mu\text{M}$ ; Fig. 2). Adrenalectomy and corticosterone replacement prevented LTP impairment in both models (*db/db* mice,  $F_{1,36} = 5.15$ ,  $P = 0.03$ ; STZ-treated rats,  $F_{1,35} = 5.90$ ,  $P = 0.02$ ). Baseline synaptic transmission was not different in *db/db* mice and controls, irrespective of corticosterone manipulation (**Supplementary Fig. 3a** online). However, in rats, adrenalectomy and corticosterone replacement reduced baseline synaptic transmission, in both diabetic and nondiabetic rats ( $F_{1,39} = 3.65$ ,  $P = 0.03$ ; **Supplementary Fig. 3c**). No alterations in the paired-pulse depression that is characteristic of this pathway were observed in either model (**Supplementary Fig. 3b,d**). Taken together, these findings suggest that diabetes causes a primarily postsynaptic deficit in dentate gyrus plasticity that is reversible by lowering corticosterone.

Adult-generated neurons show a number of distinct electrophysiological properties. Among these is the transient capacity for GABAergic excitation<sup>33,34</sup>. It was recently demonstrated that changes in adult neurogenesis correlate with changes in medial perforant path LTP in the absence, but not in the presence, of picROTOXIN<sup>35,36</sup>. We confirmed this in slices from wild-type mice that had been infused with the antimetabolic drug cytosine arabinoside (AraC), which effectively reduced progenitor cell proliferation (BrdU-labeled cells with vehicle,  $4,440 \pm 822.6$ ; with AraC,  $696.0 \pm 230.9$ ;  $t_{10} = 5.08$ ,  $P = 0.0005$ ; Figs. 3 and 4a). We also counted pyknotic cell profiles to determine whether antimetabolic treatment might influence cell death; there was no significant difference between vehicle- and AraC-treated mice in the number of pyknotic cells in the dentate gyrus (vehicle,  $216 \pm 54$ ; AraC,  $450 \pm 160$ ; mean  $\pm$  s.e.m.;  $t_7 = 1.58$ ,  $P = 0.16$ ).



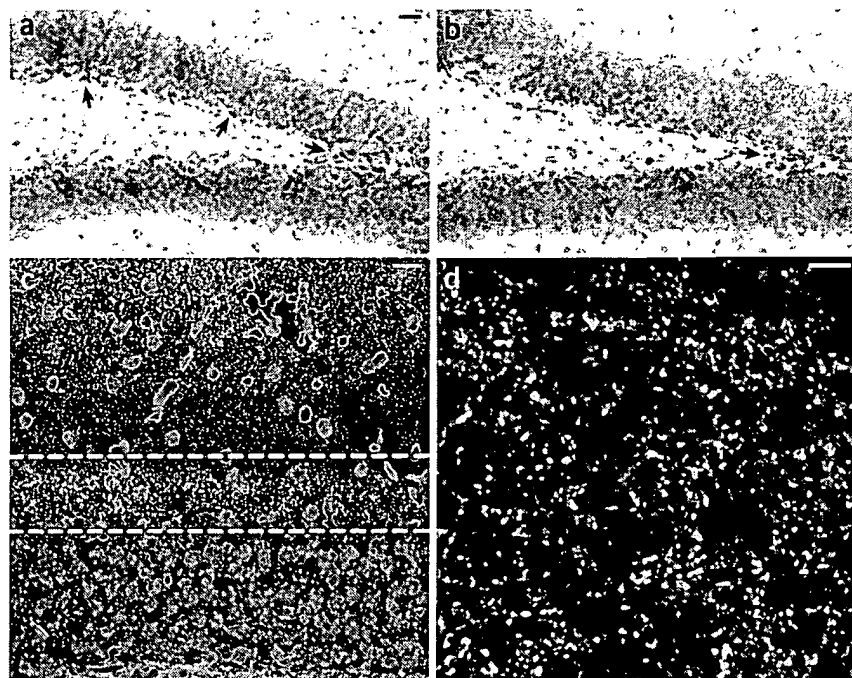


**Figure 3** AraC treatment reduces cell proliferation, without altering synaptic marker immunoreactivity. (a, b) Dentate gyri after a single injection of 300 mg kg<sup>-1</sup> BrdU with a 24 h survival period, from a mouse infused with vehicle (a) and a mouse infused with AraC (b). Arrows, BrdU-labeled cells. Scale bar (a, b), 30 μm. (c) Confocal micrograph showing synaptic marker expression in the inner third of the dentate molecular layer, where the medial perforant path synapses are located. Outline, anatomical region where scans were taken for analysis of synaptophysin labeling and where electrodes were positioned for electrophysiological recordings in slices. Scale bar, 20 μm. (d) Micrograph taken at the resolution and scale used for analysis of synaptophysin labeling (see **Supplementary Methods**). Scale bar, 10 μm.

LTP to a level similar to that in controls (*db/db* mice,  $F_{1,33} = 3.10$ ,  $P = 0.04$ ; STZ-treated rats,  $F_{1,39} = 5.24$ ,  $P = 0.03$ ; **Fig. 2c,e**). These results suggest that diabetes alters synaptic plasticity through multiple mechanisms involving both changes in new neurons and changes in the mature neuronal population.

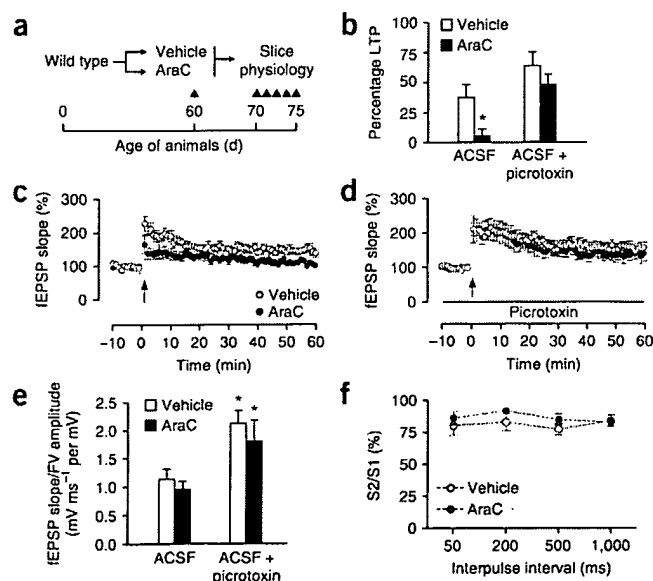
To evaluate whether AraC treatment might alter synaptic marker expression in the anatomical region where medial perforant path synapses are located, we used immunofluorescence labeling for synaptophysin. There were no differences in the area or intensity of synaptophysin immunofluorescence in AraC- and vehicle-treated mice, suggesting no loss of synapses among the larger population of mature granule neurons (optical intensity index with vehicle,  $1.1 \times 10^6 \pm 3.1 \times 10^5$ ; with AraC,  $1.2 \times 10^6 \pm 2.1 \times 10^5$ ;  $t_{10} = 0.21$ ,  $P = 0.84$ ; **Fig. 3c,d**). In slices from AraC-treated mice, we observed selective deficits in medial perforant path LTP recorded in plain artificial cerebrospinal fluid (ACSF) (**Fig. 4b,c**). These deficits were not detected when recordings were made in the presence of picrotoxin (100 μM; **Fig. 4b,d**). Although there was a significant effect of picrotoxin on the input-output curve, there was no effect of AraC treatment (**Fig. 4e**). There was also no effect of AraC infusion on paired-pulse depression, recorded in plain ACSF (**Fig. 4f**).

To measure LTP in diabetic animals under conditions that would permit the activation of newly generated neurons, we induced LTP in the absence of picrotoxin. Diabetic rodents showed impaired LTP, and maintaining low corticosterone through adrenalectomy restored

#### Corticosterone-mediated impairment of cell proliferation

To assess what role elevated corticosterone might play in the diabetes-induced suppression of hippocampal cell proliferation, we administered a single injection of the DNA synthesis marker bromodeoxyuridine (BrdU; 300 mg per kilogram body weight intraperitoneally) to adrenalectomized and sham-operated rodents with and without diabetes (**Fig. 5a,b**). In *db/db* mice, adrenalectomy and corticosterone replacement prevented the reduction in BrdU labeling in the dentate gyrus that we observed in sham-operated *db/db* mice 2 h after injection ( $F_{1,31} = 5.82$ ,  $P = 0.02$ ; **Figs. 5 and 6**). Similarly, in STZ-diabetic rats, adrenalectomy and corticosterone replacement before the induction of experimental diabetes prevented the decrease in BrdU-labeled cell number observed in sham-operated diabetic rats ( $F_{1,41} = 10.76$ ,

**Figure 4** Antimitotic treatment selectively impairs dentate gyrus LTP recorded in the absence of picrotoxin. (a) Experimental design for studies using minipump delivery of antimitotic drugs. (b) Comparison of the amount of LTP in vehicle- and AraC-infused mice when recordings were made in the presence or absence of the GABA<sub>A</sub> antagonist picrotoxin (100 μM). \* $P < 0.05$ ,  $2 \times 2$  ANOVA. (c) LTP at medial perforant path synapses in the dentate gyrus was impaired in AraC-infused mice. (d) LTP recorded in the presence of picrotoxin was not influenced by AraC infusion. (e) The relationship between the slope of the dendritic field potential and the amplitude of the axonal fiber volley was influenced by picrotoxin, but not by AraC treatment. (f) Presynaptic paired-pulse depression measured in plain ACSF was not altered by treatment with AraC. Error bars, s.e.m.; fEPSP, field excitatory postsynaptic potential; FV, fiber volley (the amplitude of the response among presynaptic axons); S1 and S2, slopes of the first and second fEPSPs, respectively.



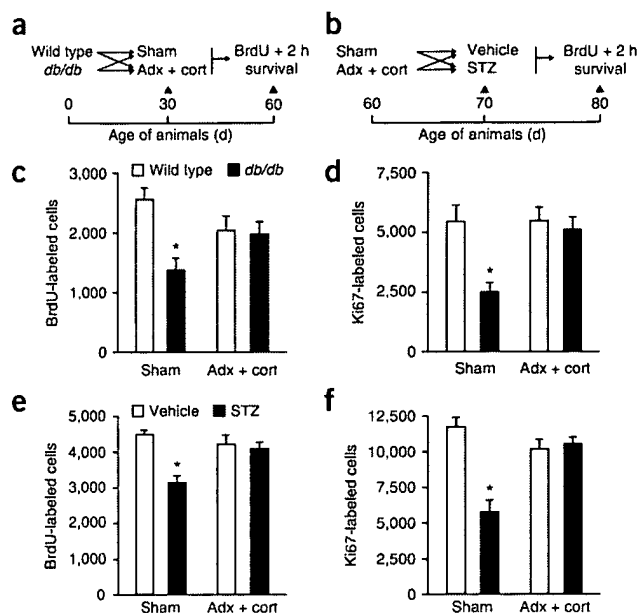


**Figure 5** Elevated corticosterone contributes to the suppression of dentate gyrus cell proliferation in diabetic rodents. **(a)** Design for studies in type 2 diabetic mice. **(b)** Design for studies in type 1 diabetic rats. **(c)** Sham-operated *db/db* mice showed reduced BrdU labeling in the dentate gyrus, whereas *db/db* mice that received adrenalectomy and corticosterone replacement were not different from nondiabetic mice. **(d)** Labeling for the endogenous proliferation marker Ki67 was reduced in sham-operated type 2 diabetic mice, whereas type 2 diabetic mice that had been adrenalectomized and given corticosterone replacement were not different from nondiabetic mice. Legend in **c** applies to **d**. **(e)** Type 1 diabetic rats with intact adrenal glands had fewer BrdU-labeled cells in the dentate gyrus; this reduction was not observed in type 1 diabetic rats with normal levels of corticosterone. **(f)** Labeling for the endogenous proliferation marker Ki67 followed a similar pattern: diabetic rats with intact adrenal glands had significantly fewer Ki67-labeled cells than controls, whereas diabetic rats that received adrenalectomy and low-dose corticosterone replacement were not significantly different from nondiabetic rats. Legend in **e** applies to **f**. Error bars, s.e.m.; Adx + cort., adrenalectomized with 25  $\mu\text{g ml}^{-1}$  corticosterone replacement.

$P = 0.002$ ; Fig. 5e, Supplementary Fig. 4a,b online). There was no effect of adrenalectomy and corticosterone replacement in vehicle-treated rats or in wild-type mice.

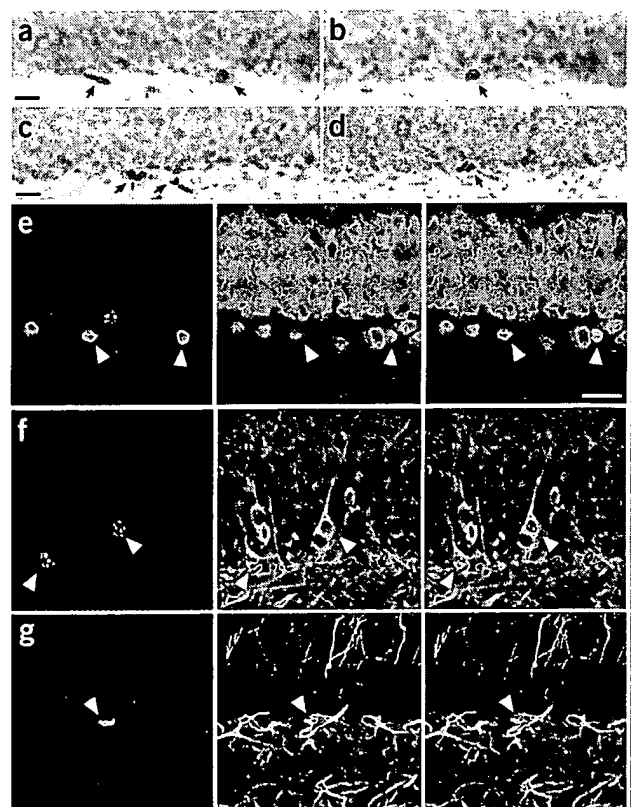
Diabetes has been associated with neurovascular pathologies, which could alter the availability of the exogenous marker BrdU. For an index of hippocampal cell proliferation that would not be influenced by availability, we used the endogenous proliferative marker Ki67. Labeling for Ki67 followed the same pattern as labeling for BrdU; sham-operated diabetic rodents had fewer Ki67-labeled cells, whereas diabetic rodents that had been adrenalectomized and given corticosterone replacement were not significantly different from nondiabetic controls (*db/db* mice,  $F_{1,20} = 5.24$ ,  $P = 0.03$ ; STZ-treated rats,  $F_{1,35} = 5.89$ ,  $P = 0.02$ ; Figs. 5d,f and 6c,d; Supplementary Fig. 4c,d). There were no effects of adrenalectomy and corticosterone replacement on Ki67 labeling in nondiabetic wild-type mice or vehicle-treated rats. These results indicate that lowering corticosterone prevents the decrease in hippocampal progenitor cell proliferation in insulin-resistant and insulin-deficient diabetes.

### Lasting suppression of adult neurogenesis with diabetes

To evaluate whether suppression of hippocampal cell proliferation in diabetic animals translates into a reduction in adult neurogenesis, we

**Figure 6** Hippocampal cell proliferation and neurogenesis is reduced in a mouse model of type 2 diabetes. **(a)** BrdU-labeled cells (arrows) in the proliferative dentate subgranular zone of a wild-type mouse 2 h after injection. **(b)** BrdU-labeled cells (arrows) in the subgranular zone of a *db/db* homozygous mouse. **(c)** Progenitor cells expressing the endogenous proliferation marker Ki67 (arrows) in the dentate gyrus of a wild-type mouse. **(d)** Cells labeled with antibodies to Ki67 (arrows) in the dentate gyrus of a *db/db* mouse. **(e)** Cells positive for both the proliferative marker BrdU (red, left) and the mature neuronal marker NeuN (green, middle) 3 weeks after injection (merged image shown to the right). **(f)** Double labeling with BrdU (red) and Tuj1 (green), also 3 weeks after injection (merged image shown to the right). **(g)** Cells double-labeled with antibodies to BrdU (red) and the astroglial marker GFAP (green) 3 weeks after injection (merged image shown to the right). For **e–g**, the far right panel shows the merged image across the z axis. Scale bars, 20  $\mu\text{m}$ . Scale bars in **a** and **c** apply to **b** and **d**, respectively; scale bar in **e** applies to **f** and **g**.

administered a single injection of BrdU (300  $\text{mg kg}^{-1}$  intraperitoneally) to diabetic and nondiabetic rodents and killed them three weeks later. In *db/db* mice, we observed a reduction in the number of BrdU-labeled cells in the dentate gyrus (mean  $\pm$  s.e.m. for wild type,  $860 \pm 69$ ; for *db/db*,  $416 \pm 85$ ;  $t_8 = 4.05$ ,  $P = 0.004$ ). There was no difference in the proportion of cells expressing the mature neuronal marker NeuN (wild type,  $98 \pm 1.22$ ; *db/db*,  $96 \pm 1.87$ ;  $t_8 = 0.89$ ,  $P = 0.39$ ; Fig. 6e) or the immature neuronal marker Tuj1 (wild type,  $93 \pm 0.96$ ; *db/db*,  $93 \pm 1.26$ ;  $t_8 = 0.03$ ,  $P = 0.97$ ; Fig. 6f). There was also no change in the percentage of BrdU-labeled cells expressing the astroglial marker GFAP (wild type,  $7.35 \pm 1.01$ ; *db/db*,  $8.92 \pm 2.51$ ;  $t_8 = 0.58$ ,  $P = 0.57$ ; Fig. 6g). Because the analyses were made separately, in adjacent series of stereological sections, values reflect relative expression of each marker among



the BrdU-labeled cell population. However, the absence of any proportionate difference in the expression of neuronal and glial markers suggests that differentiation of newly generated cells was not affected.

Similarly, in STZ-diabetic rats, there were fewer cells labeled with BrdU relative to the number in vehicle-treated controls (mean  $\pm$  s.e.m. for vehicle,  $3,728 \pm 412$ ; for STZ,  $2,070 \pm 466.6$ ;  $t_9 = 2.66$ ,  $P = 0.02$ ). There was no change in the proportion of cells positive for both BrdU and the neuronal markers NeuN (vehicle,  $91.33 \pm 2.81$ ; STZ,  $84 \pm 5.21$ ;  $t_9 = 1.30$ ,  $P = 0.23$ ; **Supplementary Fig. 4e**) or Tuj1 (vehicle,  $87 \pm 2.40$ ; STZ,  $86.67 \pm 1.33$ ;  $t_{10} = 0.24$ ,  $P = 0.81$ ; **Supplementary Fig. 4f**). The percentage of BrdU-labeled cells expressing GFAP, a marker of astrocytes, was not altered in type 1 diabetic rats (vehicle,  $7.33 \pm 1.91$ ; STZ,  $9.33 \pm 1.33$ ;  $t_{10} = 0.86$ ,  $P = 0.41$ ; **Supplementary Fig. 4g**). However, coincident with the reduction in BrdU-labeled cell number, these data indicate a net reduction in the number of new neurons and astrocytes for both insulin-resistant mice and insulin-deficient rats.

#### Corticosterone regulates glucose and insulin concentrations

To determine whether lowering corticosterone might prevent or alter the impact of experimental diabetes, we measured insulin and glucose in serum from diabetic and nondiabetic rodents that had been adrenalectomized or sham-operated. In both diabetes models, sham-operated diabetic rodents showed corticosterone concentrations that were comparable to those reported in nondiabetic rats after an acute stressor<sup>32</sup> (**Table 1**). In the type 1 diabetes model, preventing the elevation of corticosterone did not alter STZ-induced hyperglycemia (**Table 1**). Effects were similar in serum samples from fed and fasted rats (fed glucose,  $F_{1,41} = 10.19$ ,  $P = 0.002$ ; fasting glucose,  $F_{1,13} = 90.36$ ,  $P < 0.001$ ; **Table 1**). Likewise, adrenalectomy and corticosterone replacement had no impact on the ability of STZ to reduce insulin ( $F_{1,33} = 25.57$ ,  $P < 0.001$ ; **Table 1**). There was no long-term effect of STZ diabetes on feeding or body weight (**Supplementary Table 1** online). Because we administered corticosterone replacement through the drinking water, it is important to note that despite the higher volume of solution consumed by adrenalectomized rats in both the STZ-treated and vehicle-treated conditions ( $F_{1,15} = 23.78$ ,  $P < 0.001$ ; **Supplementary Table 1**), these animals maintained serum corticosterone concentrations that were similar to those of sham-operated nondiabetic controls (**Table 1**).

*db/db* mice respond differently than STZ-treated rats to adrenalectomy and corticosterone replacement. In this model, adrenalectomy and corticosterone replacement reversed the increase in fasting glucose in *db/db* mice ( $F_{1,39} = 21.38$ ,  $P < 0.001$ ; **Table 1**). However, postprandial glucose in adrenalectomized *db/db* mice remained higher than those of nondiabetic controls ( $F_{1,33} = 47.46$ ,  $P < 0.001$ ; **Table 1**). Lowering corticosterone also attenuated hyperinsulinemia ( $F_{1,23} = 5.69$ ,  $P = 0.03$ ; **Table 1**). Both sham-operated and adrenalectomized *db/db* mice weighed more than wild-type mice ( $F_{1,31} = 32.43$ ,  $P < 0.001$ ) and consumed more food ( $F_{1,48} = 51.90$ ,  $P < 0.001$ ) (**Supplementary Table 1**). *db/db* mice characteristically show polydipsia, and we observed this in sham-operated *db/db* mice but not in *db/db* mice that had received adrenalectomy and corticosterone replacement ( $F_{1,42} = 14.77$ ,  $P = 0.004$ ; **Supplementary Table 1**).

**Table 1** Endocrine characteristics of type 1 and type 2 diabetes in rodents with different levels of corticosterone

		Fasting glucose (mg dl <sup>-1</sup> )	Fed glucose (mg dl <sup>-1</sup> )	Insulin (ng ml <sup>-1</sup> )	Corticosterone (ng ml <sup>-1</sup> )
Wild type	Sham	71.77 (8.63)	140.65 (15.67)	1.41 (0.15)	46.16 (15.99)
	Adx + cort	64.80 (1.87)	95.95 (20.65)	1.41 (0.14)	18.85 (3.95)
<i>db/db</i>	Sham	330.27 (21.01)*	334.12 (41.09)*	3.16 (0.68)*	258.55 (43.11)*
	Adx + cort	98.40 (17.51)	328.88 (19.83)*	1.03 (0.17)	11.24 (2.21)
Vehicle	Sham	30.19 (5.77)	129.86 (21.72)	2.07 (0.27)	53.08 (17.72)
	Adx + cort	44.74 (2.23)	170.87 (11.74)	1.73 (0.27)	19.87 (4.56)
STZ	Sham	290.96 (35.94)*	318.46 (16.76)*	0.79 (0.09)*	418.24 (18.26)*
	Adx + cort	221.08 (14.80)*	263.06 (11.29)*	0.91 (0.16)*	30.14 (5.78)

Data were analyzed using  $2 \times 2$  ANOVA; Values are means with s.e.m. in parentheses. Sham, sham-operated; Adx + cort, adrenalectomized with corticosterone replacement.

\* $P < 0.05$  relative to sham-operated nondiabetic controls.

To evaluate whether levels of insulin and glucose in the hippocampus were altered in diabetic rodents, we measured them in whole-hippocampal homogenates from STZ-diabetic rats and *db/db* mice. We observed no effect of STZ diabetes on hippocampal glucose or insulin concentrations (glucose with vehicle,  $23.34 \pm 4.08$  mmol mg<sup>-1</sup>; with STZ,  $24.24 \pm 5.96$  mmol mg<sup>-1</sup>;  $t_{10} = 0.12$ ,  $P = 0.90$ ; insulin with vehicle,  $1.55 \pm 0.15$   $\mu$ mol mg<sup>-1</sup>; with STZ,  $1.81 \pm 0.25$   $\mu$ mol mg<sup>-1</sup>;  $t_{10} = 0.86$ ,  $P = 0.42$ ). Similarly, concentrations of glucose and insulin in the hippocampus of *db/db* mice were not different from those in wild-type mice (glucose in wild type,  $10.73 \pm 1.85$  mmol mg<sup>-1</sup>; in *db/db*,  $13.48 \pm 1.16$  mmol mg<sup>-1</sup>;  $t_6 = 1.26$ ,  $P = 0.25$ ; insulin in wild type,  $1.26 \pm 0.15$   $\mu$ mol mg<sup>-1</sup>; in *db/db*,  $1.60 \pm 0.21$   $\mu$ mol mg<sup>-1</sup>;  $t_6 = 1.32$ ,  $P = 0.25$ ). Although these results do not preclude a change in the availability or sensitivity to glucose and/or insulin at the level of individual cells, they do provide indirect support for the idea that another factor, namely corticosterone, contributes to the impairment of hippocampal plasticity in diabetic rodents.

#### Corticosterone mediates learning impairments in *db/db* mice

Because adrenalectomy removes not only endogenous corticosterone but also the primary source of peripheral epinephrine, we replicated our previous experimental design with an additional group of *db/db* mice that were adrenalectomized and given a high replacement dose of corticosterone through the drinking water ( $250 \mu$ g ml<sup>-1</sup> in 0.9% saline; **Fig. 7a**). This regimen resulted in circulating corticosterone concentrations similar to those of sham-operated *db/db* mice (mean  $\pm$  s.e.m.,  $333.28 \pm 47.38$  ng ml<sup>-1</sup>). We tested these mice in the Morris water maze and object recognition tasks. In support of our earlier result, *db/db* mice that had received adrenalectomy and  $25 \mu$ g ml<sup>-1</sup> corticosterone replacement learned the location of the hidden platform more rapidly than sham-operated *db/db* mice and adrenalectomized *db/db* mice receiving  $250 \mu$ g ml<sup>-1</sup> corticosterone replacement ( $F_{2,10} = 8.35$ ,  $P < 0.001$ ; **Fig. 7b**, **Supplementary Fig. 5a** online). *db/db* mice that had been adrenalectomized and given low-dose corticosterone replacement also showed greater improvement over successive trials on day 1, but performance on the first trial was not different from that of sham-operated *db/db* mice or that of *db/db* mice that had been adrenalectomized and given a higher dose of corticosterone (data not shown). There were no effects of any of the treatments on swimming speed (**Supplementary Fig. 5b**).

Higher doses of corticosterone also reinstated deficits in object-recognition memory. *db/db* mice that had been adrenalectomized and administered a low dose of corticosterone spent more time exploring the novel object than did sham-operated *db/db* mice. In contrast, in

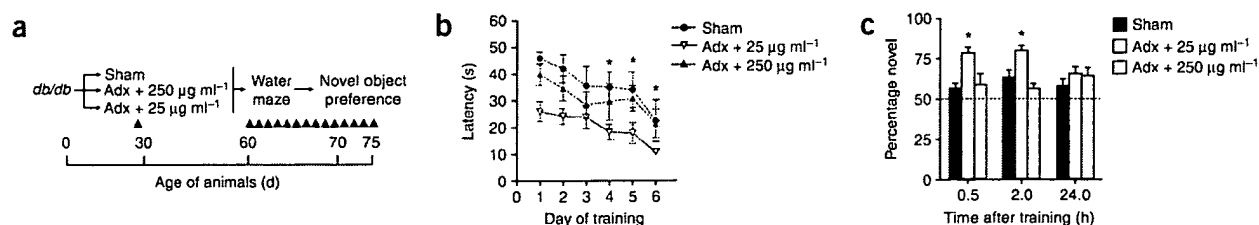


**Figure 7** A high replacement dose of corticosterone reinstates learning deficits in adrenalectomized *db/db* mice. (a) Experimental design: *db/db* mice were sham-operated or adrenalectomized (Adx); adrenalectomized mice received corticosterone replacement at 25 or 250  $\mu\text{g ml}^{-1}$  in their drinking water. One month after surgery, the mice were tested in the Morris water maze and object recognition tasks. (b) Lowering corticosterone restored hippocampal learning in insulin resistant mice, whereas a high replacement dose of corticosterone was associated with learning impairments comparable to those in sham-operated diabetic mice. Differences in performance on the first day of training in adrenalectomized *db/db* mice receiving low-dose corticosterone replacement were due to improvements over successive trials, as no differences were observed during the first trial (see Results). (c) *db/db* mice that had been adrenalectomized and given a low replacement dose of corticosterone spent more time exploring the novel object, relative to sham-operated *db/db* mice and to *db/db* mice administered a high dose of corticosterone. \* $P < 0.05$ , one-way repeated-measures ANOVA. Error bars, s.e.m.

adrenalectomized *db/db* mice that received a higher dose of corticosterone, the reduction in novel object preference was identical to that seen in sham-operated *db/db* mice ( $F_{2,8} = 11.05$ ,  $P = 0.03$ ; Fig. 7c). Again, *db/db* mice that had been adrenalectomized and administered a low dose of corticosterone showed a preference for the novel object that was similar to nondiabetic mice.

Administration of a high dose of corticosterone had complex effects on the endocrine parameters of adrenalectomized *db/db* mice. These mice showed hyperglycemia, at a level similar to sham-operated *db/db* mice (mean  $\pm$  s.e.m. fasting,  $339.30 \pm 34.10$  mg  $\text{dl}^{-1}$ ; fed,  $450.59 \pm 46.04$  mg  $\text{dl}^{-1}$ ). Serum insulin was also elevated (mean  $\pm$  s.e.m.,  $1.98 \pm 0.57$  ng  $\text{ml}^{-1}$ ). *db/db* mice receiving a high dose of corticosterone showed increased water intake, similarly to sham-operated *db/db* mice (mean  $\pm$  s.e.m.,  $52.73 \pm 7.24$  ml  $\text{d}^{-1}$ ). However, their food intake and body weights were similar to those of wild-type mice (food intake,  $5.97 \pm 0.65$  g  $\text{d}^{-1}$ ; body weight,  $41.07 \pm 4.34$  g). These results suggest that elevated corticosterone contributes centrally to learning deficits and peripherally to the endocrine characteristics of diabetes.

## DISCUSSION

Diabetes is associated with several adverse effects on the brain, some of which may result primarily from direct consequences of chronic hyperglycemia. However, our findings demonstrate a pivotal role for the adrenal steroid corticosterone as a mediator of diabetes-induced impairments in hippocampal synaptic plasticity and neurogenesis, and associated cognitive deficits. Lowering corticosterone prevented the diabetes-induced impairment of learning and memory in insulin-deficient rats and insulin resistant mice. Maintaining normal physiological corticosterone also restored LTP at perforant path–dentate gyrus synapses and prevented the impairment of adult neurogenesis in the dentate gyrus. The restorative effect of lowering corticosterone was observed when recordings were made under conditions that either permitted or excluded the contribution of newly generated neurons. Enhancement of hippocampal function by normalizing corticosterone in diabetic mice or rats was completely reversed by administration of high levels of corticosterone, demonstrating that corticosterone (rather than some other adrenal-derived factor) was responsible for the adverse effects of diabetes on hippocampal plasticity. These findings strongly support a role for elevated corticosterone in impaired hippocampal plasticity and cognition induced by diabetes.

It is well established that chronic exposure to high levels of corticosterone is detrimental for learning and synaptic plasticity in nondiabetic animals<sup>24–29</sup>. The corticosterone-mediated adverse effects of diabetes were not determined by changes in insulin production,

because they occurred both in *db/db* mice with elevated insulin and in insulin-deficient rats. We also observed no change in hippocampal insulin levels under baseline conditions in diabetic mice and rats. However, this does not rule out the possibility that insulin signaling pathways might be impaired in diabetes. The effects of insulin on learning and memory oppose those of glucocorticoids at several levels. Specifically, intrahippocampal insulin<sup>37</sup> or activation of insulin signaling pathways<sup>38</sup> can block the effects of stress on learning and memory. Exposure to elevated corticosterone reduces insulin receptor signaling in many somatic tissues, including the brain<sup>39</sup>. Therefore, it is possible that the negative effect of diabetes on hippocampal plasticity may be attributable to an interaction between elevated glucocorticoids and insulin receptor signaling.

Local cerebral glucose usage is tightly linked with neural activity and cognition. In contrast, glucocorticoids inhibit glucose usage in neurons<sup>40</sup>. In normal (that is, nondiabetic) rats, hippocampus-dependent learning is correlated with a decrease in extracellular glucose, and intrahippocampal injection of glucose improves performance<sup>41</sup>. No studies so far have reported an effect of diabetes on learning-induced changes in hippocampal glucose metabolism, but alterations in basal hippocampal glucose transporter expression have been demonstrated in diabetic rats<sup>42</sup>. Although we observed no difference in glucose concentrations in whole hippocampal homogenates from insulin-resistant mice or insulin-deficient rats, our results do not preclude a role for corticosterone in modulating the diabetes-induced alterations in hippocampal glucose metabolism.

Lowering corticosterone in diabetes can restore behavioral function on tasks that recruit both new and mature neurons. While the Morris water maze task is not influenced by antimitotic treatment<sup>35,43</sup>, newly generated neurons are activated after this task at a higher rate than mature neurons<sup>44</sup>. Similar distinctions have been reported with respect to the role of adult-generated neurons in recognition memory: systemic treatment with an antimitotic reversed enhancement of performance on the novel-object preference task after environmental enrichment<sup>45</sup>, but focal cranial irradiation did not affect spontaneous alternation in the Y-maze, which also involves recognition memory<sup>35</sup>. Although it remains to be determined whether adult-generated granule neurons make a meaningful contribution to performance on these tasks under baseline conditions, the therapeutically relevant question is whether new neurons can enhance performance after neurodegeneration or injury.

The absence of an effect of corticosterone reduction on postprandial serum glucose in *db/db* mice is in line with previous studies. Adrenalectomy and corticosterone replacement do not normalize fed glucose values in the *ob/ob* mouse<sup>18</sup>. Similar results occur upon treatment with

the glucocorticoid receptor antagonist RU486 in the Zucker (*fafa*) rat, with no effect of antiglucocorticoid treatment on fed glucose levels<sup>19</sup>. In contrast, treatment with antisense oligonucleotides directed against the glucocorticoid receptor restores normal fasting glucose in Zucker diabetic rats<sup>20</sup>. Taken together, these results suggest that inhibiting the actions of corticosterone by various methods will influence fasting but not fed glucose in rodent models of type 2 diabetes.

Studies of human subjects have provided evidence that diabetes adversely affects learning and memory, but they also suggest that not all cognitive domains are equally affected. Diabetic humans show accelerated decline on tasks that require episodic memory and rapid information processing, whereas attention and language abilities are unaffected<sup>2</sup>. Because episodic memory places a greater demand on temporal lobe structures, and language and attention primarily recruit other cortical and prefrontal regions, these data have been interpreted to suggest that the hippocampus is particularly susceptible to the negative consequences of diabetes. Other studies have begun to explore the role of cortisol in diabetes-induced cognitive deficits in humans. For example, inhibition of the enzyme 11- $\beta$ -hydroxysteroid dehydrogenase 1, which locally modulates the actions of glucocorticoids in the brain by reactivating cortisol from its inactive form, was shown to ameliorate cognitive deficits in humans with type 2 diabetes<sup>46</sup>. Overall, the task-specific cognitive impairments induced by diabetes and the demonstration of improved cognitive performance in diabetic humans after treatments that alter the availability of cortisol suggest that elevated cortisol in human diabetics may also contribute to deficits in hippocampal function.

## METHODS

**Animals and surgery.** Animal care and experimental procedures followed US National Institutes of Health guidelines and were approved by the US National Institute on Aging Animal Care and Use Committee. Adult male Sprague-Dawley rats were purchased from Charles River Laboratories and housed individually for a minimum of 2 weeks before the start of experiments. We administered streptozocin through the femoral vein at a dose of 70 mg kg<sup>-1</sup> as described<sup>16</sup>. In order to be included in the study, STZ-treated rats were required to have serum glucose  $\geq 200$  mg dl<sup>-1</sup>. Male mice mutant for the leptin receptor (*db/db* mice), bred on a C57BL/6 background, were purchased from Jackson Laboratories. Age-matched male C57BL/6 mice were used as controls. Rats and mice were subjected to bilateral adrenalectomy or sham operation. Adrenalectomized rats and mice received corticosterone replacement (25  $\mu$ g ml<sup>-1</sup> or 250  $\mu$ g ml<sup>-1</sup> in 0.9% saline; Sigma) in the drinking water to manipulate glucocorticoid levels<sup>30</sup>. Corticosterone replacement was available to the animals immediately after surgery. Mice were adrenalectomized at postnatal day 30; rats were adrenalectomized at postnatal day 60. All rats and mice were administered a single injection of the DNA synthetic marker BrdU (300 mg kg<sup>-1</sup>;  $n = 6$ –8 rats or mice per group). This dosage was based on previous studies<sup>47</sup> demonstrating maximal labeling at 300 mg kg<sup>-1</sup>. Animals were put to death 2 h or 3 weeks after BrdU. In a separate experiment, 2-month-old wild-type mice were implanted with Alzet minipumps to deliver the antimitotic drug AraC into the right lateral ventricle (2.2 mg ml<sup>-1</sup>, 0.25  $\mu$ l h<sup>-1</sup>, pump model 1002; bregma coordinates anterior-posterior  $-0.3$  mm, medial-lateral  $-1.0$  mm). These mice were injected once with BrdU (300 mg kg<sup>-1</sup>;  $n = 6$ –8 mice per group) and put to death 24 h later. All mice and rats had *ad libitum* access to food and water, and the room was maintained on a 12 h light-dark schedule (lights on at 06:00). For some experiments, the animals were weighed once weekly, and their food and water were weighed on two successive days per week for 4 weeks. Food consumption was measured in grams per day, and water bottle weights were converted to volumes. The techniques for quantifying glucose, insulin and corticosterone are described in **Supplementary Methods**.

**Electrophysiology and behavioral testing.** The procedures used for slice preparation and recording are available in **Supplementary Methods**.

Procedures for water maze training and novel object preference testing are also included in **Supplementary Methods**.

**Immunohistochemistry and microscopy.** Immunolabeling for BrdU and Ki67 was carried out as described<sup>15</sup>. Full description of the methods for brightfield and fluorescence tissue labeling are available in **Supplementary Methods**. We quantified single- and double-labeled cells using standard protocols<sup>15</sup>. Detailed cell-counting criteria are available in **Supplementary Methods**. We also quantified the optical intensity of fluorescence staining for synaptophysin<sup>48</sup>; full description available in **Supplementary Methods**.

**Statistics.** Statistical analyses were made using SPSS version 11.0, with significance set at  $P < 0.05$ ; graphs were generated using Graphpad Prism 4 software. Cell counts, hormone profiles, feeding, drinking, animal weights and the amount of LTP were compared using separate  $2 \times 2$  analysis of variance (ANOVA) designs (diabetes  $\times$  surgery). Behavioral data from the Morris water maze and novel object preference task were analyzed using  $2 \times 2$  repeated-measures ANOVA. The number of BrdU-labeled cells 3 weeks after injection was compared across diabetic and nondiabetic animals using bidirectional, unpaired *t*-tests. Percentages of cells double-positive for BrdU and a cell type-specific marker were also analyzed using *t*-tests. In experiments where we administered a high dose of corticosterone to adrenalectomized *db/db* mice, we analyzed behavioral data from the Morris water maze and novel object preference tasks using one-way repeated measures ANOVA with Tukey's post hoc test.

*Note: Supplementary information is available on the Nature Neuroscience website.*

## ACKNOWLEDGMENTS

This research was supported by US National Institutes of Health National Research Service Award Predoctoral fellowship F31AG024690-03 to A.M.S. through Princeton University, and by the Intramural Research Program of the US National Institute on Aging. We thank D.L. Longo for suggestions and T. Lamb, O. Carlson, J.S. Villareal and R. Telljohann for technical assistance. We are also grateful to E. Gould and H. van Praag for comments on the manuscript.

## AUTHOR CONTRIBUTIONS

A.M.S., M.P.M. and J.M.E. contributed to the conceptual design and development of the experiments. A.M.S., K.L., T.V.A. and R.G.C. performed surgeries, ran experiments and contributed data. All authors assisted with writing and revising the manuscript.

Published online at <http://www.nature.com/natureneuroscience>

Reprints and permissions information is available online at <http://npg.nature.com/reprintsandpermissions>

1. Reaven, G.M. The insulin resistance syndrome: definition and dietary approaches to treatment. *Annu. Rev. Nutr.* **25**, 391–406 (2005).
2. Messier, C. Impact of impaired glucose tolerance and type 2 diabetes on cognitive aging. *Neurobiol. Aging* **26** (suppl. 1), S26–S30 (2005).
3. Greenwood, C.E. & Winocur, G. High-fat diets, insulin resistance and declining cognitive function. *Neurobiol. Aging* **26** (suppl. 1), 45 (2005).
4. Desrocher, M. & Rovet, J. Neurocognitive correlates of type 1 diabetes mellitus in childhood. *Child Neuropsychol.* **10**, 36–52 (2004).
5. Biessels, G.J. *et al.* Place learning and hippocampal synaptic plasticity in streptozotocin-induced diabetic rats. *Diabetes* **45**, 1259–1266 (1996).
6. Biessels, G.J. *et al.* Water maze learning and hippocampal synaptic plasticity in streptozotocin-diabetic rats: effects of insulin treatment. *Brain Res.* **800**, 125–135 (1998).
7. Li, X.L. *et al.* Impairment of long-term potentiation and spatial memory in leptin receptor-deficient rodents. *Neuroscience* **113**, 607–615 (2002).
8. Hummel, K.P., Dickie, M.M. & Coleman, D.L. Diabetes, a new mutation in the mouse. *Science* **153**, 1127–1128 (1966).
9. Leuner, B., Gould, E. & Shors, T.J. Is there a link between adult neurogenesis and learning? *Hippocampus* **16**, 216–224 (2006).
10. Kamal, A., Biessels, G.J., Urban, I.J. & Gispen, W.H. Hippocampal synaptic plasticity in streptozotocin-diabetic rats: impairment of long-term potentiation and facilitation of long-term depression. *Neuroscience* **90**, 737–745 (1999).
11. Zhang, W.J., Tan, Y.F., Yue, J.T., Vranic, M. & Wojtowicz, J.M. Impairment of hippocampal neurogenesis in streptozotocin-treated diabetic rats. *Acta Neurol. Scand.*, published online 14 September 2007 (doi:10.1111/j.1600-0404.2007.00928.x).
12. van Praag, H., Christie, B.R., Sejnowski, T.J. & Gage, F.H. Running enhances neurogenesis, learning, and long-term potentiation in mice. *Proc. Natl. Acad. Sci. USA* **96**, 13427–13431 (1999).

13. Fontan-Lozano, A. *et al.* Caloric restriction increases learning consolidation and facilitates synaptic plasticity through mechanisms dependent on NR2B subunits of the NMDA receptor. *J. Neurosci.* **27**, 10185–10195 (2007).
14. Lee, J., Duan, W. & Mattson, M.P. Evidence that brain-derived neurotrophic factor is required for basal neurogenesis and mediates, in part, the enhancement of neurogenesis by dietary restriction in the hippocampus of adult mice. *J. Neurochem.* **82**, 1367–1375 (2002).
15. Stranahan, A.M., Khalil, D. & Gould, E. Social isolation delays the positive effects of running on adult neurogenesis. *Nat. Neurosci.* **9**, 526–533 (2006).
16. Magarinos, A.M. & McEwen, B.S. Experimental diabetes in rats causes hippocampal dendritic and synaptic reorganization and increased glucocorticoid reactivity to stress. *Proc. Natl. Acad. Sci. USA* **97**, 11056–11061 (2000).
17. Chan, O. *et al.* Hyperglycemia does not increase basal hypothalamo-pituitary-adrenal activity in diabetes but it does impair the HPA response to insulin-induced hypoglycemia. *Am. J. Physiol. Regul. Integr. Comp. Physiol.* **289**, R235–R246 (2005).
18. Tokuyama, K. & Himms-Hagen, J. Increased sensitivity of the genetically obese mouse to corticosterone. *Am. J. Physiol.* **252**, 202–208 (1987).
19. Langley, S.C. & York, D.A. Effects of antigluco-corticoid RU486 on development of obesity in obese *fafa* Zucker rats. *Am. J. Physiol.* **259**, 539–544 (1990).
20. Watts, L.M. *et al.* Reduction of hepatic and adipose tissue glucocorticoid receptor expression with antisense oligonucleotides improves hyperglycemia and hyperlipidemia in diabetic rodents without causing systemic glucocorticoid antagonism. *Diabetes* **54**, 1846–1853 (2005).
21. Oei, N.Y., Everaerd, W.T., Elzinga, B.M., van Well, S. & Bermond, B. Psychosocial stress impairs working memory at high loads: an association with cortisol levels and memory retrieval. *Stress* **9**, 133–141 (2006).
22. MacLulich, A.M. *et al.* Plasma cortisol levels, brain volumes and cognition in healthy elderly men. *Psychoneuroendocrinology* **30**, 505–515 (2005).
23. Elgh, E. *et al.* Cognitive dysfunction, hippocampal atrophy and glucocorticoid feedback in Alzheimer's disease. *Biol. Psychiatry* **59**, 155–161 (2006).
24. Oitzl, M.S., Flutterm, M., Sutanto, W. & de Kloet, E.R. Continuous blockade of brain glucocorticoid receptors facilitates spatial learning and memory in rats. *Eur. J. Neurosci.* **10**, 3759–3766 (1998).
25. Wright, R.L., Lightner, E.N., Harman, J.S., Meijer, O.C. & Conrad, C.D. Attenuating corticosterone levels on the day of memory assessment prevents chronic stress-induced impairments in spatial memory. *Eur. J. Neurosci.* **24**, 595–605 (2006).
26. Alfarez, D.N., Joels, M. & Krugers, H.J. Chronic unpredictable stress impairs long-term potentiation in rat hippocampal CA1 area and dentate gyrus in vitro. *Eur. J. Neurosci.* **17**, 1928–1934 (2003).
27. Kerr, D.S., Campbell, L.W., Hao, S.Y. & Landfield, P.W. Corticosteroid modulation of hippocampal potentials: increased effect with aging. *Science* **245**, 1505–1509 (1989).
28. Korz, V. & Frey, J.U. Stress-related modulation of hippocampal long-term potentiation in rats: Involvement of adrenal steroid receptors. *J. Neurosci.* **23**, 7281–7287 (2003).
29. Pavlides, C., Watanabe, Y. & McEwen, B.S. Effects of glucocorticoids on hippocampal long-term potentiation. *Hippocampus* **3**, 183–192 (1993).
30. Gould, E., Cameron, H.A., Daniels, D.C., Woolley, C.S. & McEwen, B.S. Adrenal hormones suppress cell division in the adult rat dentate gyrus. *J. Neurosci.* **12**, 3642–3650 (1992).
31. Montaron, M.F. *et al.* Lifelong corticosterone level determines age-related decline in neurogenesis and memory. *Neurobiol. Aging* **27**, 645–654 (2006).
32. Tanapat, P., Hastings, N.B., Rydel, T.A., Galea, L.A. & Gould, E. Exposure to fox odor inhibits cell proliferation in the hippocampus of adult rats via an adrenal hormone-dependent mechanism. *J. Comp. Neurol.* **437**, 496–504 (2001).
33. Karten, Y.J., Jones, M.A., Jeurling, S.J. & Cameron, H.A. GABAergic signaling in young granule cells in the adult rat and mouse dentate gyrus. *Hippocampus* **16**, 312–320 (2006).
34. Ge, S. *et al.* GABA regulates synaptic integration of newly generated neurons in the adult brain. *Nature* **439**, 589–593 (2006).
35. Saxe, M.D. *et al.* Ablation of hippocampal neurogenesis impairs contextual fear conditioning and synaptic plasticity in the dentate gyrus. *Proc. Natl. Acad. Sci. USA* **103**, 17501–17506 (2006).
36. Snyder, J.S., Kee, N. & Wojtowicz, J.M. Effects of adult neurogenesis on synaptic plasticity in the rat dentate gyrus. *J. Neurophysiol.* **85**, 2423–2431 (2001).
37. Moosavi, M., Naghdi, N., Maghsoudi, N. & Zahedi Asl, S. Insulin protects against stress-induced impairments in water maze performance. *Behav. Brain Res.* **176**, 230–236 (2007).
38. Revest, J.M. *et al.* The MAPK pathway and Egr-1 mediate stress-related behavioral effects of glucocorticoids. *Nat. Neurosci.* **8**, 664–672 (2005).
39. Piroli, G.G. *et al.* Corticosterone impairs insulin-stimulated translocation of GLUT4 in the rat hippocampus. *Neuroendocrinology* **85**, 71–80 (2007).
40. Sapolsky, R.M. Glucocorticoid toxicity in the hippocampus: reversal by supplementation with brain fuels. *J. Neurosci.* **6**, 2240–2244 (1986).
41. McNay, E.C., Fries, T.M. & Gold, P.E. Decreases in rat extracellular hippocampal glucose concentration associated with cognitive demand during a spatial task. *Proc. Natl. Acad. Sci. USA* **97**, 2881–2885 (2000).
42. Reagan, L.P. *et al.* Localization and regulation of GLUTx1 glucose transporter in the hippocampus of streptozotocin diabetic rats. *Proc. Natl. Acad. Sci. USA* **98**, 2820–2825 (2001).
43. Shors, T.J., Townsend, D.A., Zhao, M., Kozorovitskiy, Y. & Gould, E. Neurogenesis may relate to some but not all types of hippocampal-dependent learning. *Hippocampus* **12**, 578–584 (2002).
44. Kee, N., Teixeira, C.M., Wang, A.H. & Frankland, P.W. Preferential incorporation of adult-generated granule cells into spatial memory networks in the dentate gyrus. *Nat. Neurosci.* **10**, 355–362 (2007).
45. Bruel-Jungferman, E., Laroche, S. & Rampon, C. New neurons in the dentate gyrus are involved in the expression of enhanced long-term memory following environmental enrichment. *Eur. J. Neurosci.* **21**, 513–521 (2005).
46. Sandeep, T.C. *et al.* 11 $\beta$ -Hydroxysteroid dehydrogenase inhibition improves cognitive function in healthy elderly men and type 2 diabetics. *Proc. Natl. Acad. Sci. USA* **101**, 6734–6739 (2004).
47. Cameron, H.A. & McKay, R.D. Adult neurogenesis produces a large pool of new granule cells in the dentate gyrus. *J. Comp. Neurol.* **435**, 406–417 (2001).
48. Kozorovitskiy, Y. *et al.* Experience induces structural and biochemical changes in the adult primate brain. *Proc. Natl. Acad. Sci. USA* **102**, 17478–17482 (2005).

